TECHNISCHE UNIVERSITÄT MÜNCHEN

Professur Biotechnologie der Naturstoffe

Molecular cloning and functional characterization of glycosyltransferases from *Nicotiana benthamiana* and *Mentha x piperita*

Guangxin Sun

Vollständiger Abdruck der von der Fakultät Wissenschaftszentrum Weihenstephan für Ernährung, Landnutzung und Umwelt und International Graduate School of Science and Engineering (IGSSE) TUM Graduate School der Technischen Universität München zur Erlangung

des akademischen Grades eines

Doktors der Naturwissenschaften (Dr.rer.nat.)

genehmigten Dissertation

Vorsitzende(r): Prof. Dr. Wolfgang Liebl

Prüfer der Dissertation: 1. Prof. Dr. Wilfried Schwab

2. Prof. Dr. Brigitte Poppenberger-Sieberer

Die Dissertation wurde am 18. 07. 2019 bei der Technischen Universität München eingereicht und durch die Fakultät Wissenschaftszentrum Weihenstephan für Ernährung, Landnutzung und Umwelt am 07.10. 2019 angenommen.

Acknowledgements

First, I would like to thank Prof. Dr. Wilfried Schwab for his support in applying for the scholarship, which offered me a valuable opportunity to complete my doctorate at the Technical University of Munich and consistently supported me during these four years. Special thanks for his encouragement, interesting discussions, valuable ideas and suggestions, support and guidance during the whole project. He supported me in planning my experiments, evaluating the results and drawing the right conclusions for the successful completion of this project. I would also like to thank him for helping me to join the International Graduate School of Science and Engineering (IGSSE), which gave me a good opportunity to broaden my horizons and knowledge by exchanging and studying with other PhD students from different programs. That is why I worked for three months as a visiting scientist in the group of Prof. Dr. Jon Thorson at the University of Kentucky, College of Pharmacy in the USA. During this time, I was supported by Prof. Dr. Jon Thorson; Tonya S. Vance (Administrative Operations Facilitator); other laboratory colleagues (Dr. Sherif I. Elshahawi, Tyler D. Huber, Ryan R. Hughes, Brooke R. Johnson, Dr. Khaled Attia S. Mahmoud, and Dr. Larissa Ponomareva,) and also by Marc K. Invergo, (Director of the Graduate School) in scientific research. They made my daily life easier through their support, and I would therefore like to express my sincere thanks to them.

Furthermore, I would like to appreciate Dr. Fong-Chin Huang, who has helped me a lot in my research and my life, especially at the beginning, e.g. in teaching me how to clone and construct the viral vector system, in using the LC-MS and GC-MS and in analyzing the data, in adapting to the life in Germany and so on. She was like my sister who encouraged me, helped and cared for me, which made me feel that I was not alone in Germany. I would also like to thank Dr. Thomas Hoffmann, who always helped me in a very friendly way. For example, how to build the aglycone library, how to set up the LC-MS operating system and how to analyze the data and for helpful discussions about many experiments during my doctoral studies. He also helped me to repair my computer in a friendly and patient way, which solved a very big problem for me. I want to thank Dr. Thilo Fischer for helping me get my mint material, checking my mint primers, and giving me some good ideas on cloning. I would like to thank Heike Adamski who helped me a lot with my registration and accommodation. I would

like to thank Shuai Zhao who helped me a lot in my life, especially when I just arrived in Germany. He was very friendly and patient like a brother who never left me alone. I also wish him many good results for his doctoral thesis. I would like to thank Dr. Katja Härtl, Dr. Elisabeth Kurze and Kate McGraphery, they were like sisters always very friendly and gave me a lot of help for my life and my experiments. They helped me friendly to finish German documents, to make an appointment and so on. We always talked and shared good news, which made me feel very happy and broadened my horizons. Especially Dr. Katja Härtl helped me a lot with my project and gave me many useful suggestions. I would like to thank Julian Rüdiger, who helped me a lot and gave me many good ideas and suggestions for my experiments, especially while we were in the USA. I would like to thank Dr. Isabelle Effenberger and Dr. Rafal Jonczyk, who helped me a lot with my experiments, e.g. they kindly taught me how to prepare samples for NMR, how to carry out rotary evaporation, how to carry out distillation and so on. They were both very friendly and funny. We always talked and joked together when we were in our spare time, which made me very happy. I would like to thank Nicolas Figueroa, Soraya Chebib, Emilia Romer, Annika Haugeneder, Johanna Trinkl and Dr. Dagmar Rother for their friendly help in the laboratory and with the experiments. I would also like to thank Dr. Ruth Habegger, Kilian Skowranek, Mechthild Mayershofer and Hannelore Meckl for their support in organizing the greenhouse room and ordering samples.

I also would like to thank my three good students (Michael Strebl, Maximilian Merz and Robert Blamberg) and my HiWi student (Tarik Fida) who spent time working with me on different aspects of the project. All of you supported the work with great enthusiasm and the desire to learn and to do experiments. It was a pleasure and made me very happy as a supervisor. I hope that this period was helpful for your scientific career.

Finally, I want to thank all the members of Prof. Dr. Wilfried Schwab's lab for steady helpfulness, an open ear and for a great atmosphere in the lab. I had a great time and it was a pleasure for me to work here.

Moreover, I want to thank some Chinese friends who I met in Munich, Garching and Freising (Meng Yang, Jun Yang, Kaihui Yang, Lingcong Gao, Ruixue Zhao, Xiaoting Zhai, Yun Xu, Sufu Gan, Tiandan Wu and so on) for a memorable and unique time

during my studies here in Germany. With all of you here, I felt not alone. We encouraged each other and shared ideas.

I want to thank my roommates Tami, Alice and Sara. You were very friendly and humorous. We always shared our food and talked to each other, which made my life so happy. I especially appreciated Tami, you were always so friendly and helped me to solve my life problems, drove me to the hospital, helped me cook when I was very sick and so on, without your help I would not have recovered so quickly, I will never forget your great help. Thank you very much!

Furthermore, I would like to express my sincere thanks to my parents, two older brothers and my younger sister who always supported, encouraged and helped me, even though we were in three different countries. None of this would have been possible without you.

Last but not least, I would like to thank the China Scholarship Council for their financial support. Without this scholarship, my life would not be so easy.

Guangxin Sun
Freising, July 2019

Table of Contents

Abbreviations

ABA	Abscisic acid
AdGT	*Actinidia deliciosa* Glycosyltransferase
APS	Ammonium persulfat
Asp	Aspartic acid
ATP	Adenosine triphosphate
BCIP	5-Bromo-4-chloro-3'-indoly phosphate (Na-salt)
BLAST	Basic Local Alignment Search Tool
CAZy	CArbohydrate-Active EnZymes
CCDs	Carotenoid Cleavage Dioxygenases
cDNA	complementary Deoxyribonucleic acid
CNLE	Constant Neutral-Loss Experiment
dATP	Deoxyadenosine triphosphate
dCTP	Deoxycytidine triphosphate
ddH2O	double distilled water
DMF	N,N-Dimethylformamide
DMSO	Dimethyl sulfoxide
dNTP	Deoxynucleotide
DXD	Asp-X-Asp
E	Elution fraction
E. coli	*Escherichia coli*
EDTA	Ethylenediamine tetraacetic acid
EHMF	2(or 5)-Ethyl-4-hydroxy-5(or 2)-methyl-3(2H)-furanone
EIC	Extracted Ion Chromatogram
FMT	Furanmethanethiol
GC-MS	Gas Chromatography-Mass Spectrometry
GDR	Glucose Detection Reagent
GST	Glutathione S-transferase
GTs	Glycosyltransferases
HMF	4-Hydroxy-5-methyl-3-furanone
HPLC	High Performance Liquid Chromatography
HR	Hypersensitive Response
IPTG	Isopropyl β-D-1-thiogalactopyranoside
kcat	Turnover number
kDa	Kilodalton
KM	Michaelis constant
LB	Luria-Bertani
LC-MS	Liquid Chromatography Mass Spectrometry
M	Marker
m/z	Mass-to-charge ratio
MGR	Mint Genomics Resource
mRNA	Messenger ribonucleic acid
MS	Mass spectrometry
MW	Molecular Weight
NbGT	*Nicotiana benthamiana* Glycosyltransferase

NBT	Nitro-blue Tetrazolium
NCBI	National Center for Biotechnology Information
NCEDs	9-cis-Epoxycarotenoid Dioxygenases
NMR	Nuclear Magnetic Resonance spectroscopy
NtGT	*Nicotiana tabacum* Glycoysltransferase
OD600	Optical Density at 600 nm
ORF	Open Reading Frames
PAGE	Polyacrylamide Gel Electrophoresis
PBS	Phosphate Buffered Saline
PCR	Polymerase Chain Reaction
PSPG	Putative Secondary Plant Glycosyltransferase
QRT-PCR	Quantitative Real-Time PCR
RLU	Relative Luminescence Unit
ROS	Reactive Oxygen Species
rpm	Rounds per minute
RT	Room Temperature
RT-PCR	Reverse Transcription Polymerase Chain Reaction
SA	Salicylic acid
SDS	Sodium dodecyl sulfate
SDS - PAGE	Sodium dodecyl sulfate - Polyacrylamide Gel Electrophoresis
TEMED	Tetramethylethylendiamin
TMV	Tobacco Mosaic Virus
TRIS	Tris (hydroxymethyl) aminomethane
UDP	Uridine 5-diphosphate
UDP-G	Uridine 5´-diphosphoglucose disodium salt
UDR	UDP Detection Reagent
UGTs	UDP-dependent Glycosyltransferases
UV	Ultraviolet
Vmax	Maximum reaction rate
VvGT	*Vitis vinifera* Glycosyltransferase

Abstract

Glycosylations have major impacts on the physicochemical properties of bioactive natural products as they increase the stability of small molecules, decrease their toxicity, and affect their transport and storage. Hence, targeted glycosylation of acceptor molecules is of high scientific significance. However, regio- and stereoselective chemical synthesis is challenging and expensive. Another promising approach is the enzymatic glycosylation via glycosyltransferases (GTs). They catalyze the transfer of a sugar moiety from an activated donor, usually UDP-glucose, to a broad range of acceptor molecules. Studies on novel GTs are of great scientific interest in order to investigate their properties and to identify possible applications.

Since no *GT*s from mint have yet been characterized, we selected five potential *Mentha x piperita GTs* from an expressed sequence tag (EST) database generated from mint. Candidate *GT*s strongly expressed in mint leaf tissue were chosen and their full-length nucleotide sequences could be derived from the EST data set. Similarly, *Nicotiana* species are rich sources of bioactive glycosylated metabolites but UDP-dependent glycosyltransferases (UGTs) have been rarely characterized in this genus. Therefore, UGT genes were selected from a *N. benthamiana* transcriptome database due to their high expression level in leaves, flowers and roots.

In total, six *M. x piperita* UGTs (MpUGTs) and ten *N. benthamiana* UGTs (NbUGTS) were successfully cloned. Their recombinant glutathione-S-transferase tagged (GST-tag) fusion proteins were produced in *Escherichia coli,* purified, and their catalytic activities were tested towards a series of selected aglycons. The reaction products were analyzed by LC-MS. Twelve recombinant enzymes were promiscuous and accepted a range of substrates including aliphatic alcohols, terpenoids, and phenolics. Four genes (*UGT708M2, UGT709C8, UGT709Q1 and UGT85A74*) seemed to be pseudogenes. UGT709Q1 and UGT85A74 protein sequences lacked important features of UGTs - the GSS motif and the catalytically active amino acid His. They obviously lost their catalytic activities. UGT708M2 and UGT709C8 could not accept any of the selected substrates, although their protein sequences showed high amino acid sequence identities with the related UGT708M1 and UGT709C7 sequences,

respectively. Three enzymes (UGT709C7, UGT709C6, and UGT708M1) had a narrow substrate tolerance, accepting only 15, 15 and 10 out of 40 substrates, respectively.

Because seven UGTs UGT72AY1, UGT85A73, UGT73A25, UGT73A24, UGT86C10, UGT709C6 and UGT73B24 glucosylated α- and β-ionol their activities were also tested with 7 additional norisoprenoids namely the hydroxylated C13 apocarotinoids 3-hydroxy-α-ionol, 4-hydroxy-β-ionol, 3-hydroxy-α-ionone, 4-hydroxy-β-ionone, 3-hydroxy-α-damascone, 4-hydroxy-β-damascone, and 3-oxo-α-ionol, which were obtained as crude products of a whole-cell P450 monooxygenase biotransformation. Only α-ionol, β-ionol and 3-oxo-α-ionol were available as pure substances. The reaction products were analyzed by LC-MS and the products were putatively identified by their MS and MS2 spectra and relative retention time in comparison with the substrates. UGT86C10 showed broad substrate tolerance and accepted all 9 norisoprenoid substrates. It readily glucosylated the norisoprenoids in particular 3-hydroxy-α-ionone, 4-hydroxy-β-ionone, 3-hydroxy-α-damascone, and 4-hydroxy-β-damascone. UGT73A25 showed high enzyme activity towards 3-hydroxy-α-ionol, 4-hydroxy-β-ionol, α-ionol, and β-ionol. In contrast, UGT72AY1 was almost inactive with hydroxylated ionones and damascones but showed catalytic activity with ionols in particular 3-oxo-α-ionol. This indicated that UGT86C10 is the best UGT for the production of norisoprenoid glucosides.

To characterize the eight active NbUGTs and three MpUGTs (UGT708M1, UGT709C6, and UGT86C10) in more detail regarding their particular substrate specificities, quantitative substrate screenings were performed using the UDP Glo™ assay and a selected set of substrates. All selected NbUGTs exhibited catalytic activity and specificity towards carvacrol, scopoletin, and kaempferol, except UGT85A73, which preferentially glucosylated aliphatic compounds such as perillyl alcohol and cis-3-hexenol. MpUGTs exhibited quite different catalytic activities; UGT708M1 showed highest activity towards naringenin but the overall catalytic activity was quite low. Carvacrol was the preferred substrate of UGT709C6 while UGT86C10 favored farnesol. Subsequently, kinetic analyses based on optimal conditions were performed with the UDP-Glo^{TM} assay. The specificity constant Kcat/K_M highlighted the *in vitro* preference of UGT709C6 for 1-octene-3-ol; UGT86C10 for 1-dodecanol; UGT72AY1 for scopoletin; UGT73A24 for kaempferol; and UGT73A25 for quercetin. UGT71AJ1 favored carvacrol and UGT85A73 efficiently converted cis-3-hexenol. Notably, when

the enzymatic activity of UGT72AY1 towards α-ionol and β-ionol was tested with the UDP-Glo™ assay negative values were obtained. A significant UDP-glucose hydrolase activity was assumed and experimentally confirmed exceeding the glycosylation reaction. Therefore, LC-MS was used to determine the kinetic data for α-, and β-ionol for selected UGTs.

QRT-PCR analyses confirmed that *MpUGT*s were mainly expressed in young leaves, mature leaves and flower, while in root and old leaves the genes were barely transcribed. Similarly, *NbGT*s were strongly transcribed in *N. benthamiana* leaves.

UGT708M1, UGT709C6, UGT86C10, UGT72AY1, UGT73A24 and *UGT73A25* were also transiently overexpressed in *N. benthamiana* leaves using an established viral vector system to produce active enzymes. QRT-PCR and enzyme activities analyses confirmed the successful overexpression of the agroinfiltrated genes. Overexpression of *UGTs* except for *UGT709C6* led to an increased production of ionyl-, carvacryl-, scopoletin-, quercetin-, and kaempferyl glucosides indicating that the encoded UGTs are contributing to the formation of the hexosides in *vitro*. To structurally identify natural glycoside products formed by UGT73A24 and UGT73A25 *in planta*, untargeted metabolite profiling analyses by LC-MS on extracts isolated from agroinfiltrated *N. benthamiana* leaves was performed. LC-MS analyses revealed two isomeric hexosides, which significantly accumulated in the agroinfiltrated leaves in addition to quercetin rutinoside. Enzymatic transformations of fractions of a physiologic aglycone library confirmed the hexosides as natural products of UGT73A24 and UGT73A25, which were identified as the two isomeric D-glucosides of the phytoalexin N-feruloyl tyramine. In addition, LC-MS analyses revealed that overexpression of *UGT73A24* and *UGT73A25* significantly reduced the levels of pathogen-induced metabolites in agroinfiltrated *N. benthamiana* leaves. Although homologues of *UGT73A24* and *UGT73A25* have been shown to be involved in the production of scopolin in *N. tabacum* cells after treatment with salicylate, fungal elicitors and the tobacco mosaic virus the presented results point to a multifunctional role of UGT73A24 and UGT73A25 in plant resistance.

In summary, these results provide the foundation for the biotechnological production of bioactive natural products using UGTs as well as for the functional characterization of further GTs from *Nicotiana benthamiana* and *Mentha × piperita*.

Zusammenfassung

Glykosylierungen haben große Auswirkungen auf die physikalisch-chemischen Eigenschaften bioaktiver Naturstoffe, da sie die Stabilität kleiner Moleküle erhöhen, ihre Toxizität verringern und ihren Transport und ihre Lagerung beeinflussen. Daher ist die gezielte Glykosylierung von Akzeptormolekülen von hoher wissenschaftlicher Bedeutung. Die regio- und stereoselektive chemische Synthese ist jedoch schwierig und teuer. Ein weiterer vielversprechender Ansatz ist die enzymatische Glykosylierung durch Glykosyltransferasen (GTs). Sie katalysieren den Transfer einer Zuckereinheit von einem aktivierten Donor, üblicherweise UDP-Glucose, zu einem breiten Spektrum von Akzeptormolekülen. Studien zu neuartigen GTs sind von großem wissenschaftlichen Interesse, um ihre Eigenschaften zu untersuchen und ihre möglichen Anwendungen zu identifizieren.

Da bisher noch keine GTs aus Minze charakterisiert wurden, wurden potenzielle *Mentha x piperita* GTs in einer „expressed sequence tag“ (EST)-Datenbank gesucht. Kandidaten-GTs, die stark im Blattgewebe exprimiert waren wurden ausgewählt und ihre Volllängen-Nukleotidsequenzen konnten aus einem Transkriptom-Datensatz abgeleitet werden. Ebenso sind *Nicotiana*-Arten reich an bioaktiven glykosylierten Metaboliten, aber UDP-abhängige Glykosyltransferasen (UGTs) wurden in dieser Gattung bisher selten charakterisiert. Daher wurden UGT-Gene aufgrund ihres hohen Expressionsniveaus in Blättern, Blüten und Wurzeln aus einer *Nicotiana benthamiana*-Transkriptomdatenbank ausgewählt.

Insgesamt wurden sechs *Mentha x piperita*-UGTs (MpUGTs) und zehn *Nicotiana benthamiana*-UGTs (NbUGTS) erfolgreich kloniert. Ihre rekombinanten Glutathion-S-Transferase-markierten (GST-markierten) Fusionsproteine wurden in *Escherichia coli* hergestellt, gereinigt und ihre katalytischen Aktivitäten gegenüber einer Reihe von ausgewählten Aglyka getestet. Die Reaktionsprodukte wurden mittels LC-MS analysiert. Zwölf rekombinante Enzyme akzeptierten eine Reihe von Substraten, einschließlich aliphatischer Alkohole, Terpenoide und Phenole. Vier Gene (*UGT708M2, UGT709C8, UGT709Q1 und UGT85A74*) schienen Pseudogene zu sein. Den Proteinsequenzen UGT709Q1 und UGT85A74 fehlten wichtige Merkmale von UGTs - das GSS-Motiv und die katalytisch aktive Aminosäure His. Sie haben

offensichtlich ihre katalytischen Aktivitäten verloren. UGT708M2 und UGT709C8 konnten keines der ausgewählten Substrate akzeptieren, obwohl ihre Aminosäuresequenzen eine hohe Ähnlichkeit mit der verwandten UGT708M1 bzw. UGT709C7 aufwiesen. Drei Enzyme (UGT709C7, UGT709C6 und UGT708M1) hatten eine enge Substrattoleranz und glukosylierten nur 15, 15 bzw. 10 von 40 Substraten. Da sieben UGTs UGT72AY1, UGT85A73, UGT73A25, UGT73A24, UGT86C10, UGT709C6 und UGT73B24 α- und β-Ionol glukosylierten wurden ihre Aktivitäten auch gegenüber 7 zusätzlichen Norisoprenoiden getestet wurden, nämlich den hydroxylierten C13-Apocarotinoiden 3-Hydroxy-α-ionol, 4-Hydroxy-β-ionol, 3-Hydroxy-α-ionone, 4-Hydroxy-β-ionone, 3-Hydroxy-α-damascone, 4-Hydroxy-β-damascone und 3-Oxo-α-ionol, die als Rohprodukte einer Ganzzell-P450-Monooxygenase-Biotransformation erhalten wurden. Nur α-Ionol, β-Ionol und 3-Oxo-α-ionol waren als Reinsubstanzen erhältlich. Die Reaktionsprodukte wurden mit LC-MS analysiert und die Produkte mit Hilfe ihrer MS- und MS2-Spektren und ihrer Retentionszeit im Vergleich zu den Substraten identifiziert. UGT86C10 zeigte eine breite Substratakzeptanz und glukosylierte alle 9 Norisoprenoid-Substrate. Es glukosylierte bevorzugt die Norisoprenoide 3-Hydroxy-α-ionon, 4-Hydroxy-β-ionon, 3-Hydroxy-α-damascon und 4-Hydroxy-β-damascon. UGT73A25 zeigte eine hohe Enzymaktivität gegenüber 3-Hydroxy-α-ionol, 4-hydroxy-β-ionol, α-ionol und β-ionol. Im Gegensatz dazu war UGT72AY1 gegenüber hydroxylierten Ionen und Damasconen fast inaktiv, zeigte aber katalytische Aktivität mit Ionolen, insbesondere 3-Oxo-α-ionol. Dies deutet darauf hin, dass UGT86C10 die beste UGT für die Herstellung von Norisoprenoid-Glukosiden ist.

Um die acht aktiven NbUGTs und drei MpUGTs (UGT708M1, UGT709C6 und UGT86C10) in Bezug auf ihre jeweiligen Substratspezifitäten genauer zu charakterisieren, wurde ein quantitatives Substratscreening unter Verwendung des UDP Glo™-Assays und eines ausgewählten Satzes von Substraten durchgeführt. Alle ausgewählten NbUGTs zeigten katalytische Aktivität und Spezifität gegenüber Carvacrol, Scopoletin und Kaempferol, mit Ausnahme von UGT85A73, das vorzugsweise aliphatische Verbindungen wie Perillylalkohol und cis-3-Hexenol glykosylierte. MpUGTs zeigten hingegen deutlich unterschiedliche katalytische Aktivitäten; UGT708M1 zeigte höchste Aktivität gegenüber Naringenin, aber ihre katalytische Aktivität war sehr gering. Carvacrol war das bevorzugte Substrat von

UGT709C6, während UGT86C10 Farnesol bevorzugte. Anschließend wurden mit dem UDP-Glo™-Assay kinetische Analysen unter optimalen Bedingungen durchgeführt. Die Spezifitätskonstante Kcat/K_M unterstrich die *in vitro* Präferenz von UGT709C6 für 1-Octen-3-ol; UGT86C10 für 1-Dodecanol; UGT72AY1 für Scopoletin; UGT73A24 für Kaempferol; und UGT73A25 für Quercetin. UGT71AJ1 favorisierte Carvacrol und UGT85A73 setzte cis-3-Hexenol effizient um. Wenn die enzymatische Aktivität von UGT72AY1 gegenüber α-Ionol und β-Ionol mit dem UDP-Glo™-Assay getestet wurde, wurden bemerkenswerterweise negative Werte ermittelt. Eine signifikante UDP-Glukose-Hydrolase-Aktivität, die die Glykosylierungsreaktion übersteigt wurde deshalb angenommen und experimentell bestätigt. Daher wurden die kinetischen Daten für α- und β-Ionol für ausgewählte UGTs mittels LC-MS bestimmt.

QRT-PCR-Analysen bestätigten, dass *MpUGT*s hauptsächlich in jungen Blättern, alten Blättern und Blüten exprimiert waren, während in Wurzeln und alten Blättern die Gene kaum transkribiert wurden. Die *NbGT*s waren ebenfalls stark in *N. benthamiana* Blättern transkribiert.

UGT708M1, UGT709C6, UGT86C10, UGT72AY1, UGT73A24 und *UGT73A25* wurden auch in *N. benthamiana* Blättern überexprimiert, wobei ein etabliertes virales Vektorsystem zur Herstellung aktiver Enzyme verwendet wurde. QRT-PCR- und Enzymaktivitätsanalysen bestätigten die erfolgreiche Überexpression der agroinfiltrierten Gene. Die Überexpression von UGTs mit Ausnahme von UGT709C6 führte zu einer erhöhten Produktion von Ionyl, Carvacryl-, Scopoletin-, Quercetin- und Kaempferyl-Glukosiden, was darauf hinweist, dass die kodierten UGTs in vitro zur Bildung der Hexoside beitragen. Um natürliche Glykosidprodukte, die von UGT73A24 und UGT73A25 *in planta* gebildet werden, strukturell zu identifizieren, wurden ungerichtete Metabolitenprofilanalysen mittels LC-MS an Extrakten durchgeführt, die aus agroinfiltrierten *N. benthamiana* Blättern isoliert wurden. LC-MS-Analysen lieferten zwei isomere Hexoside, die sich zusätzlich zu Quercetin-Rutinosid in den agroinfiltrierten Blättern signifikant anreicherten. Enzymatische Umsetzungen von Fraktionen einer physiologischen Aglykabibliothek bestätigten die Hexoside als natürliche Produkte von UGT73A24 und UGT73A25, die als die beiden isomeren D-Glucoside des Phytoalexins N-feruloyltyramin identifiziert werden konnten. Zusätzlich zeigten LC-MS-Analysen, dass eine Überexpression von *UGT73A24* und *UGT73A25*

die Gehalte an pathogeninduzierten Metaboliten in agroinfiltrierten *N. benthamiana* Blättern signifikant verringerte. Obwohl gezeigt wurde, dass Homologe von UGT73A24 und UGT73A25 nach Behandlung mit Salicylat, Pilzerregern und dem Tabakmosaikvirus an der Produktion von Scopolin in *N. tabacum*-Zellen beteiligt sind, deuten unsere Ergebnisse auf eine multifunktionale Rolle der UGTs bei der Pflanzenresistenz hin.

Zusammenfassend bilden diese Ergebnisse die Grundlage für die biotechnologische Herstellung von bioaktiven Naturprodukten mit UGTs und liefern wichtige Informationen für die funktionelle Charakterisierung weiterer GTs aus *Nicotiana benthamiana* und *Mentha × piperita*.

1. Introduction

1.1 Tobacco

Nicotiana species are indigenous plants of America, but today they grow naturally across much of the world and their products have long been used both medicinally and recreationally by human societies (Jassbi et al., 2017). The genus *Nicotiana* includes an extensive group of plants in the nightshade family (Solanaceae) of which some are important crop and medicinal plants due to their ornamental properties and the psychoactive, medicinal, and toxic activities of their natural products (Goodin et al., 2008). Their secondary or specialized metabolites have different functions in the plants including protection to biotic stress factors like pathogens, and herbivores (Baldwin, 1999), or biotic stress such as drought and salinity as well as promoting outcrossing and dispersal (Jassbi et al., 2017). Since *Nicotiana* species are a rich source for bioactive plant secondary metabolites including diterpenes alcohols, aromatic compounds, isoprenoids (Wahlberg and Enzell C.R., 1987), pyridine alkaloids, flavonoids, and volatiles (Nugroho and Verpoorte, 2002) their production and biological activities have been extensively studied. Some of the metabolites, such as sugar esters, sesquiterpenoids, and acyclic hydroxygeranyllinalool diterpene glycosides (HGL-DTGs) are produced by trichomes, which are found on the surface of the leaves (Jassbi et al., 2008; Nugroho and Verpoorte, 2002). Therefore, the cultivated tobacco (*N. tabacum*), with more than 2500 structurally known metabolites, is chemically very well studied and is updated by ongoing research (Figure 1 and 2) (Xu et al., 2017). Many metabolites in tobacco are glycosylated but only a few glycosyltransferases that produce glycosides have been isolated and characterized from *Nicotiana*. An UDP-glucose: hydroxycoumarin 7-O-glucosyltransferase (CGTase) which converts scopoletin to its glycoside scopolin (Figure 2) was purified from tobacco cells and characterized (Taguchi et al., 2001). Similarly, NtGT1a and NtGT1b showed glucosylation activity against flavonoids, coumarins, and naphthols (Taguchi et al., 2003).

The cultivated tobacco was the first plant to be genetically modified (Bevan et al., 1983), and many genetic manipulation possibilities have been developed in *N. tabacum* to accurately study the function of individual metabolites (Wang and Bennetzen, 2015).

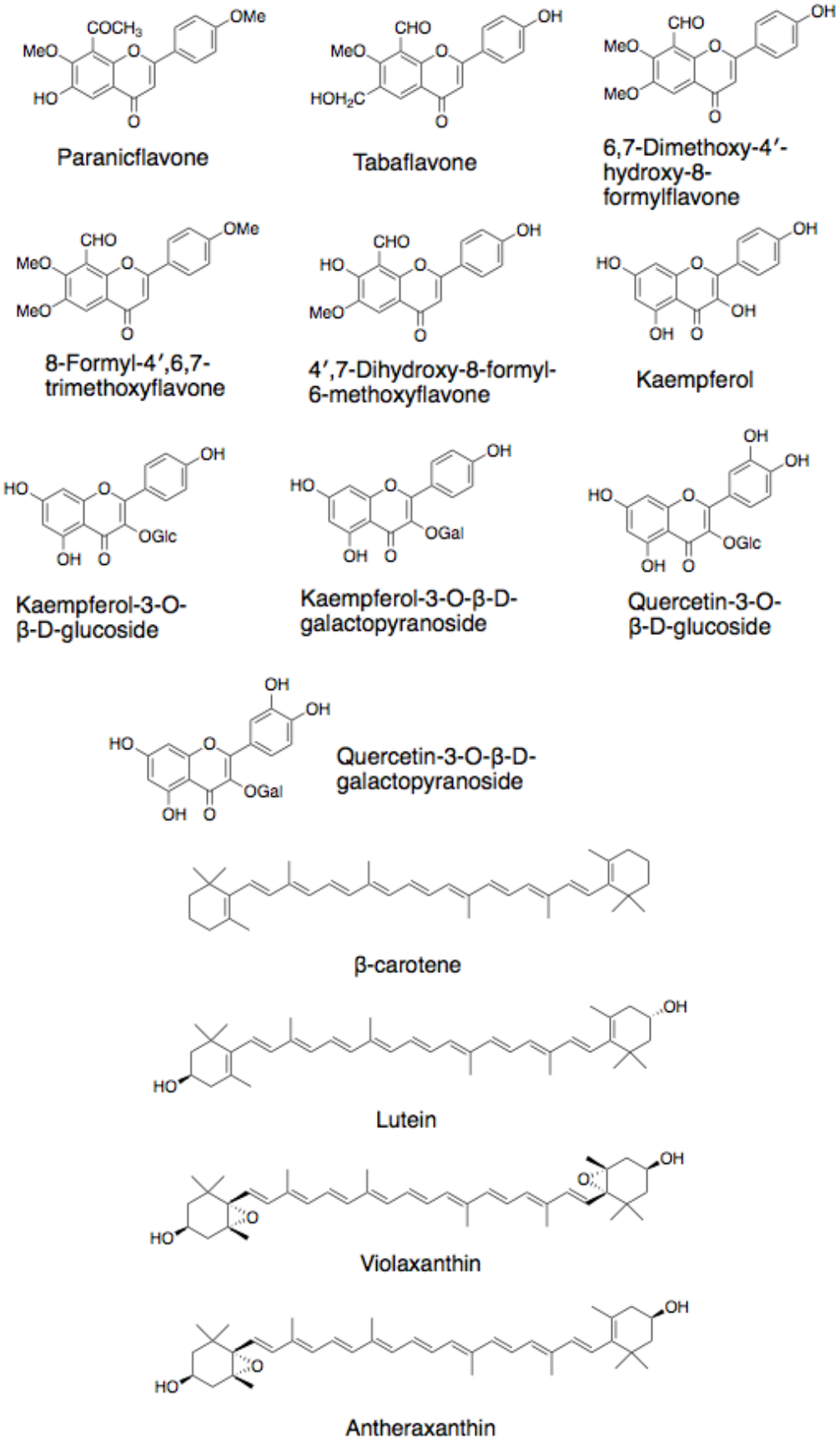

Figure 1. Some bioactive flavonoids and major carotenoids found in *Nicotiana.* Me methyl, Gal galactose, Glc glucose. (Jassbi et al., 2017).

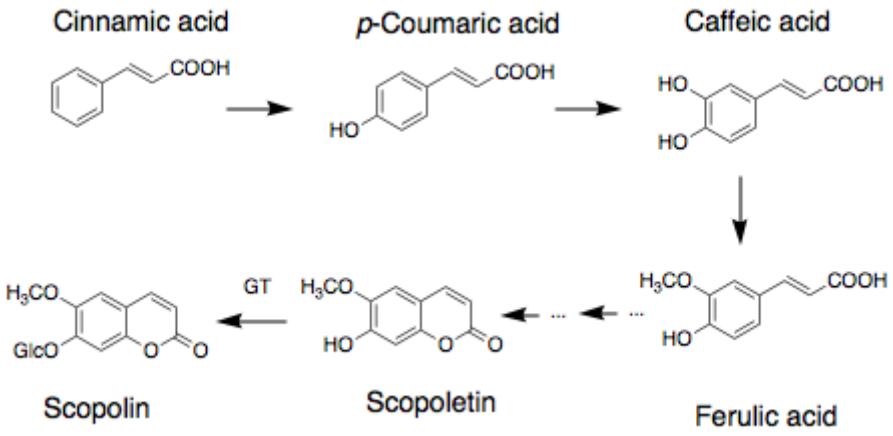

Figure 2. Proposed biosynthetic pathway of scopolin (scopoletin glucoside). GT glucosyltransferase, Glc glucose. (Chong et al., 2002).

Since the genetic methods established in cultivated tobacco have been applied to, and expanded in, other *Nicotiana* species, several *Nicotiana* species are now widely used as model organisms in scientific research (Goodin et al., 2008). Thus, tobacco research has enabled significant advances in plant science and biotechnology over the last decade, contributing to the clarification of scientific and agronomic issues in genetics, phytopathology, photosynthesis, nutrition and plant growth (Gulati et al., 2013; Mhlongo et al., 2016a; Onkokesung et al., 2012; Xu et al., 2017; Zhao et al., 2018). In addition, research with tobacco plants has already given an important contribution far beyond the frontiers of agricultural science. Tobacco is currently used in bioengineering pharmaceutical laboratories as a manufacturing platform for the production of avarious drugs and therapeutic agents (Yao et al., 2015).

The wild tobacco *N. benthamiana* is used extensively as a host for agroinfiltration experiments to functionally analyze foreign and endogenous genes (Goodin et al., 2008). It is also an important model in intraspecies and inter-plant interaction studies and plant molecular biology (Jassbi et al., 2017). The wild coyote tobacco, *N. attenuata*, is a model organism in molecular chemical ecology, which investigates the ecological roles of plant metabolites. The use of genetic methods to manipulate gene transcript levels has enabled high-throughput *in vivo* screenings to elucidate the biological functions and the biosynthetic production of secondary metabolites in *Nicotiana* species (Gachon et al., 2004; Reed and Osbourn, 2018).

Nicotiana benthamiana is a popular and widely used model plant in biology. It is quite susceptible for a variety of plant pathogens, e.g. bacteria, fungi and viruses, which

makes it an interesting species for plant pathogen research. Furthermore, since it can be genetically modified very efficient, it is used for virus induced gene silencing or transient protein expression (Goodin et al., 2008).

When geraniol synthase (GES) genes from *Valeriana officinalis* and *Lippia dulcis*, whose encoded proteins catalyze the formation of geraniol from geranyl diphosphate in one step, were agroinfiltrated in tobacco leaves for localization and enzyme activity studies, not only geraniol was detected as reaction product, but also geraniol glycosides (Dong et al., 2013). This led to the conclusion, that there are aleady endogenous enzymes with glycosylation activity towards geraniol in tobacco (Dong et al., 2013). Similar observations have been made in studies on cytochrome P450 enzymes known to hydroxylate geraniol (Höfer et al., 2013). Different variants of the monooxygenase genes were agroinfiltrated in combination with *GES* in tobacco. In addition to geraniol also various glycosylated forms of geraniol and hydroxygeraniol were detected, concluding that there are endogenous glycosyltransferases present in *N. benthamiana* (Höfer et al., 2013). Thus, *N. benthamiana* appears to be a good candidate to investigate glycosyltransferases acting on small molecules.

1.2 Peppermint (*Mentha piperita*)

The genus *Mentha* (a member of Lamiaceae family), which is commonly known as mint, includes approximately 25–30 species (Ali et al., 2002) and has been recognized for its medicinal, therapeutic and aromatic properties since ancient times (Kumar et al., 2011). These plants are of great economic importance and widely used as medicinal and aromatic herbs. They can be used in cooking of daily items (such as food and tea), pharmaceuticals (eg. against fever, cough, infection, and inflammation) (Champagne and Boutry, 2013; Dorman et al., 2003) and in the production of aromatic products (such as flavour and cosmetic). *Mentha* species have been reported to possess several biological effects, including anticancer, antimicrobial, antioxidant (Canadanovic-Brunet et al., 2005), antidiarrheal, and anti-inflammatory activities (Tang et al., 2016; Wang et al., 2018; Zaia et al., 2016), in addition to their therapeutic potential in the cardiovascular field of medicine (Shaikh et al., 2014). These biological activities are significantly correlated with their total phenol flavonoid content (Manosroi et al., 2006; Santos et al., 2014).

The chemical composition of mint oils has been widely investigated, as they are used for flavors and fragrances. Comparative few studies have been done to characterize the flavonoid glycosides of mint extracts and few compounds have been identified. Apigenin-7-O-glucuronide, 7-O-glucoside and 7-O-rutinoside (isorhoifolin), 4'-O-caffeoyl esters of apigenin glycosides (piperitoside and menthoside), 7-O-rutinosides of diosmetin (diosmin), luteolin 7-O-glucoside, 7-O-rutinoside, and 7-O-glucuronide, eriodictyol (eriocitrin) and hesperetin (hesperidin) have been found (Hoffman and Lunder, 1984). The genus Mentha is a good candidate for the discover of new bioactive compounds because flavonoids (Koşar et al., 2004), bicyclic lactones (Villasenor and Sanchez, 2009), phenolic acids (Koşar et al., 2004), triterpenes (Monte et al., 1997), aliphatic glycosides (Yamamura et al., 1998), lignans, and monoterpenes (She et al., 2010) were reported from its various species. Flavonoids in mint generally occur as sugar conjugates, principally as O-glycosides and are the most abundant metabolite class.

Peppermint (*Mentha x piperita*) is a sterile (hexaploid) hybrid mint created from watermint (*Mentha aquatica)* and spearmint *(Mentha spicata)* (Ahkami et al., 2015; Shariatmadari et al., 2015). This clonal plant has since been grown worldwide and is easily propagated by vegetative methods. It is used for commercial purposes and as an experimental material. Peppermint is one of the most important medicinal and aromatic plants of the genus mint. An important product from the members of the mint genus is the mint essential oil, which has several biological effects and can be isolated with ease by steam distillation (Chakraborty and Chattopadhyay, 2008). *In vitro,* peppermint has strong antioxidant and antitumor effects, significant antimicrobial and antiviral activities, and antiallergic potential. The essential ingredients of mint oils are menthol and menthone (Ahkami et al., 2015; McKay and Blumberg, 2006). These plant oils also contain phenolic glycosides as main components (Sgorbini et al., 2015). Flavone glycosides (Salin et al., 2011) and menthol glycoside (Sgorbini et al., 2015) have been isolated from *Mentha* species, but glycosyltransferases have not yet been characterized in mint.

Menthol (Figure 3) and related monoterpenes are representatives of the smallest members (C_{10}) of the very large class of terpenoid (isoprenoid) natural products, which today comprise more than 40,000 defined structures. Menthol ($C_{10}H_{20}O$) is a naturally occurring compound of plant origin, which gives plants of the *Mentha* species the

typical minty smell and flavour. The monoterpene is produced synthetically or obtained from the essential oil of several mint plant species such as *Mentha piperita* (peppermint) and *Mentha arvensis* (cornmint), together with traces of menthone, the ester menthyl acetate and other compounds. Peppermint and cornmint oils, obtained by steam distillation from the fresh flowering tops of the plants, contain 50% and 70-80% of (-)-menthol, respectively (Eccles, 1994). Pure (-)-menthol can be obtained from cornmint oil by recrystallization from low-boiling point solvents. Peppermint oil is not used for the production of menthol due to its high price. Menthol is extracted or synthesised from precursor molecules isolated from other essential oils such as eucalyptus oil, citronella oil, and Indian turpentine oil.

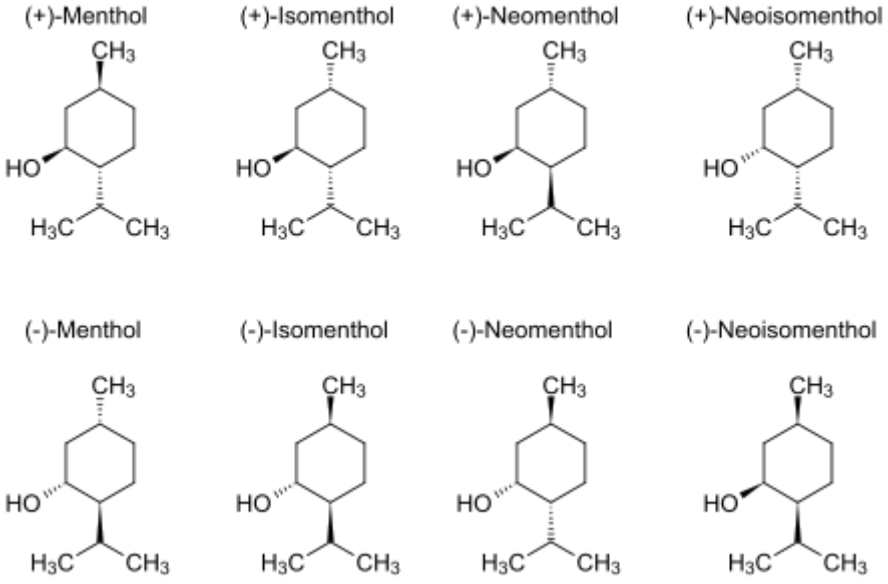

Figure 3. Eight isomers of menthol.

Menthol is a cyclic terpene alcohol with three asymmetric carbon atoms in its cyclohexane ring and, therefore, occurs as four pairs of optical isomers named (-)- and (+)- menthol, (-)- and (+)- isomenthol, (-)- and (+)- neomenthol, and (-)- and (+)- neoisomenthol (Bauer et al., 1990) (Figure 3). Among the optical isomers, (-)-menthol is the one that occurs most widely in nature. It is considered a fragrance and flavor compound, has the characteristic peppermint odour and exerts a cooling sensation when applied to skin and mucosal surfaces. For this reason, it is widely used in many confectionary goods, cosmetics, oral health care products, pharmaceuticals, teas and tobacco products. The other isomers of menthol have a similar, but not identical odour

and do not have the same cooling property as (-)-menthol. The isomers differ slightly in their boiling points, which range from 211.7 to 218.6 °C. They also differ in their physical characteristics. At room temperature, (+)-neomenthol is a colourless liquid while isomenthol and menthol are white crystals.

(−)-Menthol is the best-known monoterpene and its multistep biosynthetic pathway has been analyzed in detail. The biosynthesis of (−)-menthol and its isomers starting from the primary metabolism requires at least eight enzymatic steps, and all enzymes involved have been identified and characterized (Croteau et al., 2005). The reaction sequence begins with the cyclization of the universal monoterpene precursor geranyl diphosphate to the parent olefin (−)-(4S)-limonene (Figure 4).

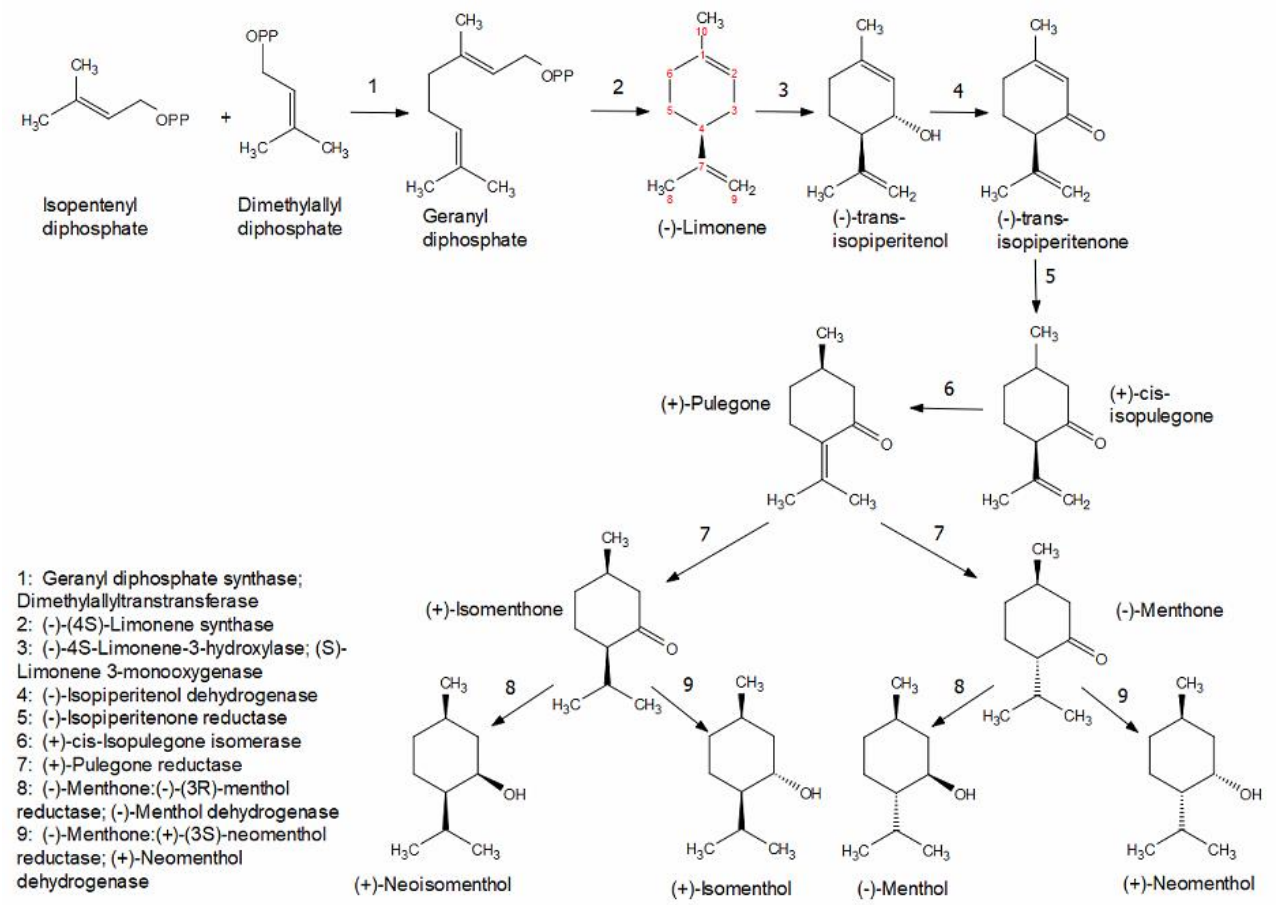

Figure 4. Biosynthesis of menthol and its stereoisomers in peppermint (*Mentha x piperita*). (http://langelabtools.wsu.edu/mgr/pathways/peppermint_terpenoids) .

Following hydroxylation at C3, a series of four redox transformations and an isomerization reaction occur in a general metabolic strategy termed the “allylic oxidation–conjugate reduction” scheme. The enzymatic reactions install three chiral

centers on the substituted cyclohexane ring to yield (−)-(1R, 3R, 4S)-menthol (Figure 4). More specifically, the biosynthesis of (−)-menthol and its isomers takes place in the secretory gland cells of the peppermint plant (Figure 5).

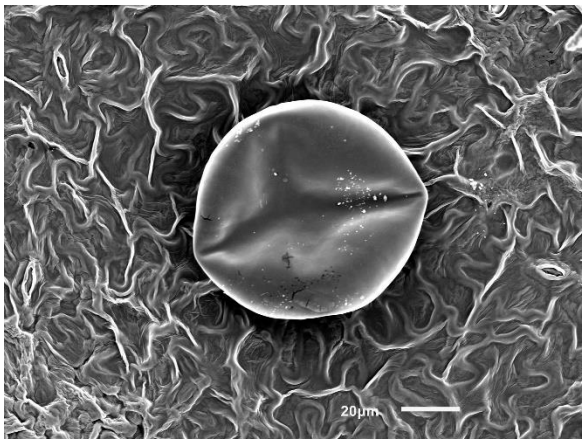

Figure 5. Mint gland cell (https://blogs.edgehill.ac.uk) .

The biosynthesis of menthol has been exploited as a model in a series of studies to probe developmental and regulatory aspects of monoterpene metabolism (Croteau et al., 2005)

1.3 Glycosylation and Glycosyltransferases

Glycosylation is a key modification of small molecules in organisms and one of the most important tailoring mechanisms of bioactive natural products in plants (Yang and Tanaka, 1997). It serves as a general storage principle of aroma compounds (Maicas and Mateo, 2005), increases structural diversity (Jones and Vogt, 2001), and enhances stability and solubility. Glycosylation of metabolites facilitates their storage and accumulation in plants (Wang, 2009), reduces the toxicity of potential toxic agents, is important for metabolic homeostasis of plant cells (Bowles et al., 2005) and involved in plant hormone homeostasis (Poppenberger et al., 2005). Besides, glycosylation of endogenous toxic chemicals allows their storage in high concentrations and determines their controlled release after attack by herbivores or pathogens (Vogt and Jones, 2000).

Studies have shown that many endogenous secondary metabolites from *Nicotiana* (Heiling et al., 2016; Jassbi et al., 2010; Kodama et al., 1984; Pang et al., 2007; Yuan et al., 2018) and *Mentha* are decorated with sugars (Brahmi et al., 2017; Guedon and Pasquier, 1994; Guvenalp et al., 2015; Mohammad Hosein Farzaei et al., 2017;

Pereira and Cardoso, 2013) and newly formed metabolites are subjected to glycosylation (Dong et al., 2016; Dong et al., 2013). In plants, glycosylation is catalyzed by uridine diphosphate dependent glycosyltransferases (UGT), which constitutes a large family of enzymes that are involved in the biosynthesis of small molecule glycosides. They transfer carbohydrates from nucleotide-sugar donors (e.g. UDP-glucose, UDP-galactose, UDP-rhamnose, UDP-xylose, UDP-xylulose, UDP-glucuronide, and UDP-glucuronic acid) to acceptors (Huang et al., 2015; Singh et al., 2013), usually alcohols and acids but also amines and thiols producing *O*-glycoside, glucose esters, *N*-, and *S*-glycosides, respectively (Schwab et al., 2015b). The range of acceptor molecules, also called aglycons, extends from carbohydrates, antibiotics, sugars, lipids, proteins, nucleic acids, to other small molecules (Schwab et al., 2015b; Yonekura-Sakakibara and Hanada, 2011). Glycosylation is not restricted to molecules from endogenous or exogenous sources (Walter et al., 2000). The low substrate specificity of GTs allows them to not only glycosylate previously already known aglycons, but also novel, xenobiotic compounds from either exogenous (Pflugmacher et al., 2000) or endogenous sources (Bak et al., 1999). GTs show high catalytic efficacy and regio- and stereospecificity, which allow organisms to modulate the structure and function of secondary metabolites. (Bungaruang et al., 2013; Williams et al., 2008).

A UGT classification is available on the CAZy (CArbohydrate-Active EnZymes) website (http://www.cazy.org/GlycosylTransferases.html). Until now there are more than 105 GT families described in the CAZy database. The members of each family have the same three-dimensional fold while several of the UGT families, which were defined based on sequence similarities, have similar 3-D structures. It seems that 3-D structures are better conserved than sequences. Family 1 has the largest number of members and contains more than 15,000 sequences of prokaryotes and eukaryotes. Members of family 1 display a 44 amino acid C-terminal signature motif designated as the plant secondary product glycosyltransferase (PSPG)-box (Figure 6), which is involved in sugar donor binding (Schwab et al., 2015b).

Figure 6. The plant secondary product glycosyltransferase box (PSPG box).

Ten of those amino acids directly interact with the UDP-sugar. Since UGTs have the ability to change the stability, solubility and toxicity of natural products, they play a major role in detoxification of xenobiotics, metabolic homeostasis, and the biosynthesis, transport and storage of secondary metabolites (Bowles et al., 2006; Yonekura-Sakakibara and Hanada, 2011).

1.4 Structure of glycosyltransferases

In general, there are two major structural types, GT-A fold and GT-B fold, for nucleotide sugar-dependent enzymes, but a third one, called GT-C was found for the soluble domains of lipid phosphosugar-dependent GTs (Lairson et al., 2008), and a forth, GT-D, was identified recently (Liang et al., 2015). In the protein data bank (https://www.rcsb.org/), crystal structures of 40 GTs with GT-A fold, 58 with GT-B fold and 2 members of the GT-C fold are available. GT-D was found for the crystal structure of a glucosyltransferase participating in the biosynthesis of bacterial O-glycans (Liang et al., 2015). The GT-A fold is composed of an open twisted β-sheet, which is surrounded by α-helices on both sides. The overall architecture of the GT-A fold looks like two abutting Rossmann-like folds (Lairson et al., 2008), which are tightly associated with the central β-sheet (Breton et al., 2006). Furthermore, members of the GT-A superfamily have an Asp-X-Asp (DXD) amino acid motif, which binds a divalent metal ion, mostly Mn^{2+} or Mg^{2+} (Lairson et al., 2008; Liang et al., 2015). This is essential for the catalysis, since it is stabilizing the pyrophosphoryl group of the UDP sugar in the enzyme's active site (Hu and Walker, 2002). Plant GTs are inverting GTs and show a GT-B fold (Liang et al., 2015). This fold consists of two separate N- and C-terminal domains with a central β-sheet flanked by two α-helices each. These domains are less tightly associated and form a cleft in between (Breton et al., 2006; Lairson et al., 2008; Wang, 2009). The catalytic site is located in the cleft, which contains the nucleotide sugar donor that mainly interacts with the C-terminal domain

(Wang, 2009). The sugar acceptor mainly binds to the N-terminal domain (Osmani et al., 2009; Wang, 2009), forming several helices and loops. Thus, the N-terminal end between the different GTs is more variable, since GTs use only a few different sugar donors, while they convert a variety of acceptors (Kumar et al., 2012). The GT-C fold commonly consists of two domains which are a C-terminal globular domain and a N-terminal transmembrane domain (Liang et al., 2015). There is a DXD motive found in the first extramembrane loop, where probably the active site is located (Lairson et al., 2008; Liang et al., 2015).

1.5 Uridine-diphosphate dependent glycosyltransferases in *Nicotiana*

Although glycosylation is an important process in plant physiology, as it affects the biological activity of natural products due to dissolution, transport, stabilization, or inactivation of signalling molecules (Song et al., 2018), endogenous UGTs that acting on small molecules have rarely been analysed in *Nicotiana* species (Chong et al., 2002).

One exception are two highly similar tobacco genes *Togt1* and *2* (tobacco glucosyltransferase 1 and 2), which are induced by salicylic acid (SA), and during the hypersensitive response (HR) of tobacco to tobacco mosaic virus (TMV) (Chong et al., 2002; Fraissinet-Tachet et al., 1998; Gachon et al., 2004; Hino et al., 1982; Matros and Mock, 2004). These genes are highly similar to *IS5a* and *IS10a* (Horvath and Chua, 1996). HR is part of the defence mechanism of induced disease resistance in plants, which leads to the induction of several metabolic changes and the production of reactive oxygen species (ROS). *In-vitro* functional analysis of recombinant TOGT revealed that the protein can glucosylate a wide range of phenylpropanoids, in particular scopoletin (6-methoxy-7-hydroxycoumarin, Figure 2). In TMV infection, the antimicrobial scopoletin accumulated in tobacco leaves as its glucoside scopolin (Figure 2), which is accompanied by bright blue fluorescence under UV light in the tissues surrounding the necrotic lesions. The loss of function in transgenic tobacco plants suggested the participation of TOGT in glucosylating scopoletin after TMV infection (Chong et al., 2002). As closely related UGTs might also glucosylate scopoletin and be affected by antisense inhibition a gain-of-function method was performed. The results showed that the concentration of the glucoside in *Togt-*

overexpressing plants was 2 times higher than that of wild-type plants after inoculation with TMV. Necrosis occured faster in transgenic plants but there was no significant difference in viral content (Gachon et al., 2004). In the meanwhile, additional *Nicotiana* UGTs are known to catalyze scopoletin glucosylation (e.g. NtGT1a and 1b; (Taguchi et al., 2001). They are promiscuous enzymes and can also glucosylate naphthols and flavonoids (Taguchi et al., 2001; Taguchi et al., 2000). In addition, UDP-glucose:salicylic acid glucosyltransferase (NtGT) activity was confirmed in tobacco leaves inoculated with TMV, and genes encoding respective UGTs were characterized (Enyedi and Raskin, 1993; Lee and Raskin, 1999). The tobacco salicylic acid glucosyltransferase was also active against tuberonic acid (12-hydroxyjasmonic acid; (Seto et al., 2011) and was expressed after biotrophic and wounding stress. This indicated that NtGT has a dual function and is active against both tuberonic acid and salicylic acid.

1.6 Norisoprenoids

Norisoprenoids are volatile C9-C13 fragments produced by degradation of carotenoids and constitute important classes of natural flavor compounds (Figure 7).

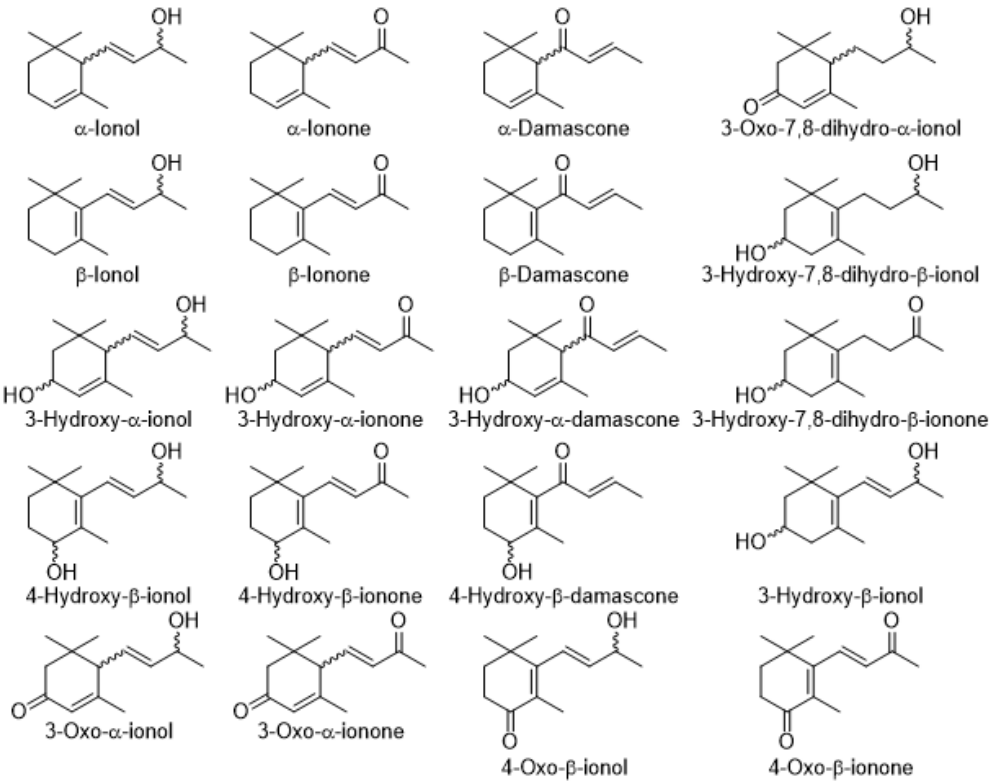

Figure 7. Selected structures of norisoprenoids

They have extremely low odor thresholds and are found in many higher plants, especially tobacco (Enzeil, 1985). Norisoprenoids can also be released from glycosidically bound norisoprenoids occurring in wine and many leaf tissues (Krammer et al., 1991; Schneider et al., 2001; Stahl-Biskup et al., 1993; Winterhalter, 1990; Winterhalter and Schreier, 1994). Well-known norisoprenoids are ionones and their regioisomers damascones (rose ketones; Figure 7). Ionon derivatives include not only natural derivatives (ionols, dihydro-ionones or irones), but also synthetic derivatives (isomethyl-α-ionone (isoraldeine), allyl-α-ionone, or n-methyl-α-ionone (raldein)), which are commercially even more important. All these compounds possess a megastigmane carbon skeleton (Winterhalter and Rouseff, 2002). Norisoprenoids have been studied in several plant species and tissues, as they are responsible for a wide range of biological properties. They show potential health benefits and contribute to the peculiar aroma properties of plant related products (Salvador et al., 2016). Some norisoprenoids have attractive sensory qualities, extremely low odor thresholds and thus have a high sensorial impact on fruit and flower aromas even at low levels, in the order of nanogram per liter of air (Brandi et al., 2011; Cataldo et al., 2016; Serra, 2015; Winterhalter and Schreier, 1994). They contribute, among others, to the aroma of tobacco, roses, tea, grapes and wine (Maldonado-Robledo et al., 2003). Norisoprenoids are produced by oxidative breakdown of carotenoids and xanthophylls catalyzed by carotenoid cleavage dioxygenases (CCDs; (Brandi et al., 2011; Ma et al., 2013; Ryle and Hausinger, 2002).

Carotenoids and most xanthophylls are a large family of fat-soluble isoprenoid compounds (mostly C40) that not only provide coloration (color range from yellow through to orange and red) (Choi et al., 2013; Walter and Strack, 2011; Yahyaa et al., 2013) to fruits and flowers but are the most widespread group of attractive natural pigments (Hirschberg, 2001; Ibdah et al., 2014; Moreno et al., 2016). They have multiple functions in photosynthesis (Busch et al., 2002; Heider et al., 2014; Lee and Schmidt-Dannert, 2002), plant defense, plant growth and development (Fernández-García et al., 2012). More than 750 types of carotenoids constitute an important precursor reservoir for the biosynthesis of bioactive compounds in bacteria, fungi, yeast, plants and even animals (Ibdah et al., 2014; Moreno et al., 2016; Takaichi, 2011). In general, carotenoids are well known for their high antioxidant activities due of their highly unsaturated backbones (Moreno et al., 2016; Stahl and Sies, 2003). Not

only can they quench reactive oxygen species they can also serve to sacrifice themselves under conditions of oxidative stress (Walter and Strack, 2011). Since carotenoids possess a series of highly conjugated double-bonds in the central chain, they are unstable and can be oxidatively cleaved in a site-specific way (Ma et al., 2013; Mein et al., 2011).

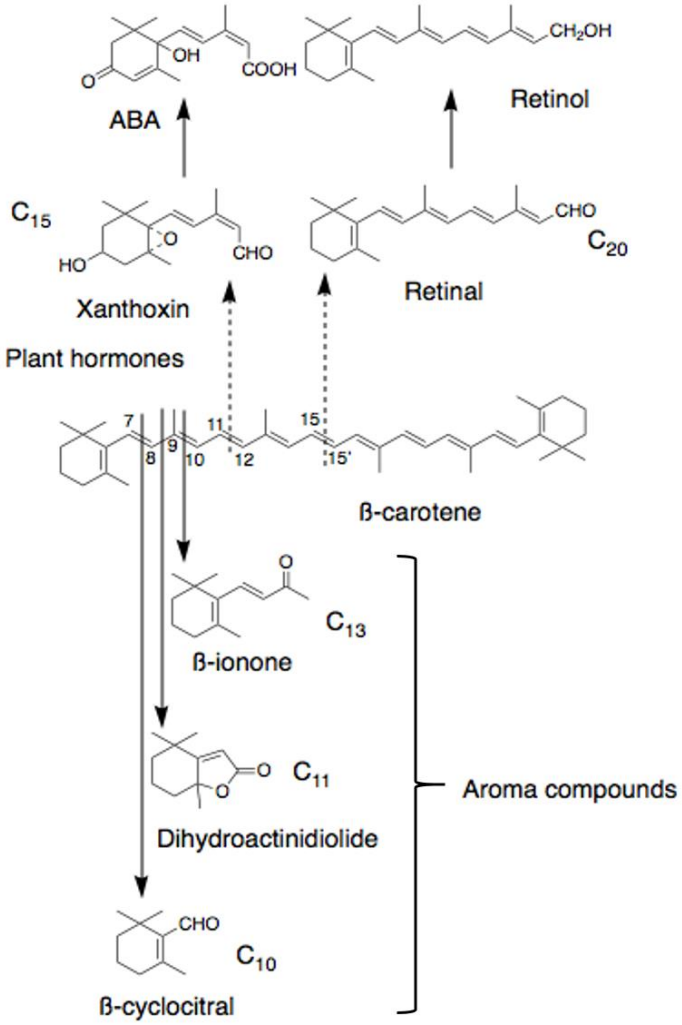

Figure 8. Carotenoid cleavage products and the biosynthetic route for abscisic acid (ABA) and retinol (Rodríguez-Bustamante and Sánchez, 2007).

The oxidative cleavage of carotenoids not only regulates their accumulation but also produces a number of apocarotenoids (Ma et al., 2013; Walter et al., 2010). Apocarotenoids are an important group of secondary metabolites that are often found in plants as glycosides. Some of the apocarotenoids, including norisoprenoids, have pleasant aroma and flavour properties (Winterhalter and Rouseff, 2002) and have attracted the attention of the food and chemistry industries. In higher plants,

apocarotenoids have important metabolic functions (Walter et al., 2010; Zhang et al., 2018) and include plant growth regulators such as the plant hormone abscisic acid (Yahyaa et al., 2015; Yahyaa et al., 2013; Zeevaart, 1988), pigments (bixin, crocin) (Bouvier et al., 2002; Frusciante et al., 2014; Rubio et al., 2008), aroma and scent compounds (α- and β-ionone), as well as signaling compounds (strigolactones) (Bouwmeester et al., 2007; Gomez-Roldan et al., 2008; Kohlen et al., 2012; Petitpierre et al., 2012; Zeevaart, 1988). After formation of the carbon chain by oxidative cleavage of carotenoids and xanthophylls, apocarotenoids can be further modified by enzymatic transformation (e.g. oxidation and dehydrogenation) or by acid-catalyzed conversions. The norisoprenoids are products of the oxidative cleavage at the 9,10 bonds of carotenoids and xanthophylls such as astaxanthin, β-carotene, lutein and zeaxanthin (Winterhalter and Rouseff, 2002; Rodríguez-Bustamante et al., 2005). Tobacco leaves are rich in lutein, which can be degraded during air-curing of the leaves to ionones and their derivatives, such as megastigmatrienones and β-damascenone, all of them are typical components of tobacco aroma (Burton and Kasperbauer, 1985; Maldonado-Robledo et al., 2003; Sánchez-Contreras et al., 2000)

In many plant tissues, numerous secondary metabolites, including C13-norisoprenoids, are glycosylated and accumulate as non-volatile odorless glycosides (Winterhalter and Schreier, 1994). C13-norisoprenoid glycosides play an important role as flavour precursors, but in some cases, also physiological activities have been reported (Berger, 2007; Winterhalter and Schreier, 1994). These abundant glycosidically bound compounds can be hydrolyzed during processing of the plant tissue to generate volatile aroma compounds. As norisoprenoid glycosides are aroma precursors that have been neglected over a longer period, studies on the structural elucidation and reactivity of these natural products have been intensified in recent years. (Winterhalter and Schreier, 1994).

Carotenoid-derived aroma compounds have been detected in leaf products (e.g. tea, tobacco, and mate) but also in many vegetables (melon and tomato). They have been found in fruits (apple, grapes, passionfruit, quince, nectarine, and starfruit), spices (saffron and red pepper), essential oils, and other sources such as coffee, seaweed, oak wood, wine, rum, and honey (Crupi et al., 2010; Kaiser, 1993; Saini et al., 2015; Villa-Ruano et al., 2017; Vinas et al., 2012; Winterhalter and Rouseff, 2002). In most of the cases, the levels of glycosidically bound apocarotenoids exceed the

concentration of the free metabolites considerably (Berger, 2007; Gui et al., 2015; Yuan and Qian, 2016). Tobacco (*Nicotiana tabacum*) is one of the most abundant sources of carotenoid degradation products, with nearly 100 components being identified (Enzell, 1985; Winterhalter and Rouseff, 2002). However, mint has not yet been analyzed for apocarotenoids.

1.7 Aim of the thesis

Due to the multitude of plant secondary metabolites found in tobacco and mint leaves and the very limited number of biochemically characterized UGTs in *Nicotiana* and *Mentha* species we decided to functionally characterize UGTs in *N. benthamiana* and *M. x piperita*. Specific tasks were as follows

- select candidate genes from transcriptome databases (*N. benthamiana* and *M. x piperita*) due to their high expression levels in leaves
- isolate full-length genes from plant tissues (*N. benthamiana* and *M. x piperita*)
- try to transform *Escherichia coli* with the full-lengh *UGT* genes for recombinant UGT production
- produce and purify recombinant UGTs
- perform qualitative substrate screening by liquid chromatography-mass spectrometry (LC-MS) with more than 40 metabolites
- perform quantitative substrate screening by UDP-Glo™ assay with selected substrates
- determine kinetics for selected UGTs and selected substrates
- perform agroinfitration experiments with selected *UGT*s for functional characterization
- test enzymatic activity of protein extracts obtained from agroinfiltrated leaves
- perform targeted and untargeted LC-MS analysis on selected agroinfiltrated leaves to identify natural substrates not included in the substrate screening
- identify the natural glycosides produced by the studied UGT

2. Material and Methods

2.1 Material

2.1.1 Chemicals

Commercial chemicals and solvents were purchased in analytical grade from the following companies: Sigma-Aldrich, Promega, Roth, Merk and Fluka, unless otherwise noted (Table 1). Hydroxycinnamoyl amides were obtained from Phytolab, Vestenbergsgreuth, Germany. Prof. Rita Bernhardt (Institut für Biochemie der Universität des Saarlandes) kindly provided hydroxylated C13 apocarotinoids produced by whole-cell P450 monooxygenase biotransformations.

Table 1. List of used chemical (not including the substrates).

Chemical	Formula	MW [g mol^{-1}]	Company
Acetic acid	$C_2H_4O_2$	60.05	Carl ROTH
30% Acrylamide, Rotiphorese® Gel 30	C_3H_5NO	71.08	Carl ROTH
Agarose	$C_{12}H_{18}O_9$	306.27	Sigma-Aldrich
Ammonium persulfate (APS)	$(NH_4)_2S_2O_8$	228.2	Carl ROTH
Ampicillin sodium salt	$C_{16}H_{18}N_3NaO_4S$	397.39	Carl ROTH
Brilliant blue G	$C_{47}H_{48}N_3NaO_7S_2$	854.02	Sigma-Aldrich
5-Bromo-4-chloro-3-indoly phosphate (BCIP) (Na-salt)	$C_8H_4BrClNO_4PNa_2$•$1.5H_2O$	397.46	Carl ROTH
Chloramphenicol	$C_{11}H_{12}Cl_2N_2O_5$	323.15	Carl ROTH
dNTP (mixed A+T+D+C)			PROMEGA
N,N-Dimethylformamide (DMF)	C_3H_7NO	73.09	Carl ROTH
Ethanol	C_2H_5OH	46.07	Merck
Ethylenediamine tetraacetic acid (EDTA)	$C_{10}H_{14}N_2Na_2O_8$•$2H_2O$	372.24	Merck
L-Glutathione reduced	$C_{10}H_{17}N_3O_6S$	307.33	Carl ROTH
Glycin	$C_2H_5NO_2$	75.07	Carl ROTH
Isopropanol	C_3H_8O	60.1	Carl ROTH
Isopropyl β-D-1-thiogalactopyranoside (IPTG)	$C_9H_{18}O_5S$	238.3	Carl ROTH
Magnesium chloride	$MgCl_2$	95.21	Carl ROTH
Magnesium sulfate	$MgSO_4$	120.31	Carl ROTH
Methanol	CH_3OH	64.7	Carl ROTH

Milk powder			Carl ROTH
Nitro-blue tetrazolium (NBT)	$C_{40}H_{30}Cl_2N_{10}O_6$	81.65	Carl ROTH
Phosphoric acid	H_3PO_4	97.99	Sigma-Aldrich
Potassium chloride	KCl	74.56	Carl ROTH
Potassium dihydrogen phosphate	KH_2PO_4	136.09	Carl ROTH
Sodium chloride	NaCl	58.44	Carl ROTH
Sodium dihydrogen phosphate dihydrate	$NaH_2PO_4 \cdot 2H_2O$	156.01	Carl ROTH
Sodium dodecyl sulfate (SDS)	$C_{12}H_{25}NaO_4S$	288.36	Carl ROTH
Tetramethylethylendiamin (TEMED)	$C_6H_{16}N_2$	116.21	Carl ROTH
Tris	$C_4H_{11}NO_3$	121.15	Carl ROTH
Tryptone			Carl ROTH
Tween 20			Carl ROTH
Uridine 5´-diphosphoglucose disodium salt (UDP-glucose)	$C_{15}H_{22}N_2Na_2O_{17}P_2$	610.27	Sigma-Aldrich
X-Gal	$C_{14}H_{15}BrClNO_6$	408.6	Carl ROTH
Yeast extract			Carl ROTH

2.1.2 Plant material

Peppermint (*M. x piperita*) and tobacco plants (*N. benthamiana*) used for the isolation of the UGT genes were cultured at room temperature and in a growth chamber maintained at 22 ± 2 °C with a 16 h light, 8 h dark photoperiod and a light intensity of 70 ± 10 µmol m^{-2} s^{-1} respectively. For over-expression and molecular analysis, leaves were agroinfiltrated with viral vectors and harvested 7 d and 10 d after treatment.

2.1.3 Primer

Primers were used for PCR (clone) and quantitative Real-Time PCR (qRT-PCR) reactions (Table 2). *Actin* and *IS* (*interspacer gene*) were used as qRT-PCR internal reference (*Actin* was used for the analysis of *MpUGTs* in different mint tissues and *IS* was used for the analysis of *UGTs* transcript levels after agroinfiltration).

Table 2. List of primers. fw = forward, rv = reverse. OVC= overexpression vector construction.

UGTs	Direction	Sequence (5'-3')	Purpose	Restriction site
UGT709C6	fw	CGCGGATCCATGAGGTCTGAAGAAGGAAAAG	PCR	BamHI
	rv	ATAGTTTAGCGGCCGCTCAACCTACCAATGACTTAATATAC	PCR	NotI
UGT86C10	fw	CGCGGATCCATGGGAGAAATAGAGAAAAATC	PCR	BamHI
	rv	ATAGTTTAGCGGCCGCTCATACTTTTGTTGCACGAAC	PCR	NotI

UGT708M1/2	fw	CGGGATCCATGAGTAAATCGGAAAAC	PCR	BamHI
	rv	ATTTGCGGCCGCTCACTTTCTCTTGAATGA	PCR	NotI
UGT709C7/8	fw	CGGGATCCATGAGGTCTGAAGAAGGA	PCR	BamHI
	rv	ATTTGCGGCCGCTCAAACTACCAATGACTT	PCR	NotI
UGT72B35	fw	CGGGATCCATGGCGGAAACTGCTATA	PCR	BamHI
	rv	CCCTCGAGTCAATTGTTTAACACCTT	PCR	XhoI
UGT72AX1	fw	CGGGATCCATGGACATATCTACAACA	PCR	BamHI
	rv	CCCTCGAGTCAACCACACAATGACTG	PCR	XhoI
UGT72AY1	fw	GAAGATCTATGGATAGCTCACAACTT	PCR	BglII
	rv	CCCTCGAGTTACAACTCTCTGCTCCG	PCR	XhoI
UGT85A73	fw	CGGGATCCATGGGTTCCATTGGTGCT	PCR	BamHI
	rv	CCCTCGAGTTAATGTTTGGACGAAAG	PCR	XhoI
UGT73A25	fw	CGGGATCCATGGGTCAGCTCCATATT	PCR	BamHI
	rv	CCCTCGAGTTAATGTCCAGTGGAACT	PCR	XhoI
UGT85A74	fw	CGGGATCCATGGGTTCTGTTGAAGGG	PCR	BamHI
	rv	CCCCCGGGCTACTCCAGTAGCCTCTC	PCR	SmaI
UGT73A24	fw	CGGGATCCATGGGTCAGCTCCATTTT	PCR	BamHI
	rv	ATTTGCGGCCGCTTAATGATCAGTAGAACT	PCR	NotI
UGT71AJ1	fw	CGGGATCCATGAGCAAATTAGAGCTA	PCR	BamHI
	rv	ATTTGCGGCCGCTCAATTCCAGGAATCAAG	PCR	NotI
UGT72B34	fw	CGGGATCCATGGCGGAAACTGCTATA	PCR	BamHI
	rv	ATTTGCGGCCGCTCAATTGTATAACACCTT	PCR	NotI
UGT709Q1	fw	CGGGATCCATGGACCATCCCTCTCCT	PCR	BamHI
	rv	ATTTGCGGCCGCTTATTCAATGCAATTAGA	PCR	NotI
MpGT86b	fw	CGGGATCCATGGCGGCGACCTTGAAA	PCR	BamHI
	rv	GCGTCGACTCACTGCGCTCTCCTGCA	PCR	SalI
NbGTfc1	fw	CGGGATCCATGGAAGAAATCACCAGC	PCR	BamHI
	rv	CCCTCGAGTTAATATGTAAACTCATT	PCR	XhoI
NbGTms6	fw	CGGGATCCATGAGTACTTCTCAGCTA	PCR	BamHI
	rv	CCCCCGGGTTATTTAACTAGCTCCAT	PCR	SmaI
NbGTms7	fw	CGGGATCCATGGCGGAAACTCCAATA	PCR	BamHI
	rv	CCCCCGGGTCAATGGGCCAGCCCATT	PCR	SmaI
UGT709C6	fw	CGGGATCCAGATGAGGTCTGAAGAAGGA	OVC	BamHI
	rv	CCAAGCTTTCAACCTACCAATGACTT	OVC	HindIII
UGT86C10	fw	CGAGCTCATGGGAGAAATAGAGAAA	OVC	SacI
	rv	GCGTCGACTCATACTTTTGTTGCACG	OVC	SalI
UGT708M1	fw	CGGGATCCAGATGAGTAAATCGGAAAAC	OVC	BamHI
	rv	CCAAGCTTTCACTTTCTCTTGAATGA	OVC	HindIII
UGT72AY1	fw	GGGGTACCATGGATAGCTCACAACTT	OVC	KpnI
	rv	GCGTCGACTTACAACTCTCTGCTCCG	OVC	SalI
UGT73A25	fw	CGAGCTCATGGGTCAGCTCCATTTT	OVC	SacI
	rv	GCGTCGACTTAATGTCCAGTGGAACT	OVC	SalI
UGT73A24	fw	CGAGCTCATGGGTCAGCTCCATATT	OVC	SacI
	rv	GCGTCGACTTAATGATCAGTAGAACT	OVC	SalI
UGT709C6	fw	CCTTCATCATCTCCGATTTCAGCCACC	qRT-PCR	

	rv	GAAAGTCATCAGGCCATCAGCGACGT	qRT-PCR
UGT86C10	fw	CAGCTCGAGATTCGGGACTCGACATA	qRT-PCR
	rv	GAAGGTCCCAATGGTACCCCAAGGTAT	qRT-PCR
UGT708M1/2	fw	GCATCAAACGCCTAGAATTCCGCCT	qRT-PCR
	rv	GGAGATGAGAGAGAGAGGCCATGAGAG	qRT-PCR
UGT72AY1	fw	CGTGAAGCCTTGCCCAAAAT	qRT-PCR
	rv	GGATCCACCACGTCATCAGG	qRT-PCR
UGT73A25	fw	GCAAGAACCACTGGAACAGC	qRT-PCR
	rv	CAAACGGAGACACCTGGGTT	qRT-PCR
UGT73A24	fw	TGCCGCCCTAATTGTCTTGT	qRT-PCR
	rv	CTGTCTCTTCCCCAGATCGC	qRT-PCR
Actin	fw	CTACGAAGGCTACGCACTCC	qRT-PCR
	rv	GCAATGTAGGCCAGCTTCTC	qRT-PCR
IS	fw	ACCGTTGATTCGCACAATTGGTCATCG	qRT-PCR
	rv	TACTGCGGGTCGGCAATCGGACG	qRT-PCR

2.2 Methods

2.2.1 Transcriptomic analysis

Putative *UGT* sequences in *N. benthamiana* were extracted from the transcriptome database of the Centre for Tropical Crops and Biocommodities at the Queensland University of Technology (Brisbane, Australia; http://benthgenome.qut.edu.au/, accessed May 15th 2017; version 6.1). The PSPG sequence motif, characteristic for UGTs, of *VvGT14* (XM_002285734) from grape (*Vitis vinifera*) and *AdGT4* (AIL51400) from kiwi (*Actinidia deliciosa*) were used as the reference sequences for the tblastn search. Thirteen UGT nucleotide sequences (*NbGTfc1, UGT72B35, UGT72AX1, UGT72AY1, UGT85A73, UGT73A25, UGT85A74, NbGTms6, NbGTms7, UGT73A24, UGT71AJ1, UGT72B34,* and *UGT709Q1*) were chosen according to their total transcript abundances, predicted functions, amino acid sequence consensus, and their expression levels in leaves (Supplemental Figure S1). Nucleotide and amino acid sequence analyses were performed using Geneious (http://www.geneious.com/).

Similarly, in order to detect putative *UGTs* in *Mentha x piperita* (MpGTs), a database research was performed using the transcriptome data from the Mint Genomics Resource (MGR) at Washington State University (http://langelabtools.wsu.edu/mgr/home). Five candidate genes *MpGT86b, UGT709C6, UGT709C7/8, UGT708M1/2* and *UGT86C10* were chosen as they are highly expressed in leaf tissue and their full-length nucleotide sequences could be deduced from the transcriptomic data set.

Furthermore, their translated amino acid sequences were analyzed for the PSPG (putative secondary plant glycosyltransferase) motif and their expression in the leaves of the plant were verified.

Based on the nucleotide sequences of the *UGTs* and restriction sites within the coding sequences, primers for ligation into the pGEX-4T1 vector were designed (Table 2).

2.2.2 Cloning and construction of expression plasmids

Total RNA was isolated from *M. x piperita* and *N. benthamiana* leaves by RNeasy plant mini kit (QIAGEN, Hilden, Germany) and cetyltrimethylammonium bromide (CTAB) extraction (Liao et al., 2004), respectively, and then treated with Moloney Murine Leukemia Virus (M-MLV) Reverse Transcriptase (Promega) containing DNase I (Fermentas, St. Leon-Rot, Germany) and oligo(dT) primers for reverse transcription into cDNA. The transcribed cDNA was used as a template for the PCR reaction, and all PCR reactions were carried out in a total reaction volume 30 µl. The procedure was carried out at 98 °C for 2 minutes, one cycle; at 98 °C for 30 sec, at 55 °C for 30 sec, at 72 °C for 1 min, 35 cycles; at 72 °C for 10 minutes, one cycle, the final temperature was keep at 8 °C, using appropriate primers (Table 2). After extraction of the correct DNA fragments using the PCR Clean-up Gel Extraction Kit (Macherey-Nagel), the DNA fragments and the vector DNA were digested with the same restriction enzymes and ligated into the pGEX-4T-1 vector. The recombinant plasmids (pGEX-4T1-*UGTs*) were transformed into *E. coli* NEB 10β. After colony PCR and restriction enzyme digestion analysis, positive plasmids were sequenced and stored as cryostock cultures at −80 °C.

2.2.3 Heterologous protein expression

Protein expression was performed with *E. coli* BL21 (DE3) pLysS containing the pGEX-4T-1 vector and the *UGT* sequence. A pre-culture was prepared by adding 2 µl of the cryostock culture to 10 ml LB liquid medium containing 100 µg/ml ampicillin and 34 µg/ml chloramphenicol and the culture was incubated overnight at 37 °C and 160 rpm. The following day, two different harvest cultures were prepared: a 50 ml harvest culture for subsequent crude protein extraction and a 400 ml harvest culture for protein purification. For both, aliquots of the overnight pre-culture were diluted to 1:100 with LB medium containing 100 µg/ml ampicillin and 34 µg/ml chloramphenicol. Cultures were incubated at 37 °C and 160 rpm for 2-3 h, until the optical density OD_{600} reached

0.6. Protein expression was induced by adding isopropyl-β-D-thiogalactopyranoside (IPTG) at a final concentration of 0.2 mM, and cells were incubated at 18 °C and 180 rpm for at least 20 h. The 50 ml culture was centrifuged at 4 °C and 8,000 rpm for 20 min and the pellet resuspended in 5 ml of 2 mM Na-phosphate buffer pH 8.0 followed by centrifugation at 4 °C and 8,000 rpm for 10 min. The pellet was subjected to a freeze thaw cycle, resuspended in 2 ml of 2 mM 2 Na-phosphate buffer, pH 8.0 and sonicated (Sonopuls HD 2070 homogenizer) for 6 cycles, 30 sec each cycle, with 10% power and 30 sec pause in between. The supernatant was collected by centrifugation at 8,000 rpm and 4 °C for 10 min and stored at −20 °C. The 400 ml culture was centrifuged at 5,100 rpm and 4 °C for 20 min and the pellet resuspended in 30 ml 1x phosphate-buffered saline (PBS) buffer (pH 7.3) and centrifuged at 5,100 rpm and 4 °C for 10 min. The pellet was subjected to a freeze thaw cycle, resuspended in 10 ml 1x PBS buffer (pH 7.3) and the cells disrupted by sonication (10 cycles with 15% power). The suspension was centrifuged at 13,200 rpm and 4 °C for 30 min. The glutathione-S-transferase (GST)-fusion proteins were purified with a GST Bind resin (Novagen, Darmstadt, Germany) following the manufacturer's instructions. After 2 h the proteins were eluted and quantified (Bradford, 1976). The recombinant proteins were verified by SDS-PAGE and Western blot using anti-GST antibody and goat anti-mouse IgG fused to alkaline phosphatase. Proteins were visualized by colorimetric detection of alkaline phosphatase using 5-bromo-4-chloro-3-indolyl-phosphate and nitroblue tetrazolium.

2.2.4 Enzyme activity assay by LC–MS

The recombinant proteins were assayed for glycosylation activity with different substrates and the products were identified by LC-MS (Table 3). The reaction was performed in 50 µl of 100 mM Tris-HCl buffer (pH 7.5) with 1 mM UDP-glucose, 600 µM substrate (all the substrate were dissolved in dimethyl sulfoxide (DMSO)) and 50 µl crude protein, at 30 °C and 400 rpm, for 17 h in the dark. The reaction was stopped by heating 10 min at 75 °C, centrifuged at room temperature (RT) and 14,800 rpm for 10 min, twice. Fifty µl of the clear supernatant was used for LC-MS analysis.

Samples were analyzed on an Agilent 6340 HPLC, which consisted of a capillary pump and a variable wavelength detector. The column was a LUNA C18 100A 150 x 2 mm (Phenomenex). LC was performed with the following binary gradient system: solvent A, water with 0.1% formic acid; and solvent B, methanol with 0.1% formic acid. The

gradient program used was as follows: 0–3 min 100% A to 50% A / 50% B; 3-6 min 50% A / 50% B to 100% B; 6–14 min hold 100% B; 14–14.1 min 100% B to 100% A; 14.1–25 min hold 100% A. The flow rate was 0.2 ml/min. Attached to the LC was a Bruker esquire 3000plus mass spectrometer with an ESI interface that was used to record the mass spectra. The ionization voltage of the capillary was 4,000 V and the end plate was set to –500 V. MS spectra were recorded in alternating polarity mode and nitrogen was used as nebulizer gas at 30 p.s.i. and as dry gas at 330 °C and 9 l/ min (Ring et al., 2013). Data were analyzed with Data Analysis 5.1 software (Bruker Daltonics).

Table 3. Diagnostic ions and wavelengths used for the detection of glucoside products by LC-MS formed by UGTs.

	Substrate	Diagnostic ions	*m/z*	Wavelength
1	Carvacrol	[M+HCOO]-	357	210
2	Thymol	[M+HCOO]-	357	210
3	Menthol	[M+HCOO]-	363	210
4	Isomenthol	[M+HCOO]-	363	210
5	Neomenthol	[M+HCOO]-	363	210
6	Eugenol	[M+HCOO]-	371	210
7	Raspberry ketone	[M+HCOO]-	371	210
8	2-Phenylethanol	[M+HCOO]-	329	210
9	Geraniol	[M+HCOO]-	361	210
10	Citronellol	[M+HCOO]-	363	210
11	Linalool	[M+HCOO]-	361	210
12	Terpineol	[M+HCOO]-	361	210
13	Nerolidol	[M+HCOO]-	429	210
14	Farnesol	[M+HCOO]-	429	210
15	Maltol	[M+H]+	289	280
16	Furaneol	[M+HCOO]-	335	280
17	trans-2-Hexenol	[M+HCOO]-	307	210
18	cis-3-Hexenol	[M+HCOO]-	307	210
19	1-Octene-3-ol	[M+HCOO]-	335	210
20	1-Hexanol	[M+HCOO]-	309	210
21	1-Octanol	[M+HCOO]-	337	210
22	1-Decanol	[M+HCOO]-	365	210
23	1-Dodecanol	[M+HCOO]-	393	210
24	Isorhamnetin	[M+HCOO]-	523	210
25	Galangin	[M-H]-	431	280
26	Naringenin	[M+H]+	435	280
27	7,3-Dihydroxyflavone	[M+H]+	417	210
28	Quercetin	[M+H]+	465	280
29	α-Ionol	[M+HCOO]-	401	280
30	β-Ionol	[M+HCOO]-	401	280

31	3-Oxo-α-ionol	[M+HCOO]-	415	280
32	Retinol	[M+HCOO]-	493	280
33	FMT(Furanmethanethiol)	[M+HCOO]-	321	280
34	Hydroquinone	[M+HCOO]-	317	280
35	Kaempferol	[M–H]-	447	280
36	Scopoletin	[M+HCOO]-	399	280
37	Mandelonitrile	[M+HCOO]-	340	280
38	S-Perillyl alcohol	[M+HCOO]-	359	210
39	Benzyl alcohol	[M+HCOO]-	315	280
40	Mandelic acid	[M+HCOO]-	359	280
41	α-Bisabolol	[M+HCOO]-	429	280
42	Lavandulol	[M+HCOO]-	361	210
43	Borneol	[M+HCOO]-	361	210
44	Eucalyptol	[M+HCOO]-	361	210
45	L-Carveol	[M+HCOO]-	359	210
46	Fenchyl alcohol	[M+HCOO]-	361	210
47	4-Carvomenthenol	[M+HCOO]-	361	210
48	Ethyl 4-hydroxy-3-methoxy-cinnamate	[M+HCOO]-	429	210
49	Tyramine	[M+HCOO]-	344	210
50	trans-Ferulic acid	[M+HCOO]-	401	210
51	p-Coumaric acid	[M+HCOO]-	371	210
52	Caffeic acid	[M+Na]+	365	210
53	n-Caffeoyl-O-methyl tyramine	[M+H]-	476	280
54	N-p-trans-Coumaroyl tyramine	[M+H]-	446	280
55	N-trans-Feruloyl tyramine	[M+H]-	476	280

2.2.5 Kinetic assay

The UDP-Glo™ Glycosyltransferase Assay (Promega, Mannheim, Germany) was used to determine the kinetic parameters of UGTs according to the manufacturer's instruction. The UDP-Glo™ assay is specific for enzymes that use UDP-sugars as an activated sugar donor. During the glycosylation reaction, equal amounts of UDP and glycoside are released. A UDP Detection Reagent (UDR) is added to convert UDP into ATP, which is generating a light signal in a luciferase reaction. The luminescence signal can be detected by a microplate reader and correlated with the UDP concentration and thus with the glycoside formed.

The enzymatic reactions were carried out in 50 mM Tris HCl (pH 7.5), 100 µM UDP-glucose, 100 µM substrate (dissolved in DMSO), and purified protein (100 µl in total). For the blank reaction, 1 µl DMSO was added instead of the substrate. Triplicates were performed for every measurement. The reaction was started by the addition of

UDP-glucose and immediately incubated at 30 °C for 20 min. The reaction was stopped by the addition of 5 µl of UDR and incubated for 60 min at room temperature in the dark, followed by measurement of luminescence using a CLARIOstar Microplate-reader (BMG Labtech, Ortenberg, Germany). To maximize the enzyme activity, the optimal reaction conditions were determined for each UGT using the UDP Glo™ assay. Each reaction was carried out at least twice. The optimal protein amount was determined using 0.25, 0.5, 1, 2, 3, 4, and 6 µg of purified proteins (Table 4, Table 5). The optimal pH was evaluated by testing three different kind of buffers in a range of pH 4.0-11.5, citric acid buffer (pH 4.0, 5.0, 5.5, and 6.0), sodium phosphate buffer (pH 6.0, 6.5, 7.0, 7.5, and 8.0), and Tris-HCl (pH 7.5, 8.0, 8.5, 9.0, 9.5, 10.0, 10.5, 11.0 and 11.5). The incubation time was examined in a range of 5–30 min with 5 min intervals. Different incubation temperatures of 15–60 °C in 5 °C steps were tested. A UDP calibration curve was generated and used for the UDP Glo™ kinetic analysis. The data was fitted to the Michaels-Menten equation using a nonlinear regression (Solver) to calculate K_M and V_{max}.

LC-MS analysis was used to determine the kinetic parameters of UGT72AY1. Enzyme assays were performed in triplicates in 100 mM Tris-HCl buffer (pH 7.5) containing 1 mM UDP-glucose, 10–1200 µM substrate (dissolved in DMSO), and 1 µg purified protein in a total volume of 200 µl. The reaction was started by adding UDP glucose and incubated immediately at 40 °C with continuous shaking at 400 rpm in the dark for 40 min. Subsequently, the reaction was stopped by heating 10 min at 75 °C. The sample was centrifuged at RT and 14,800 rpm for 10 min, twice. Fifty µl clear supernatant was taken for LC-MS analysis.

Table 4. The optimal reaction conditions determined with UDP-Glo™ for UGTs from mint.

	UGT709C6	**UGT86C10**	**UGT708M1**
Substrate	Carvacrol*[1]	Geraniol*[2]	Naringenin*[3]
Amount (µg)	0.5	1	2
Incubation time (min)	10	10	10
Temperature (°C)	45	35	40
pH	Tris 9.5	Phos 7	Phos 8

*[1] 1-Decanol was used for the determination of the optimal temperature and pH

*[2] 1-Dodecanol was used for the determination of the optimal temperature and pH

*[3] 2-Phenylethanol was used for the determination of the optimal temperature and pH

Tris: Tris-HCl buffer; Phos: Phosphate buffer

Table 5. The optimal reaction conditions determined with UDP-Glo™ for UGTs from tobacco.

	UGT 72B35	UGT 72AX1	UGT 72AY1	UGT 85A73	UGT 73A25	UGT 73A24	UGT 71AJ1	UGT 72B34
Substrate	Carvacrol	Carvacrol	Benzyl alcohol*	Perillyl alcohol	α-Ionol	Scopoletin	Carvacrol	Carvacrol
Amount (µg)	0.5	0.5	0.5	0.5	1	0.5	0.5	0.5
Incubation time (min)	10	10	10	10	10	10	10	15
Temperature (°C)	45	40	40	45	40	40	40	45
pH	7.0	8.0	7.5	8.5	8.5	7.5	8.0	8.0

* Perillyl alcohol and scopoletin were used for the determination of the optimal temperature and pH, respectively

2.2.6 Tissue specificity analysis of MpUGTs with qRT-PCR

Quantitative real-time PCR analysis was performed on *M. x piperita* root, lateral stem, main stem, young leaf, mature leaf, old leaf and flower. After grinding to fine powder in liquid nitrogen with a mortar and pestle, RNA was extracted with RNeasy plant mini kit (QIAGEN, Hilden, Germany) according to the manufacturer's protocol. One µg RNA was used for reverse transcription. The qRT-PCR analysis was carried out with the SensiFAST™ SYBR Hi-ROX Kit (Bioline, Luckenwalde, Germany) following the manufacturer's instructions. Each reaction consisted of 5 µl 2 x SYBR, 1 µl cDNA and a final primer concentration of 400 nM in a total volume of 10 µl. *Actin* was used as an internal control for normalization (Table 2). The reactions were run on a StepOnePlus™ system (Applied Biosystems™, Waltham, MA, USA). The thermal cycling conditions were 2 min at 95 °C followed by 40 cycles of 5 sec at 95 °C, 10 sec at 59 °C and 1 min at 72 °C, ending in a melting curve detection of 15 sec at 95 °C, 1 min at 60 °C, and 15 sec at 95 °C. Subsequently, 2% agarose gel electrophoresis was applied to confirm that the desired amplicon had been generated and the relative expression level was analyzed by applying a modified $2^{\Delta\Delta\text{-Ct}}$ method taking reference genes and gene specific amplification efficiencies into account (Hellemans et al., 2007).

2.2.7 Construction of plasmids for transient over-expression

The full-length open reading frames (ORF) of *UGT709C6, UGT86C10, UGT708M1/M2, UGT72AY1, UGT73A24* and *UGT73A25* were amplified by PCR from the plasmid pGEX-4T1-*UGTs* using the OVC (overexpression vector construction) primers listed in Table 2. The PCR products were double digested with restriction enzymes and ligated into the pICH11599 vectors (Marillonnet et al., 2005; Marillonnet et al., 2004), which were digested with the same restriction enzymes as for the inserts to obtain pICH11599-*UGTs.* The recombinant genes were subjected to sequencing to confirm the sequence of the inserts.

2.2.8 Agroinfiltration into *N. benthamiana* leaves

Various modules are delivered to plant cells using a viral vector system (Marillonnet et al., 2005; Marillonnet et al., 2004). Three pro-vectors, pICH17388, pICH14011 and pICH11599 were used. Since the gene of interest cannot be expressed by the 3' module (pICH11599) alone, because the construct lacks a subgenomic promoter, the 5' module (pICH17388) and the 3' module (pICH11599) must be assembled inside a plant cell with the help of site-specific recombinase (pICH14011) to produce a fully functional RNA replicon. The vectors pICH11599, pICH17388, pICH14011, pICH11599-UGT709C6, pICH11599-UGT86C10, pICH11599-UGT708M1, pICH11599-UGT72AY1, pICH11599-UGT73A25 and pICH11599-UGT73A24 were separately transformed into the *Agrobacterium tumefaciens* strain AGL0 using the freeze-thaw technique (Höfgen and Willmitzer, 1988) and integrity was confirmed by PCR. Overnight-grown *Agrobacterium* cultures were centrifuged at 5,000 g for 5 min and resuspended in infiltration solution (10 mM 2-N-morpholino-ethanesulfonic acid, (MES), pH 5.5, containing 10 mM $MgSO_4$). *Agrobacterium* strains carrying each pro-vector module were mixed and infiltrated into *N. benthamiana* using a syringe without a needle as described (Huang et al., 2010) . *UGT709C6, UGT86C10, UGT708M1, UGT708M2, UGT72AY1, UGT73A24* and *UGT73A25* were separately infiltrated into *N. benthamiana*. The empty pICH11599 vector was also infiltrated into *N. benthamiana* as a negative control. The infiltrated plants grew under the same condition, and the leaves were harvested 7 days and 10 days after the infiltration.

2.2.9 Enzyme extraction and analysis

N. benthamiana leaves infiltrated with *Agrobacterium* and wild type leaves were ground to fine powder in liquid nitrogen with a commercial blender (Personal Blender PB 250, Tribest, Buxtehude, Germany). The powder (100 mg) was resuspended in 300 µl of protein extraction buffer (50 mM sodium phosphate buffer, pH 7.5, 5 mM β-mercaptoethanol, 10 mM EDTA and 0.1% Triton X-100). The homogenate was centrifuged at 13,400 rpm and 4 °C, for 10 min. Total protein content was determined by Bradford assay. The enzyme activity assay was performed in a reaction volume of 200 µl, which included 100 mM Tris-HCl buffer (pH 7.5), 500 µM UDP-glucose, 600 µM acceptor substrate, and 100 µl of crude protein extract from *N. benthamiana* leaves. The reaction was initiated by the addition of UDP-glucose, incubated at 30 °C with constant shaking for 1 or 2 h, and was stopped by heating at 75 °C for 10 min. Denaturated proteins were removed by centrifugation at 14,800 rpm and RT for 10 min, twice. Fifty µl of the solution was used for LC-MS analysis.

2.2.10 Metabolite analysis of agroinfiltrated leaves

Metabolites in individual *N. benthamiana* leaves were analyzed 7 d after agroinfiltration. The material was ground to a fine powder in liquid nitrogen and kept at -80 °C prior to analysis. For metabolite analysis, 500 mg powder was used and was prepared in triplicates for each UGT. A 250-µl aliquot of the internal standard solution (4-methylumbelliferyl-β-D-glucuronide and Biochanin A in methanol, each 0.2 mg/ml), and 250 µl methanol were added to 500 mg of powder, vortexed and sonicated for 10 min. The solution was centrifuged at 13,400 rpm and 4°C for 10 min. The residue was re-extracted with 500 µl methanol. Methanol was removed in a speed vacuum concentrator and the residue was redissolved in 60 µl of 50 % methanol. The clear supernatant was used for LC-MS analysis after additional centrifugation (13,400 rpm and 4°C for 20 min). The column was a LUNA C18 100A 150 x 2 mm (Phenomenex). A binary gradient system using water with 0.1% formic acid (solvent A) and methanol with 0.1% formic acid (solvent B) was performed as follows: 0–30 min 100% A to 50% A / 50% B; 30–35 min 50% A / 50% B to 100% B; 35–50 min hold 100% B; 50–55 min 100% B to 100% A; 55–65 min hold 100% A. The flow rate was 0.2 ml/min and UV spectra were recorded from 190–600 nm. For MS analysis an Esquire 3000 Plus Ion Trap Mass Spectrometer (Bruker Daltonic) using an ESI interface was attached (Ring et al., 2013).

2.2.11 Quantitative real-time PCR analysis of agroinfiltrated leaves

Quantitative real-time PCR analysis was performed on *N. benthamiana* leaves, 7 d (NbUGTs) and 10 d (MpUGTs) after agroinfiltration. The leaves were ground into a fine powder with liquid nitrogen and RNA was extracted with RNeasy plant mini kit (QIAGEN, Hilden, Germany) according to the manufacturer's protocol. One µg RNA was used for reverse transcription. The qRT-PCR was carried out with the SensiFAST™ SYBR Hi-ROX Kit (Bioline, Luckenwalde, Germany) following the manufacturer's instructions. *IS* was used as an internal control for normalization (Table 2). The reactions were performed to the chapter 2.2.6.

2.2.12 Establishment of aglycone library and activity assay

To identify the natural substrates of UGTs, 1 kg tobacco leaves were used to prepare a tobacco physiological aglycone library as a source of natural acceptor molecules. The extraction procedure is summarized in Figure 9. Preparative LC using a Jasco LC system (Jasco GmbH, Groß-Umstadt, Germany) yielded thirty LC fractions. The system consisted of two Jasco PU-2087 Plus pumps connected to a Jasco UV-2075 Plus variable wavelength detector set at 210 nm and an Advantec CHF122SC fraction collector (Tokyo Seisakusho Kaisha Ldt., Japan) with a Synergi 4u Fusion-RP 80, 25 cm x 21.5 mm column (Phenomenex, Aschaffenburg, Germany). A binary gradient system using water containing 0.1% formic acid (solvent A) and 100% methanol containing 0.1% formic acid (solvent B) was performed as follows: 0-2 min 100% A, 2–40 min 100% A to 100% B, 100% B for 40-50 min, 100% A for 50-60 min. The flow rate and injection volume was 7 ml/min and 420 µl, respectively. Fractions were collected for 1 min (corresponding to 7 ml fractions). A run lasted 30 min.

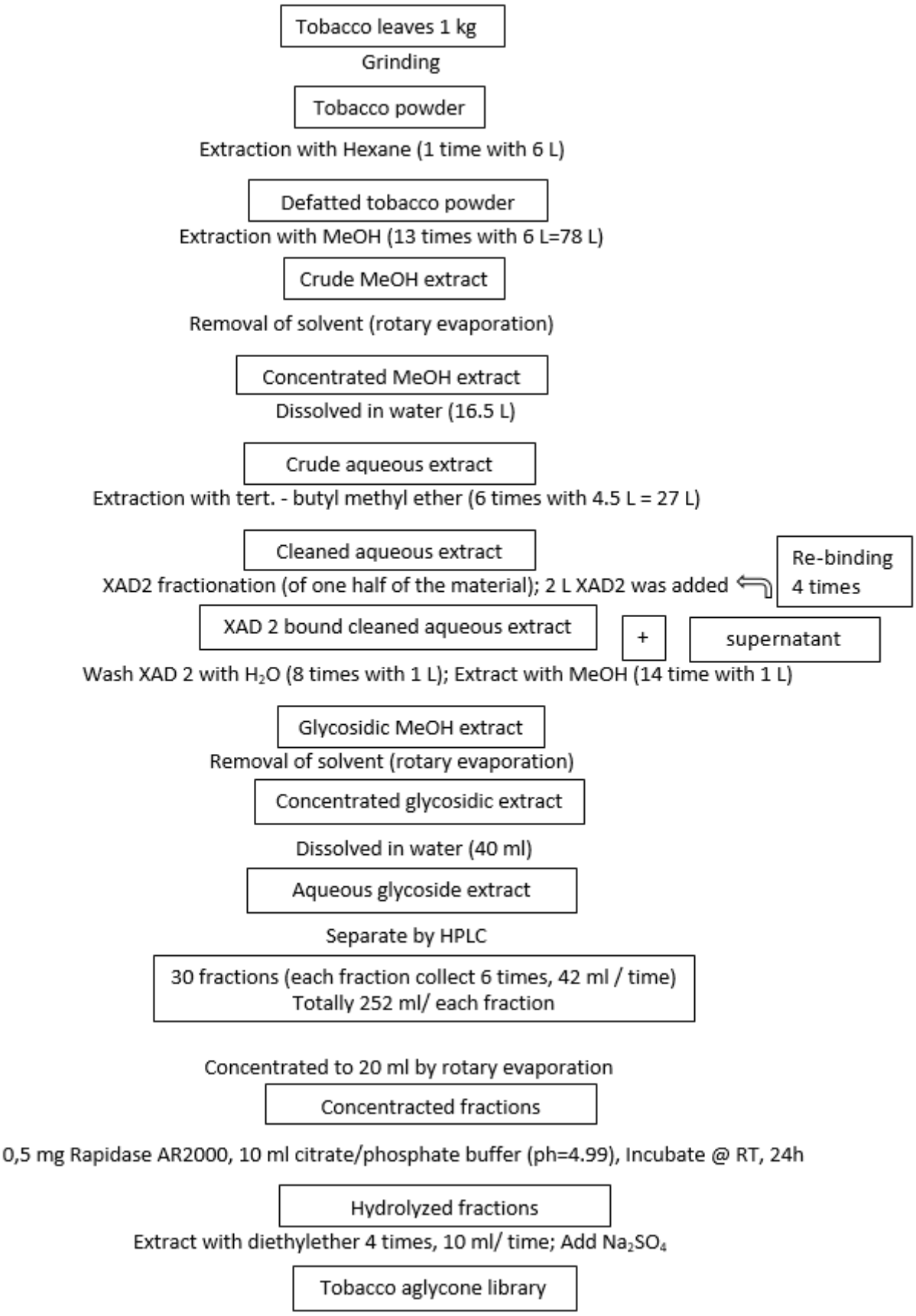

Figure 9. Preparation and screening of the tobacco aglycon library.

2.2.13 High resolution mass spectrometry

The system used for high resolution mass data was a Sciex TripleTOF 6600 mass spectrometer (Sciex, Darmstadt, Germany) connected to a Shimadzu Nexera X2 system (Shimadzu, Kyoto, Japan) operating in positive electrospray ionization mode. We are very grateful to AK Professor Thomas Hofmann (Lebensmittelchemie und Sensorik; Dr. Timo Stark) for using the device.

2.2.14 UDP-glucose hydrolase activity assay by UDP Glo™ and Glucose Glo™

In order to determine the hydrolase activity of UGT72AY1 and the ratio of the released amount of UDP and glucose, the UDP-Glo™ glycosyltransferase assay (Promega) and the Glucose-Glo™ assay (Promega) were performed side by side. The Glucose-Glo™ Assay couples glucose oxidation and NADH production with a bioluminescent NADH detection system. In this process, glucose dehydrogenase catalyzes the oxidation of glucose with concomitant reduction of NAD+ to NADH. In the presence of NADH, a reductase enzymatically reduces a pro-luciferin substrate to luciferin. Luciferin is detected in a luciferase reaction using Ultra-Glo™ rLuciferase and ATP, and the amount of light produced is proportional to the amount of glucose in the sample. The Glucose-Glo™ assay was used according to the manufacter's instruction.

2.2.15 UDP Glo™ and Glucose Glo™ calibration curve

To determine UDP-glucose hydrolase enzyme activity of UGTs the released amount of UDP and glucose was quantified. Therefore, UDP and glucose calibration curves were generated with known UDP and glucose concentrations (provided by the kits). The UDP and glucose dilutions were prepared in 50 mM Tris-HCl, pH 7.5 and 1x PBS buffer, pH 7.3, respectively. For the regular UDP-Glo™ assay, 5 µl UDP dilution was mixed directly with 5 µl UDP Detection Reagent (UDR), incubated in the dark at room temperature (RT), and the luminescence was measured after 60 min. For the modified UDP-Glo™ assay and Glucose-Glo™ assay, 5 µl Inactivation Solution (0.6 M HCl) (the volume ratio is 1:8) was added to 40 µl solution, shaken at 500 rpm, RT, for 5 min to stop the reaction, followed by adding 5 µl Neutralization Solution (1 M Tris base), RT, shaken at 500 rpm for 1 min. The mixtures can be stored at RT for up to 2 hours or at –20°C for longer storage. Before use, the products were thawn and sightly centrifuged. Then, 5 µl of the solution were added to 5 µl fresh UDR (UDP-Glo™) or GDR (Glucose-Glo™) reaction mix, in a 384 well plate, mixed while shaking the plate for 30-60 sec

and incubated in the dark at RT for 60 min. The measured Relative Luminescence Unit (RLU) was plotted against the known UDP or glucose concentration (calibration curves) and the calibration equations were calculated. The calibration equations were used to calculate the UDP and glucose amount and the enzyme activities.

3. Results

3.1 Selection of UGTs

3.1.1. *Mentha x piperita*

In order to detect putative *UGT* genes in *M. x piperita*, a database research was performed using the transcriptome data from the Mint Genomics Resource (MGR) at the Washington State University (http://langelabtools.wsu.edu/mgr/home) (Ahkami et al., 2015). Five putative candidate genes were chosen as they were highly expressed in leaf tissue and their full-length nucleotide sequences could be deduced from the transcriptomic data set. Six *UGTs* (two were obtained from the same putative candidate gene) were successful cloned and a protein sequence alignment of the encodes MpUGTs was performed with the Geneious program (http://www.geneious.com/; Figure 10). The sequences showed the characteristic features of a functional UGT of the CAZy family 1. These are the catalytically active amino acids His (Offen et al., 2006); consensus sequence position 23) and Asp (position 136), the PSPG box (Schwab et al., 2015a); position 374 to 417) and the GSS motif (Huang et al., 2018); position 485 to 487), except for UGT708M1 and UGT708M2, which lacked the catalytic Asp (Figure 10).

Table 6. Amino acids sequence identities of MpUGTs (%).

	UGT708M1	UGT708M2	UGT709C8	UGT709C7	UGT709C6	UGT86C10
UGT708M1	100	97	27	27	27	27
UGT708M2	97	100	27	27	27	28
UGT709C8	27	27	100	96	96	28
UGT709C7	27	27	96	100	97	28
UGT709C6	27	27	96	97	100	27
UGT86C10	27	28	28	28	27	100

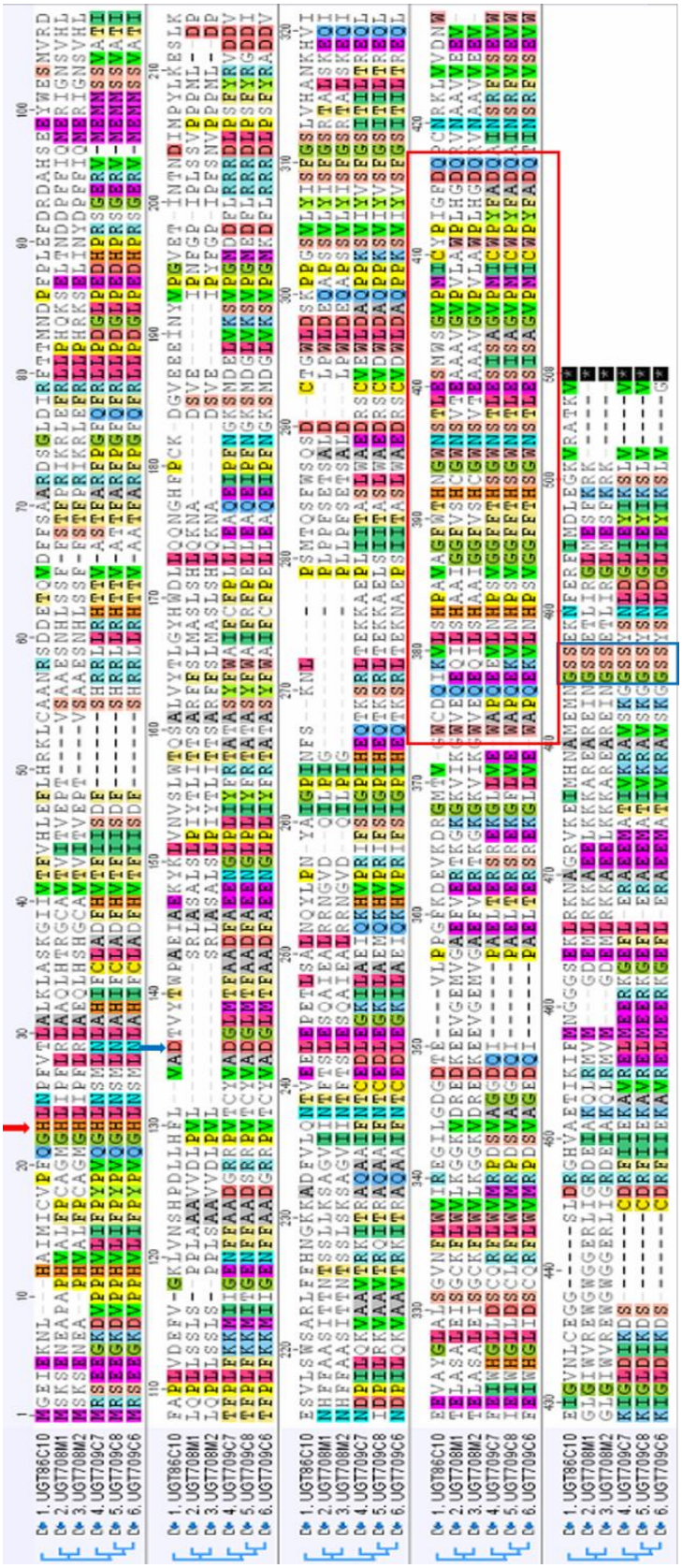

Figure 10. Amino acid sequence alignment of UGTs from *Mentha x piperita*. Red and blue arrows show the catalytically active His and Asp, respectively and the red and blue box the conserved PSPG box and GSS motif, respectively.

The protein sequences of UGT708M1/UGT708M2, UGT709C8/UGT709C7, UGT709C8/UGT709C6, and UGT709C7/UGT709C6 showed the highest amino acid sequence identities with 96.9%, 95.8%, 95.8%, and 97.3 respectively (Table 6).

3.1.2. *Nicotiana benthamiana*

To select putative UGT sequences from *N. benthamiana,* a BLAST search was performed in the transcriptome database (version 6.1) of the Centre for Tropical Crops and Biocommodities at the Queensland University of Technology (Brisbane, Australia, http://benthgenome.qut.edu.au/). The characteristic PSPG motif of VvGT14 (XM_002285734) and AdGT4 (AIL51400) are used as query sequences for tblastn searches. Thirteen putative UGT sequences were selected for characterization because of their total transcript abundance and high expression levels in leaves, root and flowers (Supplemental Figures S1). Ten NbUGT genes were successfully cloned. Protein sequence alignment of the encoded proteins was performed (Figure 11; Supplemental Figure S2) and a phylogenetic tree was constructed using the Neighbor-joining tree approach provided in the Geneious program (http://www.geneious.com/; Figure 12).

The sequences showed the characteristic features of a functional NbUGT of the CAZy family 1. They contain the catalytically active amino acids His (Offen et al., 2006); consensus sequence position 28) and Asp (position 142), the PSPG box (Schwab et al., 2015a); position 397 to 440) and the GSS motif (Huang et al., 2018); position 513 to 515), except for UGT709Q1 and UGT85A74, which lacked the catalytic His and the GSS motif, respectively (Figure 11). The selected *NbUGT* sequences are 1383 to 1470 base pairs long and encode proteins of 461 to 490 amino acids. The transcripts of the corresponding genes were mainly isolated from leaves (*UGT72B35*), stem (*UGT72AX1* and *UGT72AY1*), flower (*UGT85A73, UGT85A74*, and *UGT71J1*), callus/root/leaves (*UGT73A24, UGT73A25*, and *UGT709Q1*), and root (*UGT72B34;* Supplemental Figure S1). Phylogenetic analysis revealed the relationship of UGT73A24 and UGT73A25 with four salicylate-induced scopoletin UGTs from *N. tabacum* (Figure 12; Supplemental Figure S2; (Fraissinet-Tachet et al., 1998; Horvath and Chua, 1996) while UGT71AJ1 clustered with two UGTs from *N. tabacum* acting on naphthols, flavonoids and coumarins (Taguchi et al., 2001; Taguchi et al., 2000). The selected UGTs were only closely related to an UDP-glucose:salicylic acid UGT

characterized from *N. tabacum*, catalyzing also the glucosylation of cinnamic acid and benzoic acid derivatives (Lee and Raskin, 1999).

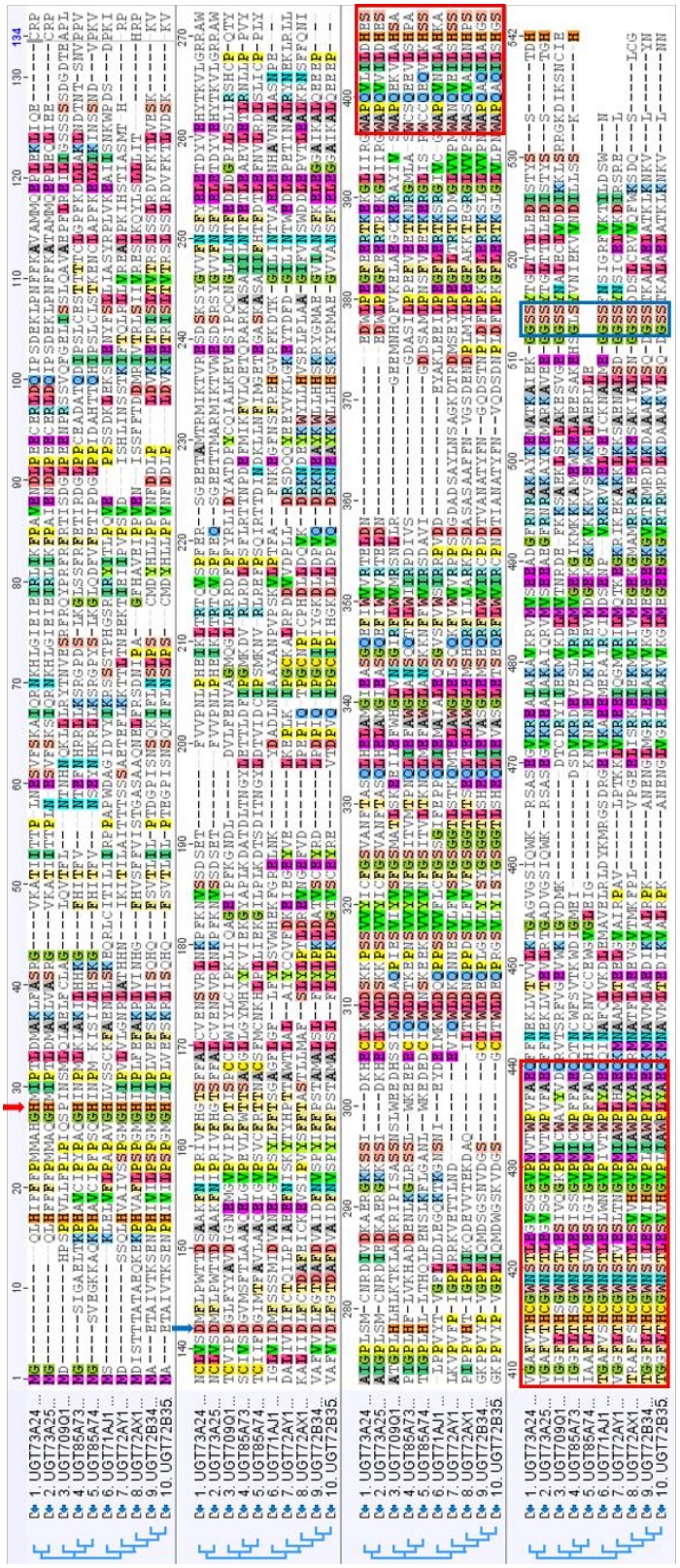

Figure 11. Amino acid sequence alignment of selected UGTs from *N. benthamiana.* Red and blue arrows show the catalytically active His and Asp, respectively and the red and blue box the conserved PSPG box and GSS motif, respectively.

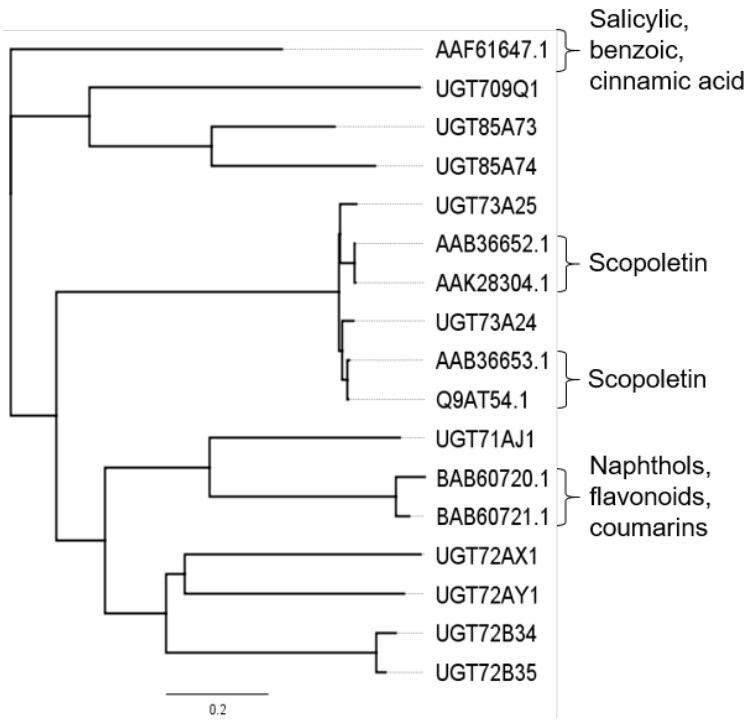

Figure 12. Phylogenetic tree of UGTs from *N. benthamiana* analysed in this study and biochemically characterized GTs from *N. tabacum*. Known substrates are shown. Default values of the Geneious program (http://www.geneious.com/) were used.

The protein sequences of UGT73A24/UGT73A25 and UGT72B34/UGT72B34 showed the highest amino acid sequence identities with 94% and 95%, respectively (Table 7).

Table 7. NbUGTs amino acids sequence identities (%).

	UGT 709Q1	UGT 71AJ1	UGT 72AX1	UGT 72AY1	UGT 72B34	UGT 72B35	UGT 73A24	UGT 73A25	UGT 85A73	UGT 85A74
UGT709Q1	100	19	21	22	21	20	23	24	33	32
UGT71AJ1	19	100	28	29	29	29	28	28	26	22
UGT72AX1	21	28	100	41	43	42	25	24	24	24
UGT72AY1	22	29	41	100	38	38	26	26	25	23
UGT72B34	21	29	43	38	100	95	27	26	23	24
UGT72B35	20	29	42	38	95	100	28	27	23	24
UGT73A24	23	28	25	26	27	28	100	94	26	24
UGT73A25	24	28	24	26	26	27	94	100	26	24
UGT85A73	33	26	24	25	23	23	26	26	100	58
UGT85A74	32	22	24	23	24	24	24	24	58	100

3.2 Cloning and expression of proteins in *E. coli*

For biochemical characterization of the encoded proteins, the *UGT* gene sequences were amplified using leaf cDNA from *Mentha x piperita* and *N. benthamiana*, respectively, as template and cloned into the pGEX-4T-1 expression vector containing an N-terminal glutathione S-transferase (GST-fusion) tag.

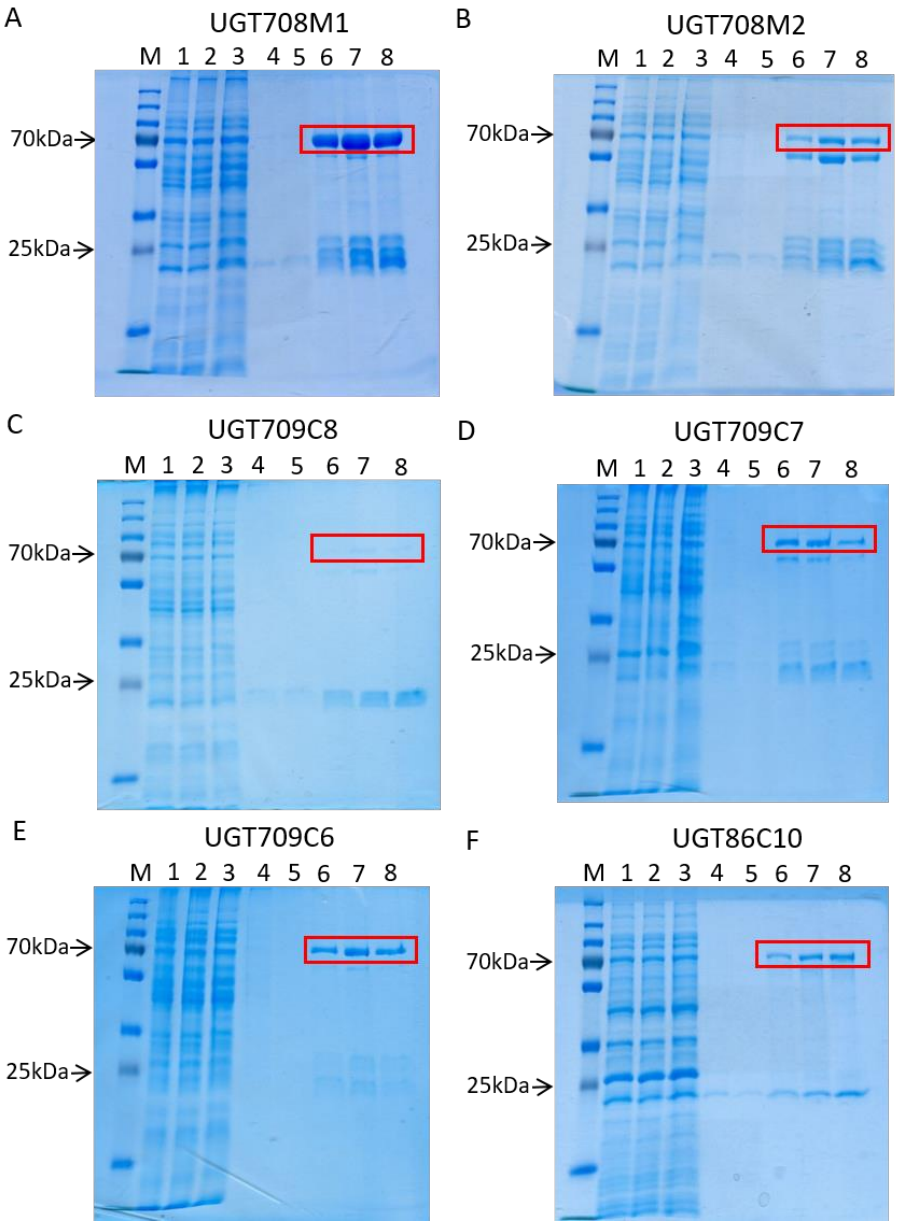

Figure 13. SDS-PAGE analysis of six recombinant UGTs from *Mentha x piperita*. Gel was stained with Coomassie Blue. M: marker proteins (PageRuler Plus Prestained Protein Ladder marker); 1 crude protein extract; 2 flow-through; 3 wash 1; 4 wash 2; 5 wash 3; 6 elution 1; 7 elution 2; 8 elution 3. Red boxes show the UGT-GST fusion proteins. **(A-F)** UGT708M1, UGT708M2, UGT709C8, UGT709C7, UGT709C6, and UGT86C10.

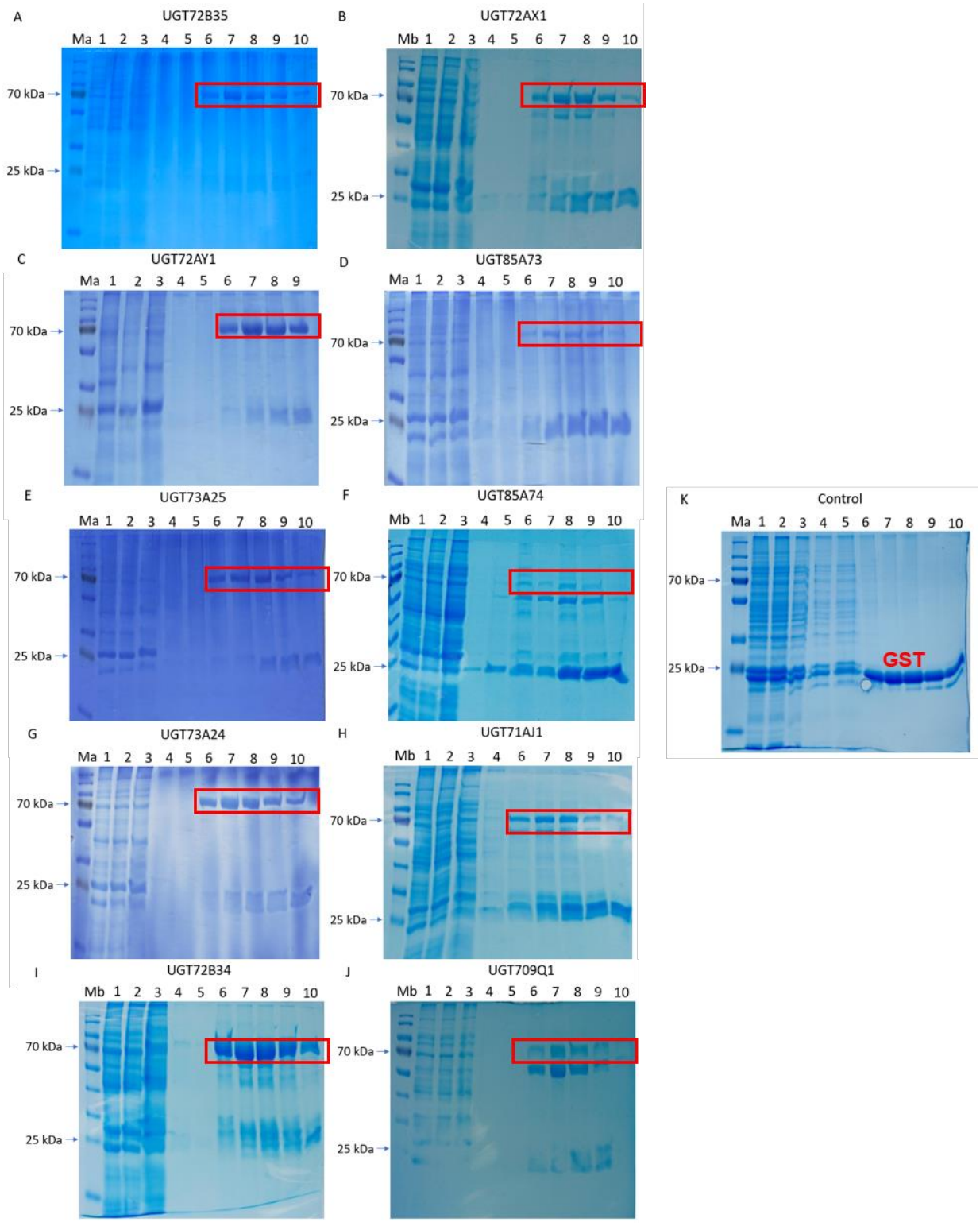

Figure 14. SDS-PAGE analysis of ten recombinant UGTs from *N. benthamiana* and an empty vector control. Gel was stained with Coomassie Blue. Ma: marker proteins (PageRuler Plus Prestained Protein Ladder marker), Mb: marker proteins (PageRuler Prestained Protein Ladder marker); 1 crude protein extract; 2 flow-through; 3 wash 1; 4 wash 2; 5 wash 3; 6 elution 1; 7 elution 2; 8 elution 3; 9 elution 4; 10 elution 5. GST glutathione S-transferase; red boxes show the UGT-GST fusion proteins. **(A-J)** UGT72B35, UGT72AX1, UGT72AY1, UGT85A73, UGT73A25, UGT85A74, UGT73A24, UGTAJ1, UGT72B34, UGT709Q1. **(K)** Empty vector control SDS-PAGE gel.

The fusion proteins were successfully generated in *E. coli* BL21 (DE3) pLysS, affinity purified and verified by SDS-PAGE (Figures 13 and 14). The SDS-PAGE analyses showed clear bands of fusion proteins at approximately 70-80 kDa in all elution fractions, whereas elution fractions 2 and 3 exhibited distinctly more intense bands than fractions 1 and 4. In addition, a band of approximately 27 kDa was visible for the GST protein and in some cases (UGT708M2, UGT709C7, UGT72AX1, UGT85A74, and UGT709Q1) protein bands at about 55 kDa pointed to untagged UGTs. Western blot analyses using an anti-GST antibody confirmed the production of UGT-GST fusion proteins.

3.3 Qualitative substrate screening by LC-MS

First, recombinant UGTs from *Mentha x piperita* and *N. benthamiana* were subjected to a substrate screening. The protein extract of each UGT was incubated with UDP-glucose as sugar donor and a variety of different potential acceptors. All MpUGTs were tested with 40 substrates, mainly aromatic compounds, aliphatic alcohols, terpenoids and phenols (Table 8). Twenty-six substrates were selected for the screening of the NbUGTs, which were known to occur naturally in *Nicotiana* species (e.g. 2-phenylethanol, 3-*cis*-hexenol, benzyl alcohol, kaempferol, scopoletin, and 3-oxo-α-ionol) and structural analogs including phenolic, branched chain, and aliphatic compounds, and a thiol (Table 9). The reaction products were analyzed by LC-MS and their structures confirmed by their MS and MS2 spectra (Table 3), relative retention time and by comparison with the spectral data of authentic reference material. The peak areas of the UGTs products were determined in the ion traces of their pseudo molecular ions, the highest value was set at 100% and the relative product levels produced by the other UGTs were determined (Tables 8 and 9).

The selected MpUGTs showed a narrow substrate tolerance, except for UGT86C10, which accepted 37 out of 40 potential substrates and converted them to glucosides. UGT708M1, UGT709C7, and UGT709C6 transformed only 10, 15 and 15 substrates out of 40, respectively. UGT709C8 and UGT708M2 showed no activity against any of the 40 potential substrates (Table 8). Although the protein sequences of UGT708M1 and UGT708M2 as well as UGT709C7 and UGT709C8 were highly similar, they showed distinct substrate preferences, indicating that the exchange of amino acids altered their function.

Table 8. Screening of potential MpUGT with 40 substrates. The reaction products were analyzed by LC-MS. The color code shows non-reactive substrate enzyme combinations in red (0%, no product detected by LC-MS) and increasing reactivities from white to green color (maximum activity in dark green corresponding to 100%).

Substrate	UGT 708M1	UGT 708M2	UGT 709C8	UGT 709C7	UGT 709C6	UGT 86C10
Carvacrol	0	0	0	100	58	0
Thymol	0	0	0	100	37	0
Menthol	0	0	0	6	4	100
Isomenthol	0	0	0	0	0	100
Neomenthol	0	0	0	100	44	72
Eugenol	0	0	0	4	2	100
Caffeic acid	100	0	0	42	34	46
Raspberry ketone	0	0	0	0	0	100
2-Phenylethanol	32	0	0	0	0	100
Geraniol	0	0	0	0	0	100
Citronellol	0	0	0	0	0	100
Linalool	0	0	0	0	0	100
Terpineol	0	0	0	0	0	100
Nerolidol	0	0	0	0	0	100
Farnesol	0	0	0	0	0	100
trans-2-Hexenol	0	0	0	0	0	100
cis-3-Hexenol	0	0	0	0	0	100
1-Octene-3-ol	0	0	0	17	8	100
1-Hexanol	0	0	0	0	0	100
1-Octanol	0	0	0	0	0	100
1-Decanol	0	0	0	0	0	100
1-Dodecanol	0	0	0	0	0	100
Isorhamnetin	42	0	0	0	0	100
7,3-Dihydroxyflavone	15	0	0	2	1	100
Maltol	29	0	0	0	17	100
Furaneol	0	0	0	0	2	100
α-Ionol	1	0	0	1	1	100
β-Ionol	0	0	0	14	9	100
3-Oxo-α-ionol	0	0	0	0	0	100
Galangin	100	0	0	0	0	39
Naringenin	9	0	0	2	0	100
Hydroquinone	0	0	0	0	0	0
Kaempferol	30	0	0	0	0	100
Scopoletin	4	0	0	23	14	100
Quercetin	0	0	0	0	0	100
Perillyl alcohol	0	0	0	1	0	100
Benzylalcohol	0	0	0	0	0	100
Lavandulol	0	0	0	9	4	100
Borneol	0	0	0	0	0	100
L-Carveol	0	0	0	12	3	100
converted substrates	10	0	0	15	15	37

Table 9. Screening of potential NbUGT with 26 substrates. The reaction products were analyzed by LC-MS. The color code shows non-reactive substrate enzyme combinations in red (0%, no product detected by LC-MS) and increasing reactivities from white to green color (maximum activity in dark green corresponding to 100%).

Substrates	UGT 71AJ1	UGT 72AX1	UGT 72AY1	UGT 72B35	UGT 72B34	UGT 73A24	UGT 73A25	UGT 85A73	UGT 85A74	UGT 709Q1
Retinol	0	0	0	0	0	0	0	0	0	0
Farnesol	0	0	21	0	0	100	37	5	0	0
α-Ionol	2	0	51	2	2	60	100	16	0	0
β-Ionol	2	3	49	2	1	76	100	24	0	0
2-Phenylethanol	0	0	56	0	0	59	26	100	0	0
Furanmethanethiol	0	0	0	0	0	0	0	0	0	0
Carvacrol	31	33	50	48	58	100	42	2	0	0
Geraniol	1	2	23	1	11	81	47	100	0	0
Hydroquinone	13	22	55	81	100	0	0	0	0	0
Kaempferol	87	18	92	100	71	24	37	5	0	0
Scopoletin	8	32	72	61	79	100	82	4	0	0
Mandelonitrile	0	4	0	0	0	0	0	100	0	0
3-cis-Hexenol	0	17	41	0	35	23	14	100	0	0
Perillyl alcohol	0	0	100	3	16	82	74	90	0	0
1-Octene-3-ol	0	25	55	2	13	56	33	100	0	0
Benzyl alcohol	10	31	32	44	100	0	0	83	0	0
Mandelic acid	0	0	0	0	0	0	0	0	0	0
α-Bisabolol	0	0	0	0	0	0	0	0	0	0
Lavandulol	2	19	33	1	16	100	73	30	0	0
Borneol	0	0	0	0	0	79	75	100	0	0
Carveol	14	29	46	5	26	25	11	100	0	0
Fenchyl alcohol	0	0	0	0	0	0	0	0	0	0
4-Carvomenthenol	0	0	0	0	0	0	0	100	0	0
Tyrosol	0	0	100	10	54	33	16	16	0	0
Myrtenol	1	5	29	3	32	37	58	100	0	0
3-Oxo-α-ionol	0	0	100	0	0	46	27	0	0	0
Converted substrates	11	13	18	14	15	17	17	19	0	0

All selected NbUGTs showed extensive substrate tolerance, with the exception of UGT85A74 and UGT709Q1, which did not convert any alcohol or thiol (Table 9). Twenty-one out of 26 potential substrates were converted to glucosides, while eight acceptors including geraniol, carvacrol, scopoletin, kaempferol, lavandulol, β-ionol, carveol, and myrtenol were glucosylated by all catalytically active UGTs. Only four alcohols (α-bisabolol, retinol, mandelic acid, and fenchyl alcohol) and the thiol furanmethanethiol remained untouched. UGT85A73 was an excellent universal enzyme of the eight active UGTs because it could glycosylate 19 different acceptors and showed the highest enzymatic activity against 9 acceptors (Table 9). In contrast, UGT85A74 and UGT709Q1 were ineffective. Since the two protein sequences lack

important features of UGTs - the GSS motif and catalytically active His in case of UGT85A74 and UGT709Q1, respectively - they apparently lost their catalytic activities.

3.4 Screening of UGTs with norisoprenoids

Since α- and β-ionol were efficiently glucosylted by six UGTs (UGT72AY1, UGT85A73, UGT73A25, UGT73A24, UGT86C10 and UGT709C6) analyzed in this study and one strawberry (*Fragaria x ananassa*) UGT (UGT73B24), recently characterized in our group, additional norisoprenoids should be tested as substrate for these UGTs. Prof. Rita Bernhardt (Institut für Biochemie der Universität des Saarlandes) kindly provided hydroxylated C13 apocarotinoids such as 3-hydroxy-α-ionol, 4-hydroxy-β-ionol, 3-hydroxy-α-ionone, 4-hydroxy-β-ionone, 3-hydroxy-α-damascone, and 4-hydroxy-β-damascone as crude products of a whole-cell P450 monooxygenase biotransformation. Only α-ionol, β-ionol and 3-oxo-α-ionol were available as pure substances. The reaction products were analyzed by LC-MS and the products were putatively identified by their MS and MS2 spectra and relative retention time in comparison with the substrates. The peak areas of monoglucosylated products were determined in the ion traces of their pseudo molecular ions $[M+Cl]^-$ and $[M+ HCOO]^-$, the highest value was set at 100% and the relative product levels produced by the other UGTs determined (Table 10).

Table 10. Norisoprenoid substrate screening. The reaction products were analyzed by LC-MS. The color code shows non-reactive substrate enzyme combinations in red (0%, no product detected by LC-MS) and increasing reactivities from white to green color (maximum activity in dark green corresponding to 100%).

substrates	UGT 72AY1	UGT 85A73	UGT 73A25	UGT 73A24	UGT 709C6	UGT 86C10	UGT7 3B24
3-Hydroxy-α-ionol	73	7	100	55	2	96	51
4-Hydroxy-β-ionol	27	2	100	90	9	81	36
3-Hydroxy-α-ionone	1	1	4	2	0	100	16
4-Hydroxy-β-ionone	6	2	67	12	4	100	36
3-Hydroxy-α-damascone	4	29	50	20	0	100	71
4-Hydroxy-β-damascone	0	15	9	0	43	100	0
α-Ionol	77	21	100	77	7	66	43
β-Ionol	51	26	100	86	23	57	25
3-Oxo-α-ionol	100	0	25	37	0	45	20

Glucosides of α-ionol and β-ionol were detected at ion traces *m/z* 391 and 401 representing $[M+Cl]^-$ and $[M+HCOO]^-$, respectively. The retention times of α-ionol glucoside and β-ionol glucoside were 11.9 min (Figure 15). Similarily, diastereomeric 3-oxo-α-ionol glucosides were detected at *m/z* 415 and 405, which eluted before 10.5 min (Figure 15). 3-Hydroxy-α-ionol monoglucoside and 4-hydroxy-β-ionol monoglucoside were visualized at ions traces *m/z* 407 $[M+Cl]^-$ and 417 $[M+HCOO]^-$ (Figures 16 and 17). The retention times of the diastereomeric 3-hydroxy-α-ionol monoglucosides and 4-hydroxy-β-ionol glucosides were 10.7 min and 11 min, respectively. Since the hydroxylated norisoprenoids used for the glucosylation assay were not pure, glucosides of the substrates and side products of the monooxygenase reaction were also found (Figures 16 and 17). As control, all substrates were also incubated with empty vector proteins. No glucoside was produced in the control samples.

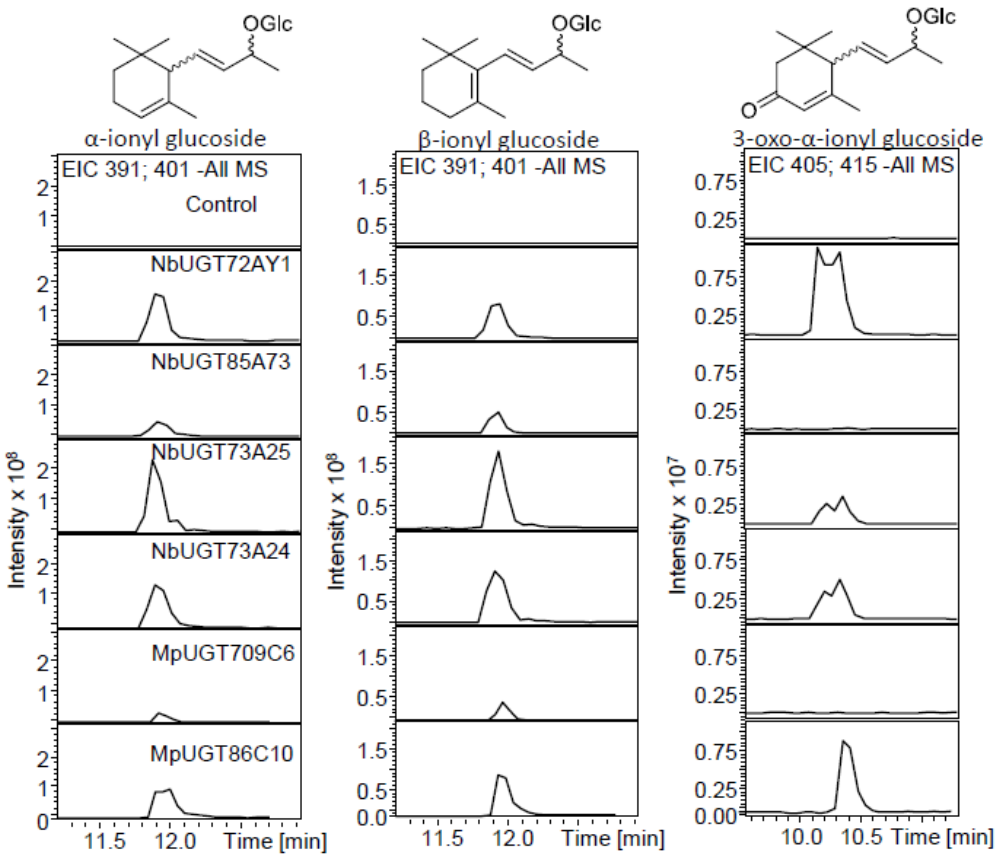

Figure 15. LC-MS analysis of glucosides produced from α-ionol, β-ionol and 3-oxo-α-ionol produced by selected UGTs. LC-MS ion traces at *m/z* 391 and 401 show α-ionol glucoside and β-ionol glucoside, while ion traces at *m/z* 405 and 415 show 3-oxo-α-ionol glucoside.

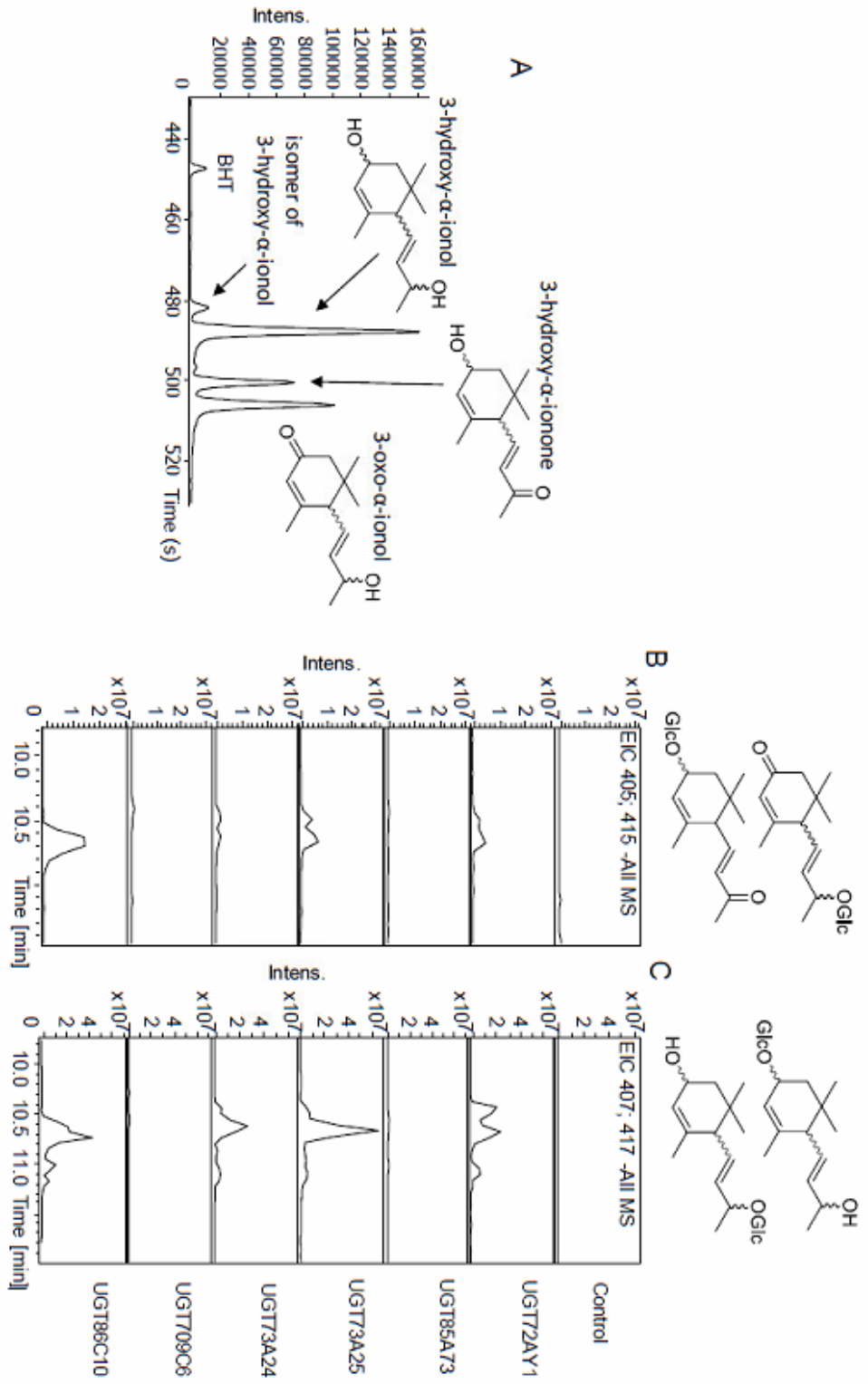

Figure 16. LC-MS analysis of monoglucosides of 3-hydroxy-α-ionol, 3-oxo-α-ionol, 3-hydroxy-α-ionone produced by selected UGTs (right, B), and GC-MS of the substrate mix (left, A) obtained by whole-cell P450 monooxygenase biotransformation. BHT butylated hydroxytoluene, LC-MS ion traces at *m/z* 405 and 415 show 3-hydroxy-α-ionone glucoside and 3-oxo-α-ionol glucoside and traces at *m/z* 407 and 417 show monoglucosides of 3-hydroxy-α-ionol.

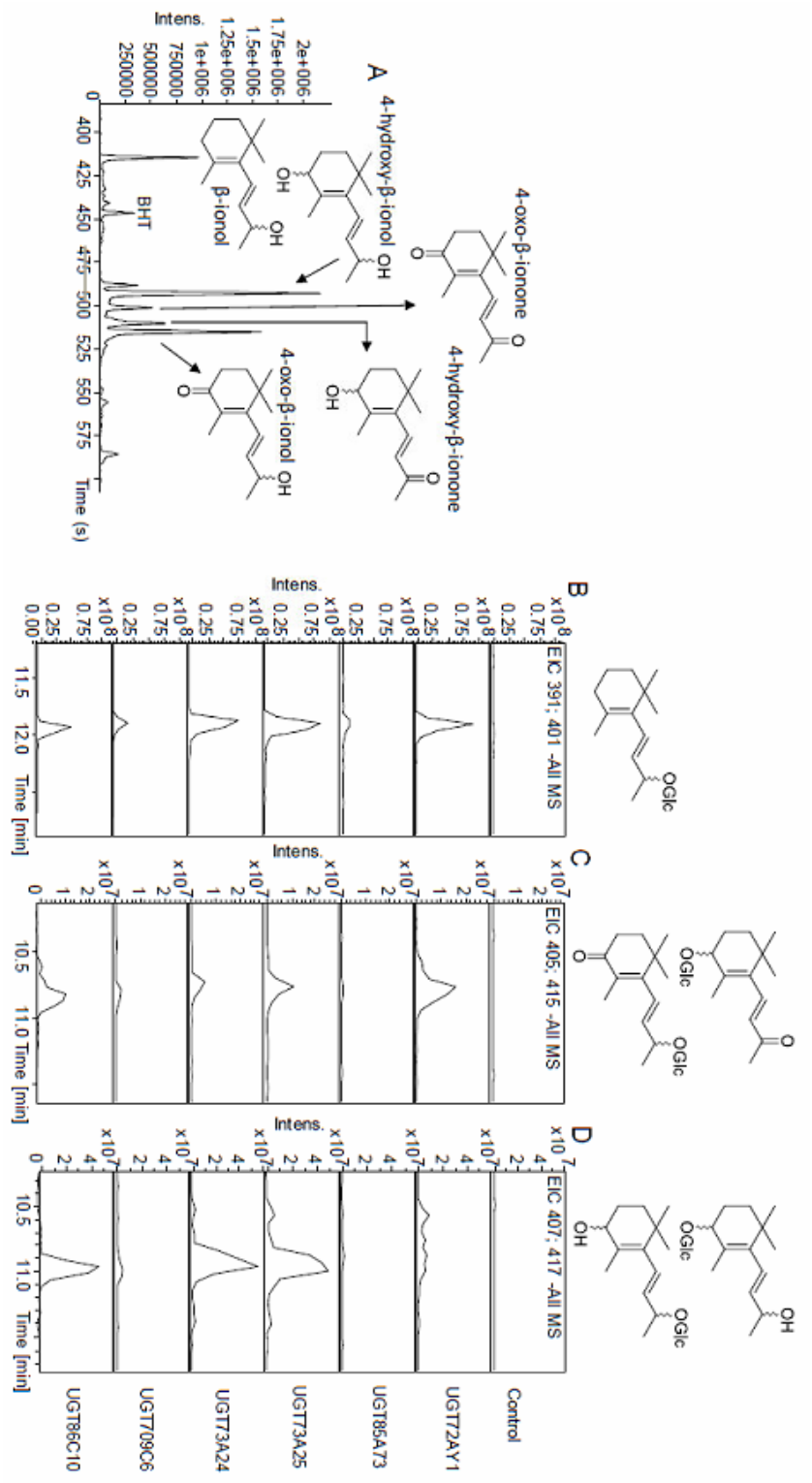

Figure 17. LC-MS analysis of monglucosides of β-ionol and 4-hydroxy-β-ionone, 4-oxo-β-ionol, and 4-hydroxy-β-ionol produced by selected UGTs (right B), and GC-MS of the substrate mix (left, A) obtained by whole-cell P450 monooxygenase biotransformation. BHT butylated hydroxytoluene, LC-MS ion traces at *m/z* 391 and 401 show β-ionol glucoside, ion traces at *m/z* 405 and 415 show 4-hydroxy-β-ionone and 4-oxo-β-ionol glucoside and ion traces at *m/z* 407 and 417 visualize 4-hydroxy-β-ionol glucosides.

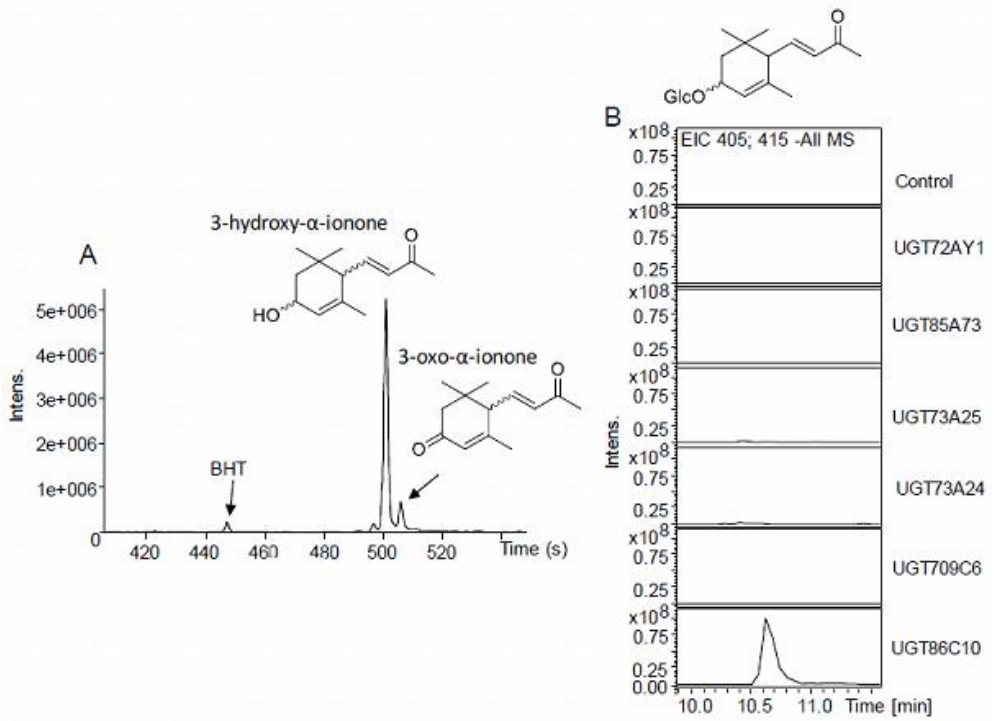

Figure 18. LC-MS analysis of monglucosides of 3-hydroxy-α-ionone produced by selected UGTs (right B), and GC-MS of the substrate mix (left, A) obtained by whole-cell P450 monooxygenase biotransformation. BHT butylated hydroxytoluene, LC-MS ion traces at *m/z* 405 and 415 show 3-hydroxy-α-ionone glucoside.

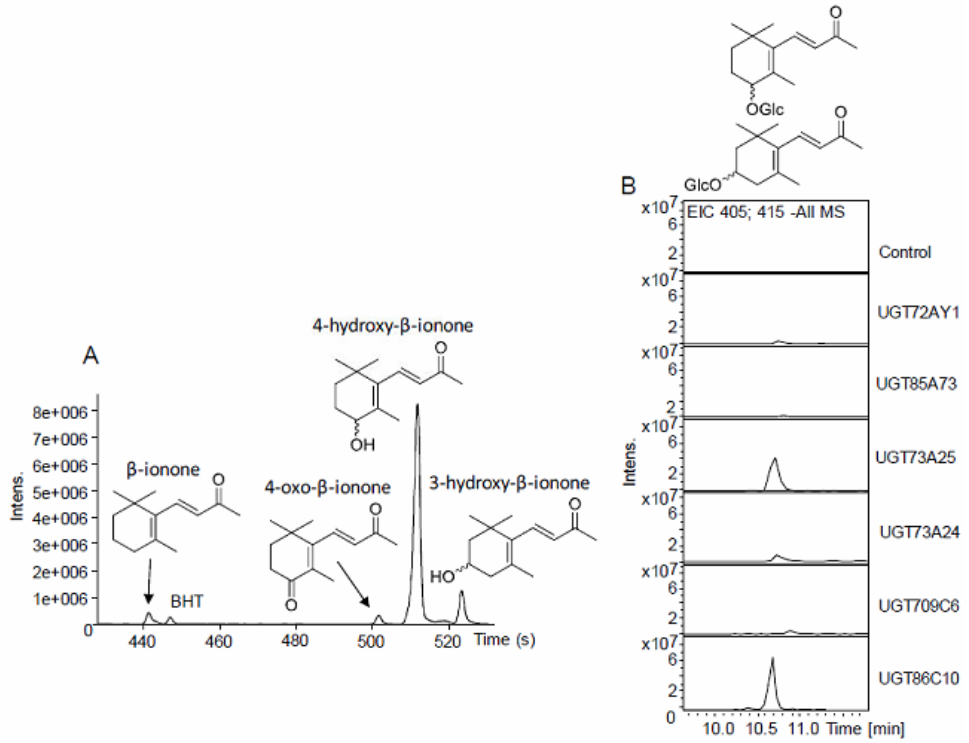

Figure 19. LC-MS analysis of monglucosides of 4-hydroxy-β-ionone produced by selected UGTs (right B), and GC-MS of the substrate mix (left, A) obtained by whole-cell P450 monooxygenase biotransformation. BHT butylated hydroxytoluene, LC-MS ion traces at m/z 405 and 415 show 4-hydroxy-β-ionone glucoside.

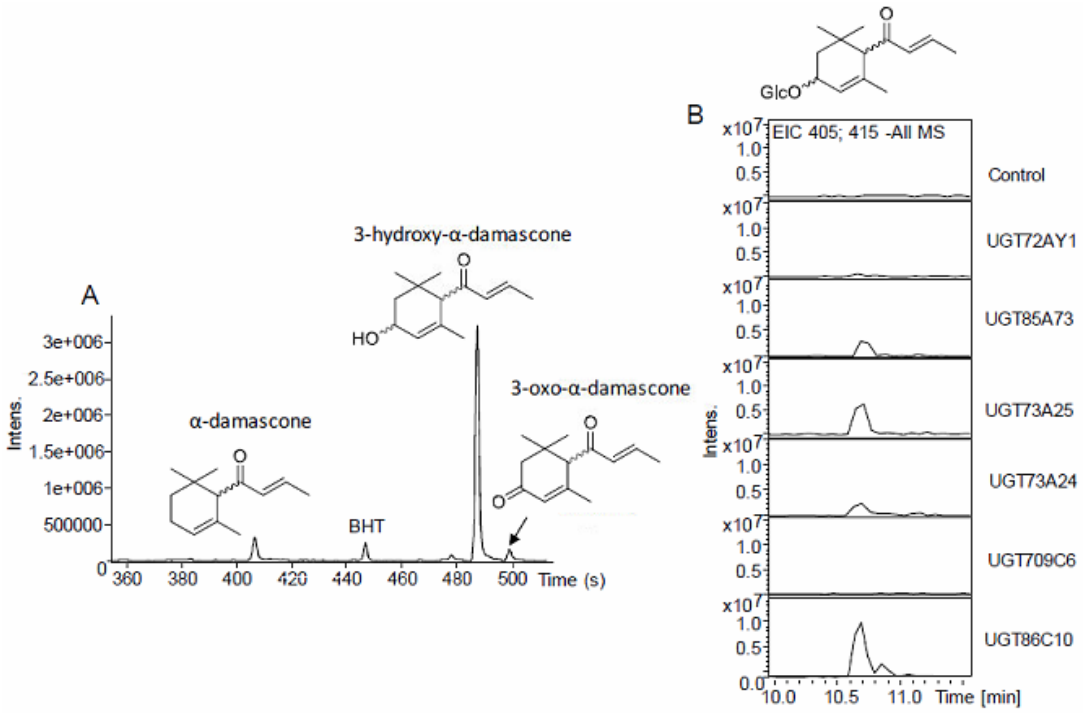

Figure 20. LC-MS analysis of monglucosides of 3-hydroxy-α-damascone produced by selected UGTs (right B), and GC-MS of the substrate mix (left, A) obtained by whole-cell P450 monooxygenase biotransformation. BHT butylated hydroxytoluene, LC-MS ion traces at *m/z* 405 and 415 show 3-hydroxy-α-damascone glucoside.

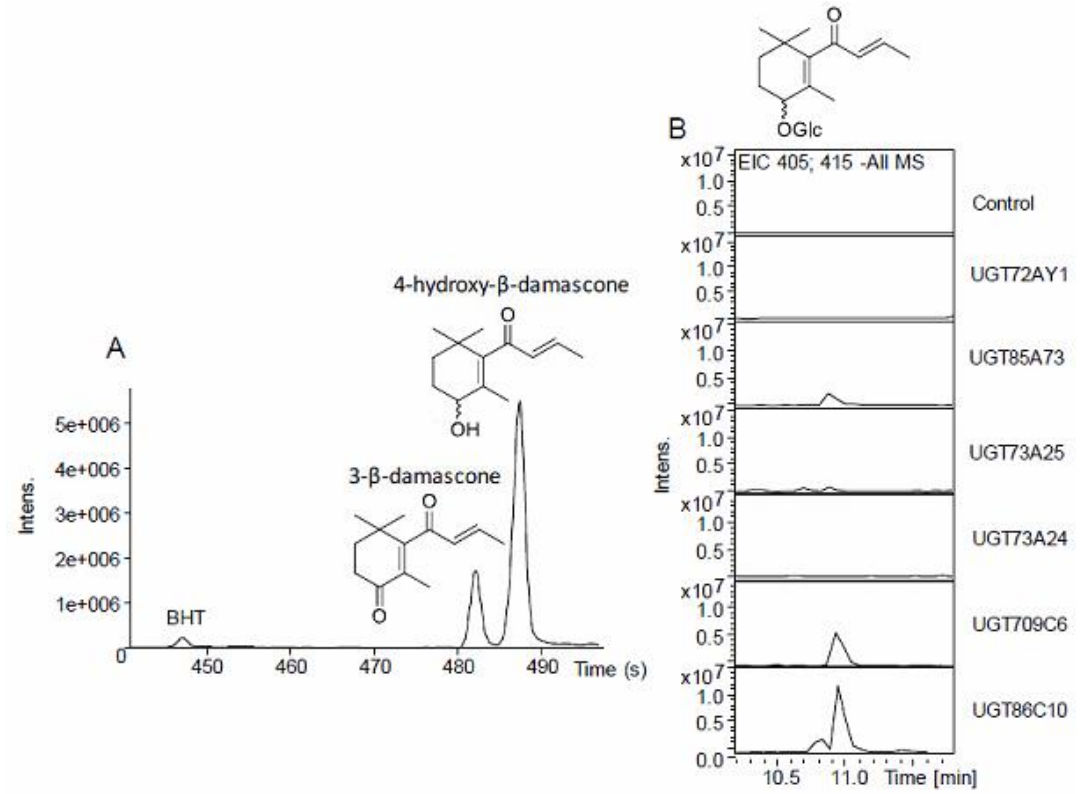

Figure 21. LC-MS analysis of monglucosides of 4-hydroxy-β-damascone produced by selected UGTs (right B), and GC-MS of the substrate mix (left, A) obtained by whole-cell P450 monooxygenase biotransformation. BHT butylated hydroxytoluene, LC-MS ion traces at *m/z* 405 and 415 show 4-OH-β-damascone glucoside.

Similarly, the enzymatic production of monoglucosides of 3-hydroxy-α-ionone, 4-hydroxy-β-ionone, 3-hydroxy-α-damascone, and 4-hydroxy-β-damascone was demonstrated (Figures 18 – 21).

UGT86C10 showed broad substrate tolerance and accepted all nine norisoprenoid substrates. It readily glucosylated 3-hydroxy-α-ionone, 4-hydroxy-β-ionone, 3-hydroxy-α-damascone, and 4-hydroxy-β-damascone. UGT73A25 showed high enzyme activity towards 3-hydroxy-α-ionol, 4-hydroxy-β-ionol, α-ionol and β-ionol. In contrast, UGT72AY1 was almost inactive with ionones and damascones but showed catalytic activity with ionol in particular 3-oxo-α-ionol (Table 10). These results indicated that UGT86C10 is the best UGT for the production of norisoprenoid glucosides.

3.5 Quantitative substrate screening by UDP Glo™ assay

3.5.1 *Mentha x piperita* UGTs

To characterize the three major MpUGTs (UGT708M1, UGT709C6, and UGT86C10) and eight active NbUGTs in more detail regarding their particular substrate specificities, quantitative substrate screening using the UDP-Glo™ assay was performed with a selected set of substrates (Figure 22).

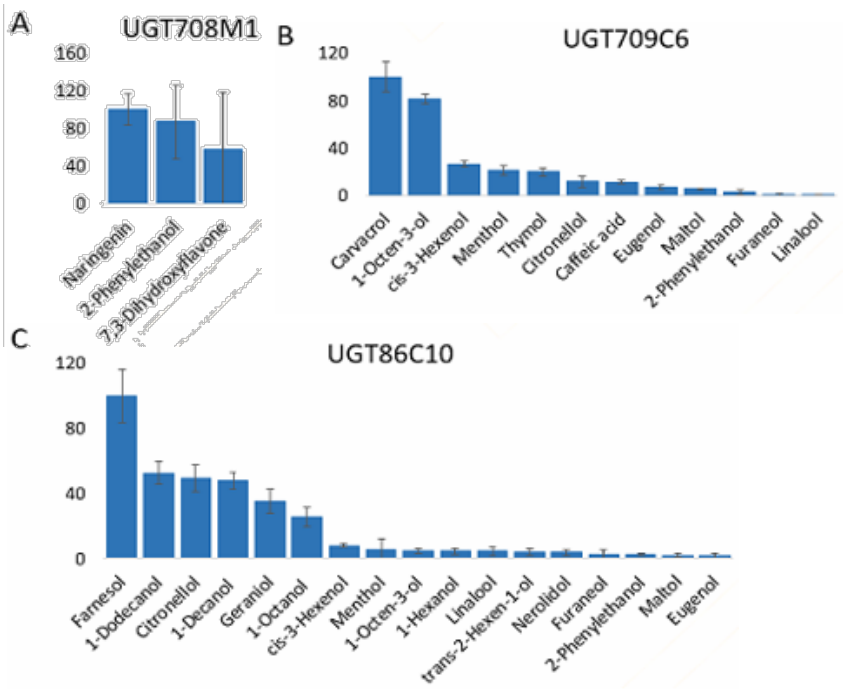

Figure 22. Quantitative substrate screening of MpUGTs by the UDP Glo™ assay. (A-C) Relative enzyme activities were calculated after measuring the release of UDP during the glucosylation reaction. The highest enzymatic activity was set to 100% and the relative enzyme activities were calculated for the other substrates.

The amounts of UDP released during the glucosylation reactions were measured and the relative catalytic activities were calculated. The highest enzyme activity was set to 100% (Figure 22). UGT708M1 showed highest activity towards naringenin (100% corresponding to 0.06 nmol/min/mg) but the overall catalytic activity was quite low. Carvacrol was the preferred substrate of UGT709C6 (23.75 nmol/min/mg) while UGT86C10 favored farnesol (54.52 nmol/min/mg).

3.5.2 *Nicotiana benthamiana* UGTs

Carvacrol was the preferred substrate of UGT72B35 (100% corresponding to 142 nmol/min/mg), UGT72AX1 (3 nmol/min/mg), UGT71AJ1 (23 nmol/min/mg), and UGT72B34 (15 nmol/min/mg; Figure 23).

UGT85A73 favored perillyl alcohol (46 nmol/min/mg), while UGT73A24 and UGT73A25 showed highest activity towards kaempferol (208 nmol/min/mg and 196 nmol/min/mg, respectively). UGT72AY1 displayed the highest activity towards scopoletin (638 nmol/min/mg), followed by carvacrol (391 nmol/min/mg) and malvidin (308 nmol/min/mg). However, in the case of UGT72AY1 negative values were obtained for some substrates, e.g. α-ionol (-107 nmol/min/mg), β-ionol (-111 nmol/min/mg), farnesol (-113 nmol/min/mg), and retinol (-135 nmol/min/mg).

We observed that the blank signal (UDP formation without substrate), which is substracted from the signal of the sample (UDP production in the presence of a putative substrate) was higher than the signal of the sample with substrate. Thus, the enzyme already formed UDP even in the absence of acceptor substrate, which would mean that UGT72AY1 shows substantial UDP-glucose hydrolase activity. The hydrolase activity was later confirmed (chapter 3.14). The substrate screening using UDP-Glo™ assay demonstrated that UGT72AY1 and UGT85A73 are highly promiscuous enzymes glucosylating a range of substrates very effectively, while UGT72B34 and UGT72AX1 show specificity for the phenol carvacrol. All selected NbGTs exhibited catalytic activity and specificity for scopoletin, carvacrol, and kaempferol, with the exception of UGT85A73, which preferably glucosylated aliphatic compounds such as perillyl alcohol and 3-cis-hexenol.

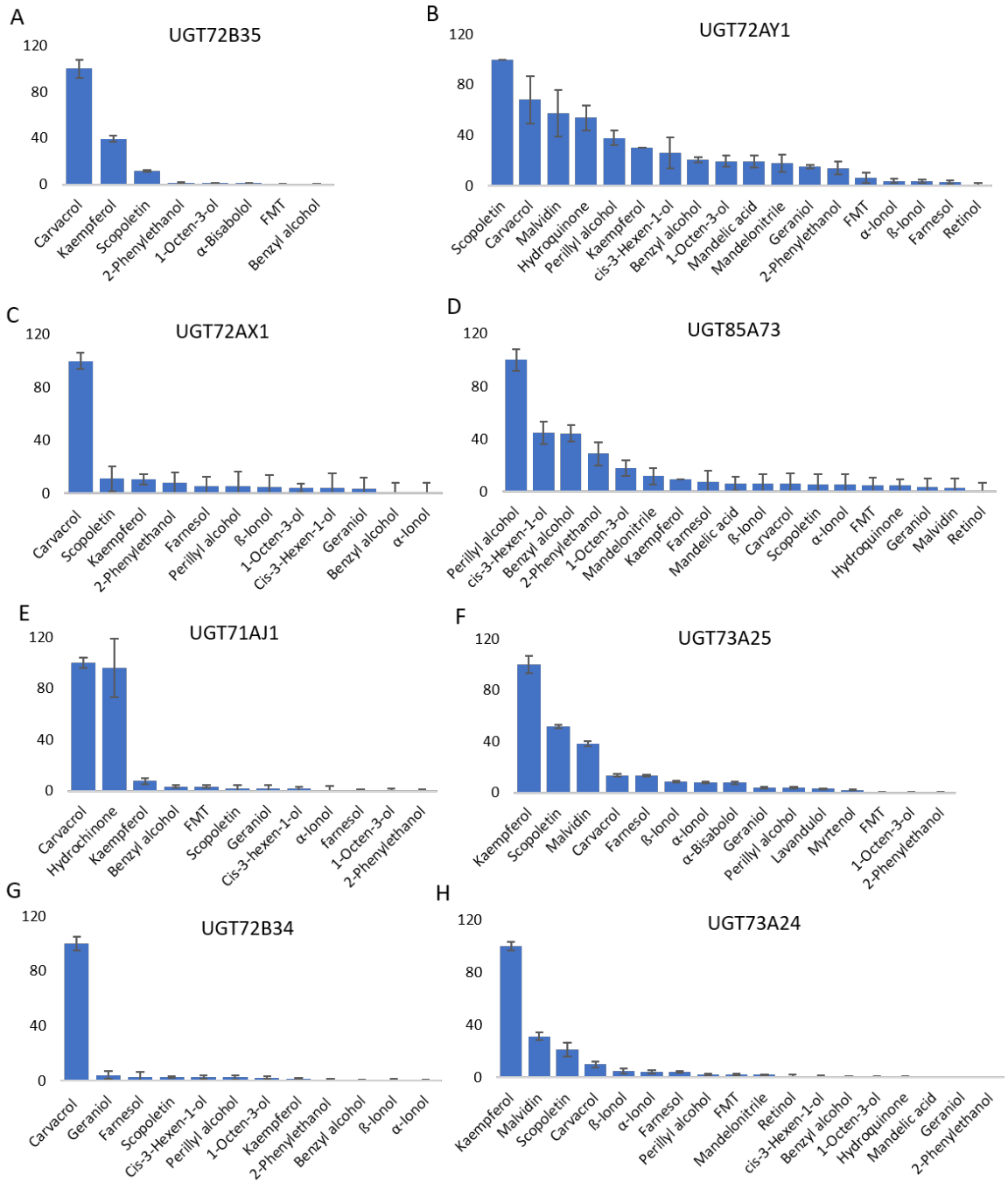

Figure 23. Quantitative substrate screening of NbUGTs by the UDP Glo™ assay. (A-H) Relative enzyme activities were calculated after measuring the release of UDP during the glucosylation reaction. The highest enzymatic activity was set to 100% and the relative enzyme activities were calculated for the other substrates. FMT is Furanmethanethiol.

3.6 Determination of kinetics by UDP Glo™

The protein amount, incubation temperature, time and pH reaction conditions were optimized for each enzyme prior to determining the kinetic data (Tables 4 and 5). At least seven different substrate concentrations were examined and the amounts of

released UDP were quantified to calculate enzyme activities. For each UGT, V_{max}, K_M, Kcat, and Kcat/K_M values of the preferred substrates were determined (Table 11 and 12).

Table 11. Michaelis-Menten parameters of UGTs from *Mentha x piperita*. Kinetics were determined using the UDP Glo™ assay accept for α- and β-ionol, which were determined by LC-MS.

	Substrates	K_M [µM]	V_{max} [nmol min^{-1} mg^{-1}]	Kcat [s^{-1}]	kcat/K_M [$M^{-1}s^{-1}$]
UGT708M1	7,3-Dihydroxyflavone	4.1 ± 0.5	0.27 ± 0.001	0.0003	83
	2-Phenylethanol	5.2 ± 5.8	0.34 ± 0.07	0.0004	82
	Naringenin	17.1 ± 16.0	0.24 ± 0.003	0.0003	18
UGT709C6	1-Octene-3-ol	235.4 ± 89.7	78.81 ± 15.03	0.1060	450
	β-Ionol	28.7 ± 7.5	7.16 ± 1.27	0.0096	336
	Carvacrol	260.8 ± 71.2	52.80 ± 12.33	0.0710	272
	2-Phenylethanol	84.4 ± 101.8	6.75 ± 2.34	0.0091	108
	Citronellol	205.6 ± 40.8	10.91 ± 0.72	0.0147	72
	cis-3-Hexenol	402.7 ± 146.5	20.94 ± 10.99	0.0282	70
	α-Ionol	27.2 ± 0.4	1.32 ± 0.10	0.0018	65
	Eugenol	37.4 ± 15.3	1.69 ± 0.33	0.0023	61
	Thymol	391.7 ± 120.1	10.41 ± 2.07	0.0140	36
	Maltol	181.7 ± 35.1	4.66 ± 0.57	0.0063	35
	Menthol	123.6 ± 81.0	2.3 ± 0.38	0.0031	25
UGT86C10	1-Dodecanol	16.2 ± 4.0	139.96 ± 21.41	0.1870	11552
	Farnesol	10.7 ± 1.8	65.53 ± 3.67	0.0875	8202
	1-Decanol	45.2 ± 8.3	76.61 ± 1.98	0.1023	2264
	Citronellol	59.5 ± 12.1	73.2 ± 5.22	0.0978	1644
	β-Ionol	6.0 ± 2.1	7.01 ± 1.42	0.0094	1575
	α-Ionol	23.8 ± 3.7	14.00 ± 0.80	0.0187	786
	Geraniol	120.1 ± 25.8	58.51 ± 9.99	0.0782	652
	1-Octanol	295.8 ± 132.6	48.09 ± 10.65	0.0643	217
	Menthol	157.3 ± 125.7	8.82 ± 1.68	0.0118	75
	cis-3-Hexenol	434.6 ± 251.6	15.64 ±1.26	0.0209	48
	1-Hexanol	6069.6 ± 8945.5	98.24 ± 130.44	0.1313	22

The Kcat values ranged from 0.014 to 0.967 s^{-1} for carvacrol, 0.012 to 0.65 s^{-1} for kaempferol, and 0.002 to 1.7 s^{-1} for scopoletin. The K_M values ranged from 11.6 to 1272.1 µM for carvacrol, 3.5 to 18.7 µM for kaempferol, and 7.3 to 912.3 µM for scopoletin. The specificity constant Kcat/K_M highlights the *in vitro* preference of UGT709C6 for 1-octene-3-ol; UGT86C10 for 1-dodecanol; UGT72AY1 for scopoletin; UGT73A24 for kaempferol; UGT73A25 for quercetin. UGT71AJ1 favored carvacrol and UGT85A73 efficiently converted cis-3-hexenol. Most of the NbUGTs showed high

catalytic activity for carvacrol, scopoletin and kaempferol while UGT86C10 is a superior biocatalyst for the glucosylation of 1-decanol. The specificity constants affirmed the *in vitro* substrate preferences of UGTs shown in Tables 8 and 9 and Figures 22 and 23.

Table 12. Michaelis-Menten parameters of UGTs from *N. benthamiana*. Kinetics were determined using the UDP Glo™ assay, accept for α- and β-ionol, which were determined by LC-MS.

	Substrate	**K_M [µM]**	**V_{max} (nmol $min^{-1}mg^{-1}$)**	**Kcat [s^{-1}]**	**kcat/KM [$M^{-1}s^{-1}$]**
UGT72B35	Carvacrol	57.9 ± 16.1	194.9 ± 12.4	0.256	4430
	1-Octen-3-ol	2.8 ± 2.4	2.3 ± 0.6	0.003	1108
	2-Phenylethanol	13.0 ± 2.4	5.3 ± 0.7	0.007	533
	Scopoletin	124.6 ± 57.9	6.8 ± 2.7	0.009	72
UGT72AX1	Carvacrol	11.6 ± 6.1	10.7 ± 1.0	0.014	1235
	Scopoletin	7.4 ± 2.0	6.7 ± 0.04	0.009	1213
UGT72AY1	Scopoletin	7.3 ± 2.4	1281.9 ± 245.2	1.704	233159
	Carvacrol	12.9 ± 0.9	708.9 ± 83.6	0.943	73362
	Kaempferol	8.9 ± 1.5	378.2 ± 29.2	0.503	56281
	Malvidin	24.9 ± 9.3	116.5 ± 13.3	0.155	6232
	Perillyl-alcohol	46.6 ± 21.1	143.1 ± 12.5	0.190	4086
	Hydroquinon	345.3 ± 84.0	419.3 ± 30.9	0.558	1615
	Myrtenol	29.4 ± 17.9	17.4 ± 3.5	0.023	786
	Tyrosol	182.2 ± 67.6	39.3 ± 8.3	0.052	287
UGT85A73	Cis-3-Hexenol	132.5 ± 52.7	384.8 ± 55.5	0.517	3903
	Benzylalcohol	55.2 ± 24.8	96.1 ± 6.8	0.129	2341
	Perillyl-alcohol	110.2 ± 12.1	177.5 ± 14.5	0.239	2166
	1-Octene-3-ol	161.5 ± 28.5	241.2 ± 14.4	0.324	2007
UGT73A25	Quercetin	4.3 ± 0.5	197.6 ± 7.7	0.264	61686
	Kaempferol	18.7 ± 3.4	440.9 ± 49.8	0.589	31516
	β-Ionol	131.4 ± 18.3	155.6 ± 7.1	0.208	1580
	Scopoletin	912.3 ± 687.8	574.1 ± 245.6	0.766	840
	α-Ionol	106.0 ± 22.2	64.4 ± 4.5	0.086	811
	Farnesol	23.1 ± 5.8	13.8 ± 2.0	0.018	797
	Carvacrol	1272.1 ± 425.9	724.2 ± 76.0	0.967	760
	Perillyl alcohol	755.6 ± 122.0	291.2 ± 47.2	0.389	514
	Geraniol	526.8 ± 313.4	191.2 ± 69.5	0.255	485
	N-caffeoyl-o-methyltyramine	159.2 ± 55.8	56.1 ± 9.0	0.075	471
	Lavandulol	1014.7 ± 364.9	310.2 ± 68.0	0.414	408
	N-p-trans-coumaroyl-tyramine	110.3 ± 29.4	9.2 ± 2.0	0.012	112
	2-Phenylalcohol	139.8 ± 59.0	7.6 ± 2.5	0.010	73
	N-trans-Feruloyl-tyramine	3030.7 ± 693.6	41.6 ± 1.0	0.056	18

UGT73A24	Kaempferol	3.5 ± 0.1	488.3 ± 28.3	0.650	187845
	Quercetin	2.2 ± 0.4	256.1 ± 33.6	0.341	158692
	Malvidin	22.3 ± 1.1	294.8 ± 26.0	0.392	17637
	Scopoletin	324.5 ± 21.2	687.9 ± 50.7	0.916	2822
	Carvacrol	881.8 ± 224.3	609.6 ± 108.3	0.811	920
	α-Ionol	32.8 ± 8.8	18.5 ± 2.5	0.025	750
	β-Ionol	34.1 ± 3.9	18.4 ± 0.2	0.024	718
	N-caffeoyl-o-methyltyramine	150.5 ± 77.0	48.7 ± 16.9	0.065	431
	Perillyl-alcohol	514.9 ± 76.1	53.5 ± 2.1	0.071	138
	N-trans-Feruloyl-tyramine	1473.2 ± 340.9	46.7 ± 1.1	0.062	42
	N-p-trans-coumaroyl-tyramine	282.6 ± 83.4	5.7 ± 1.2	0.008	27
UGT71AJ1	Carvacrol	16.0 ± 0.2	161.8 ± 5.1	0.215	13398
	Kaempferol	12.4 ± 1.3	9.0 ± 1.5	0.012	959
	Hydroquion	437.0 ± 175.7	143.5 ± 40.1	0.190	436
	β-Ionol	2.6 ± 0.6	8.4 ± 2.4	0.004	414
	Scopoletin	138.6 ± 112.5	1.3 ± 0.6	0.002	13
	Benzylalcohol	1353.7 ± 768.0	11.5 ± 4.4	0.015	11
UGT72B34	Carvacrol	50.7 ± 6.2	99.8 ± 5.4	0.131	2587
	Scopoletin	255.6 ± 76.6	10.4 ± 1.3	0.014	53

When the enzymatic activity of UGT72AY1 towards α-ionol and β-ionol was tested with the UDP-Glo™ assay negative values were obtained (Supplemental Figure S3a). As already explained above significant UDP-glucose hydrolase activity was assumed, exceeding the glycosylation reaction. The hydrolase activity could also not be inhibited by α-ionone and β-ionone (Supplemental Figure S3a). Therefore, LC-MS was used to determine the kinetic data for α-, and β-ionol (Supplemental Figure S3b) for selected UGTs. Since the kinetic parameters for α-ionol and β-ionol were determined with a different method, the values cannot be directly compared with those of the other substrates.

3.7 Tissue specificity analysis of MpUGTs in *Mentha × piperita*

To test the expression level of MpUGTs in *Mentha × piperita,* RNA was extracted from different tissues (root, side stem, main stem, young leaves, mature leaves, old leaves and flower) to perform qRT-PCR. Relative expression levels of *UGT86C10, UGT709C6,* and *UGT708M1/2* were calculated by the $2^{-\Delta\Delta CT}$ method (Figure 24). *UGT86C10* showed the highest expression level in mature leaves, while the transcripts of *UGT708M1/2* and *UGT709C6* were abundant in young leaves. Overall,

the MpUGTs are mainly expressed in young leaves, mature leaves and flower, while in root and old leaves the genes were barely transcribed.

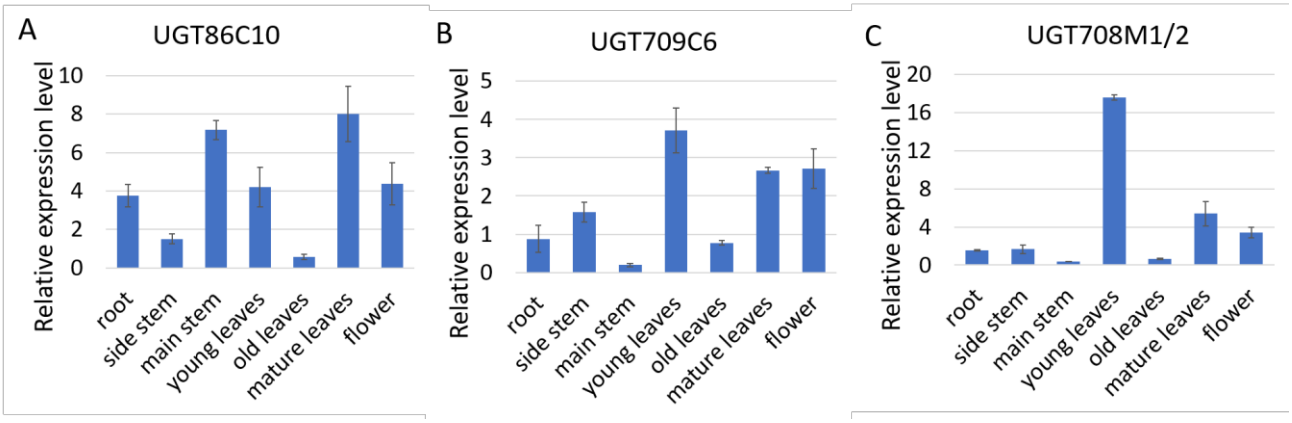

Figure 24. Relative expression levels of *UGT86C10, UGT709C6, UGT708M1*/2 in different tissues of *M. x piperita.*

3.8 Agroinfiltration of *N. benthamiana* leaves

3.8.1 QPCR analysis

Although UGT73A24 and UGT73A25 showed high sequence similarity (95% sequence identity) with two biochemically characterized scopoletin UGTs from *N. tabacum* (Fraissinet-Tachet et al., 1998; Gachon et al., 2004) our biochemical assays revealed kaempferol as the preferred substrate *in vitro*. Therefore, we transiently overexpressed *UGT73A24* and *UGT73A25* in *N. benthamiana* leaves using an established viral vector system to characterize natural acceptor substrates (Huang et al., 2010). At the same time, *UGT72AY1, UGT73B24, UGT86C10, UGT709C6, UGT708M1* and *UGT708M2* were also infiltrated. As controls, an empty vector (CO) was infiltrated and untreated wild-type leaves (WT) were used (Figure 25).

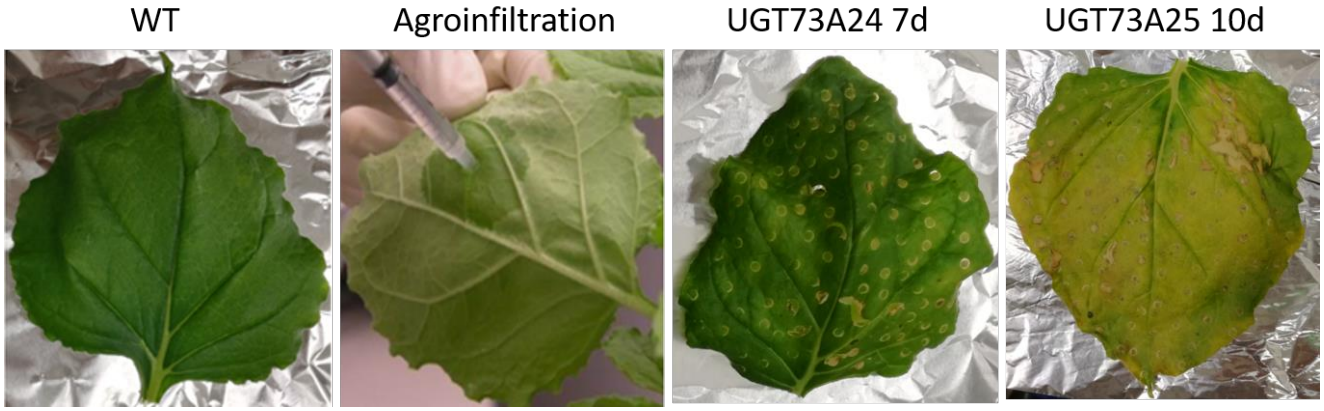

Figure 25. Agroinfiltration of *UGT73A24* and *UGT73A25* in *N. benthamiana*. Untreated leaves (WT).

Tobacco leaves were treated with Agrobacterium from the backside and harvested 7 and 10 days after agroinfiltration. During this period, the leave color changed from green to light yellow (Figure 25). To test whether the infiltrated genes were successfully expressed in *N. benthamiana* leaves, RNA and proteins were extracted from all samples for qRT-PCR and enzyme activity analyses, respectively. Quantitative transcript analyses demonstrated that *UGTs* were strongly expressed in the agroinfiltrated leaves (Figure 26). Compared with WT and CO, the transcript levels of all infiltrated genes increased significantly.

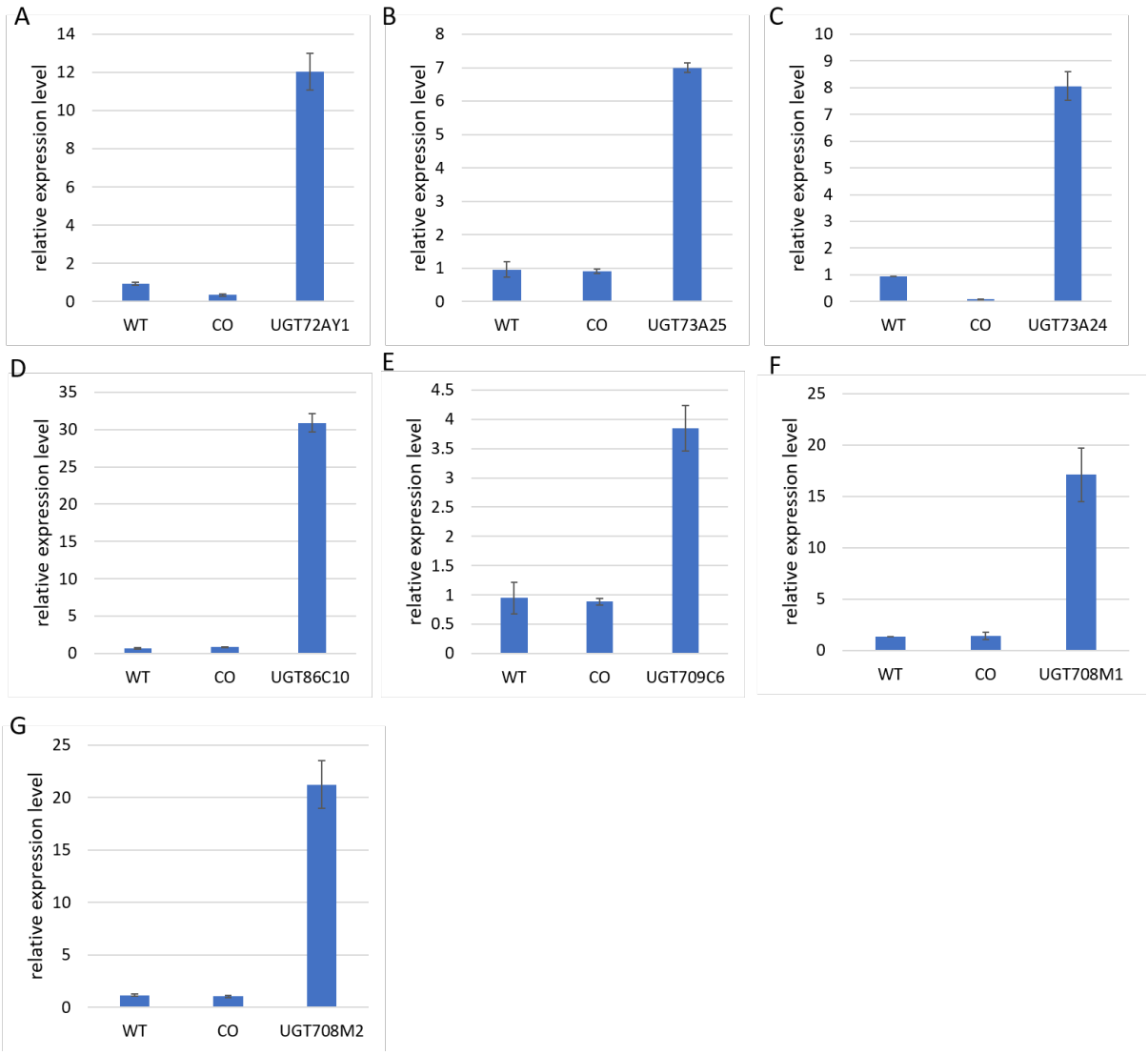

Figure 26. QRT-PCR analysis of *N. benthamiana* leaves agroinfiltrated with *UGT72AY1, UGT73A25, UGT73A24, UGT86C10, UGT709C6, UGT708M1,* and *UGT708M2***.** Untreated leaves (WT), leaves infiltrated with an empty vector control (CO). Tobacco UGTs (*UGT72AY1, UGT73A25* and *UGT73A24*) were analyzed 7 d after agroinfiltration and mint UGTs (*UGT86C10, UGT709C6, UGT708M1* and *UGT708M2*) 10 d after agroinfiltration. Triplicate analysis. Expression level of WT was set at 1.

3.8.2 Enzymatic activity of crude protein extracts

Crude protein extracts were isolated from *NbUGT*s infiltrated *N. benthaminana* leaves 7 d after agroinfiltration and used as enzyme source for *in vitro* enzyme assays. Extracts obtained from *UGT73A24*- and *UGT73A25*-infiltrated leaves readily produced glucosides when carvacrol, quercetin, scopoletin, and kaempferol were used as acceptor substrates (Figure 27). Proteins extracted from CO and WT leaves formed only minor amounts of glucosides. The highest level of scopolin was produced by extracts of leaves infiltrated with *UGT73A24,* while the infiltrated leaves of *UGT73A25* formed a greater amount of quercetin, carvacrol, and kaempferol glucoside (Figure 27). Overexpression of *UGT73A24* and *UGT73A25* resulted in increased production of glucosides, indicating that the encoded UGTs contribute to the formation of hexosides *in vitro*.

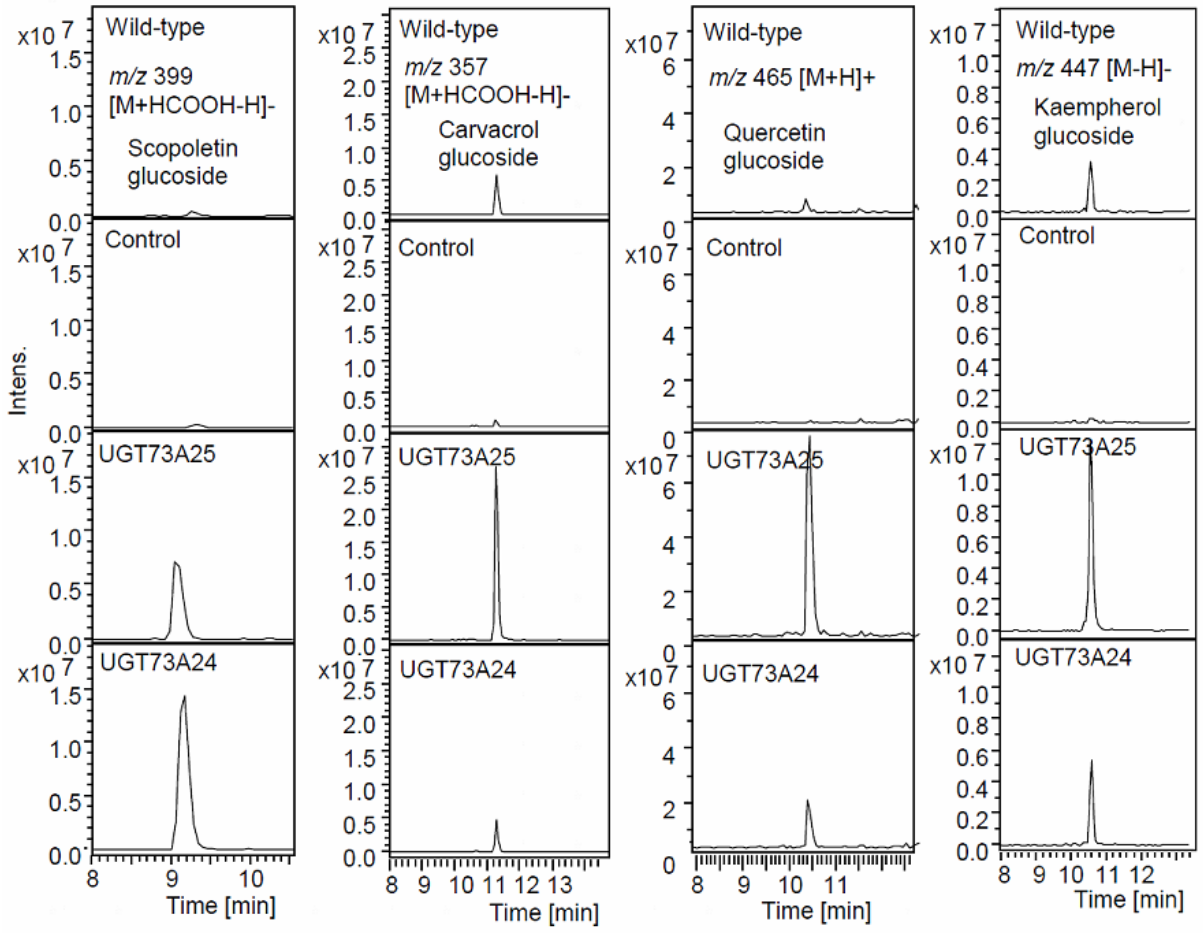

Figure 27. LC-MS analysis of products produced by protein extract isolated from *UGT73A24*- and *UGT73A25*-agroinfiltrated *N. benthamiana* leaves from different substrate. LC-MS analysis of enzymatic assays performed with protein extracts from wild-type, empty vector control, *UGT73A24*- and *UGT73A25*-infiltrated leaves and the substrates scopoletin, carvacrol, quercetin, and kaempferol.

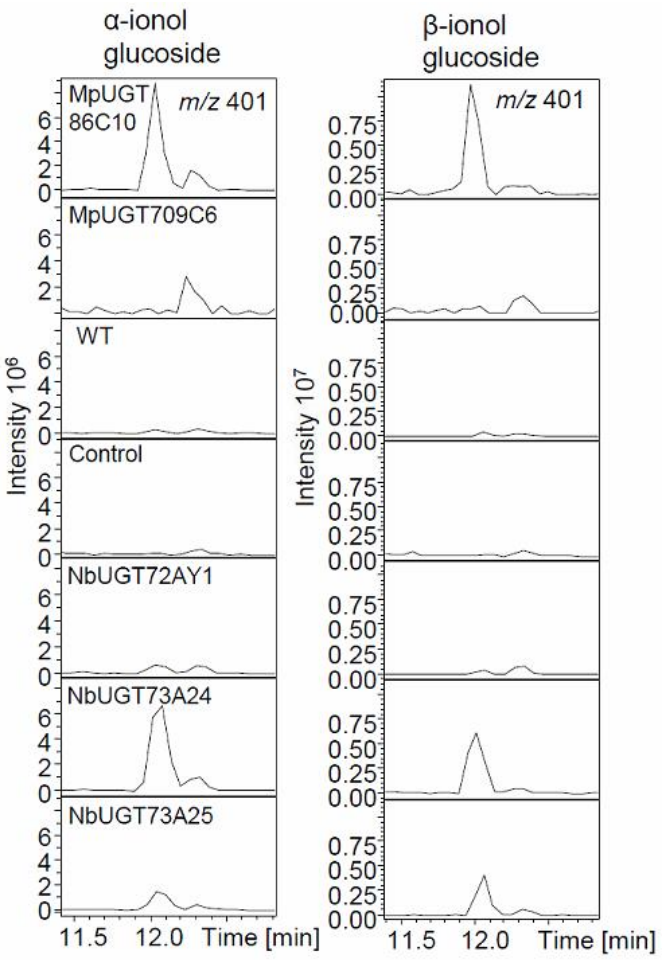

Figure 28. LC-MS analysis of products produced by crude protein extraction of *N. benthamiana* leaves agroinfiltrated with *UGT72AY1, UGT73A25, UGT73A24, UGT709C6, UGT86C10* and *UGT73B24* from α-ionol and β-ionol. Untreated leaves (WT), leaves infiltrated with an empty vector control (CO). *UGT709C6* and *UGT86C10* extracts were incubated at 30 °C, for 2 h, all other extracts were incubated at 30 °C for 1h. Extracts were isolated 7 d after agroinfiltration. Detection α-ionol glucoside (A) and β-ionol glucoside (B) at ion trace *m/z* 401 $[M+HCOO]^-$.

Additionally, crude protein extracts isolated 7 d after agroinfiltration from *UGT72AY1-*, *UGT73A25-*, *UGT73A24-*, *UGT709C6-*, *UGT86C10-*, and *UGT73B24*-infiltrated leaves were also tested with α-ionol and β-ionol as acceptors. All protein extracts produced ionol glucosides except for *UGT709C6*, while in the reaction mixtures containing wild type and control leaf extracts ionol glucosides were not found (Figure 28). The highest level of α-ionol and β-ionol glucoside was produced by UGT73A24 and UGT86C10, but the incubation time for the latter was twice a long. The results confirmed that the UGTs were successfully overexpressed in tobacco leaves and they contributed to the formation of ionol glucosides *in vitro*, except for f UGT709C6.

3.9 Untargeted metabolite profiling

Non-targeted metabolite profiling of extracts isolated from agroinfiltrated *N. benthamiana* leaves was performed by LC-MS to structurally identify natural glycoside products formed by UGT73A24 and UGT73A25 *in planta* (Figure 29).

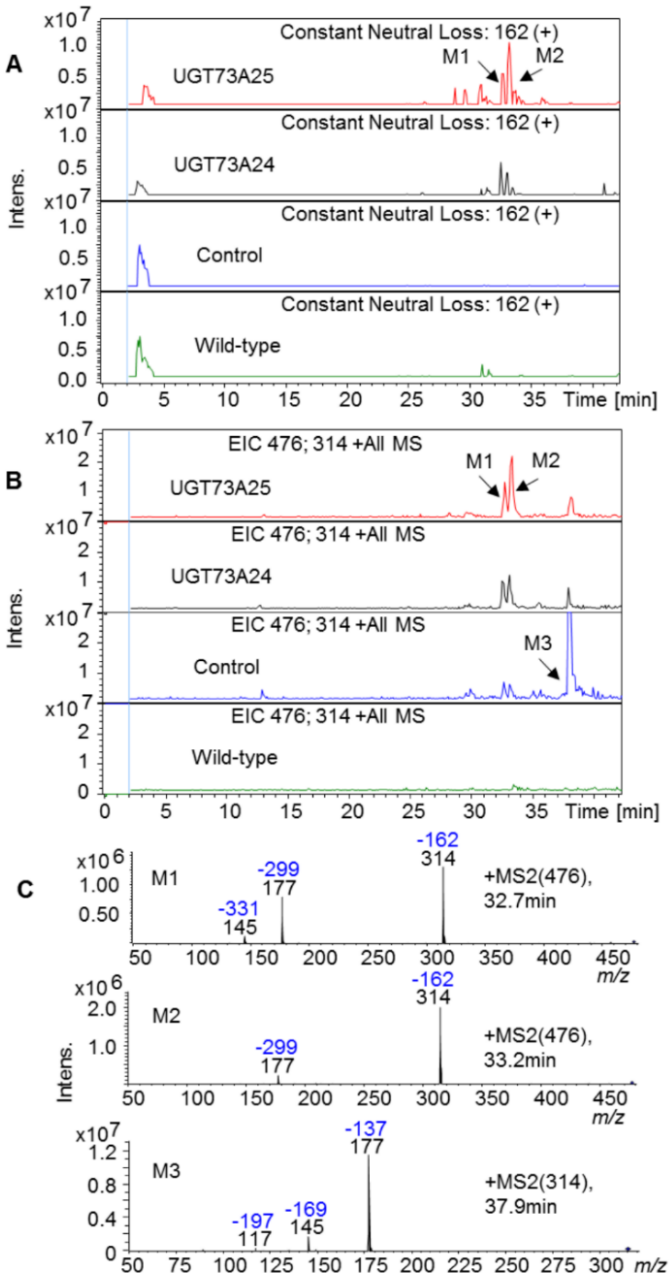

Figure 29. LC-MS analysis to detect natural hexosides produced by UGT73A24 and UGT73A25 after overexpression in *N. benthamiana*, their potential substrate and mass spectra. (A) The constant neutral loss (*m/z* 162) experiments reveal potential hexosides (M1 and M2). **(**B) Extracted ion chromatograms (EIC) at *m/z* 476 and 314 show hexosides M1 and M2 and the potential precursor substrate M3. Control and wild-type represent agroinfiltration of an empty vector and untreated leaves, respectively. **(**C**)** Product ion mass spectra (MS2) of M1, M2, and M3.

In order to reduce the amount of data we applied constant neutral-loss experiments (CNLE), as this is the most appropriate mode to find expected conjugates in a sample. We monitored the neutral loss of 162 Dalton in the product ion spectra (MS2) in positive and negative modes, indicating hexose residues. CNLE comparison of metabolites isolated from *UGT73A24*- and *UGT73A25*-infiltrated, CO, and WT leaves showed two significant signals (M1 and M2) in the ion traces of *UGT73A24* and *UGT73A25* samples, which lacked in the CO and WT samples (Figure 29). The product ion spectra (MS2) of the two metabolites confirmed the loss of a neutral fragment of 162 Dalton and showed pseudomolecular ions at *m/z* 476 $[M+H]^+$ and major fragments at *m/z* 314 $[M\text{-hexose}+H]^+$. We concluded that M1 and M2 are isomers and the major fragment ions represent the protonated aglycons. The extracted ion chromatograms (EIC) of *m/z* 476 and 314 showed a third signal (M3) in the control sample, which had been agroinfiltrated with an empty vector (Figure 29). The product ion spectrum (MS2) of metabolite M3 showed a pseudomolecular ion at *m/z* 314 $[M+H]^+$ and a major fragment ion at *m/z* 177. A comparison of MS2 of the metabolites M1, M2, and M3 led to the conclusion that M3 is the biogenic precursor of M1 and M2, and the natural substrate of UGT73A24 and UGT73A25.

3.10 Screening of aglycon libraries

Since a physiological library is a multifunctional tool for identifying natural substrates of UGTs (Bönisch et al., 2014), low molecular weight metabolites were isolated by XAD solid phase extraction from tobacco leaves (*N. tabacum*) and fractionated into 30 fractions using semi-preparative liquid chromatography. The fractions were analyzed by LC-MS (Supplemental Figure S4 and S5) and 30 aglycon libraries were generated by enzymatic hydrolysis using a glycosidase preparation (rapidase), followed by solvent extraction. The putative products (M1 and M2) of UGT73A24 and UGT73A25 were found in fraction 10 (Figure 30). M1 and M2 were hydrolysed by glycosidase (Rapidase) and reconstituted by UGT73A24 and UGT73A25, confirming that M1 and M2 are the products of both enzymes (Figure 30). High-resolution LC-MS analysis yielded the molecular formula $C_{24}H_{30}NO_9$ $[M+H]^+$ (measured *m/z* 476.1937; calculated *m/z* 476.1915). With the help of database and literature data search, M1 and M2 were finally identified as N-feruloyl tyramine 4-*O*-β-glucoside and N-feruloyl tyramine 4'-*O*-β-glucoside, respectively (Supplemental Figure S6). Thus, feruloyl tyramine (M3) serves as *in planta* substrate for UGT73A24 and UGT73A25, which produce two

isomeric forms of the glucosides (M1 and M2) in contrasting ratios (Figure 30) and different efficiencies.

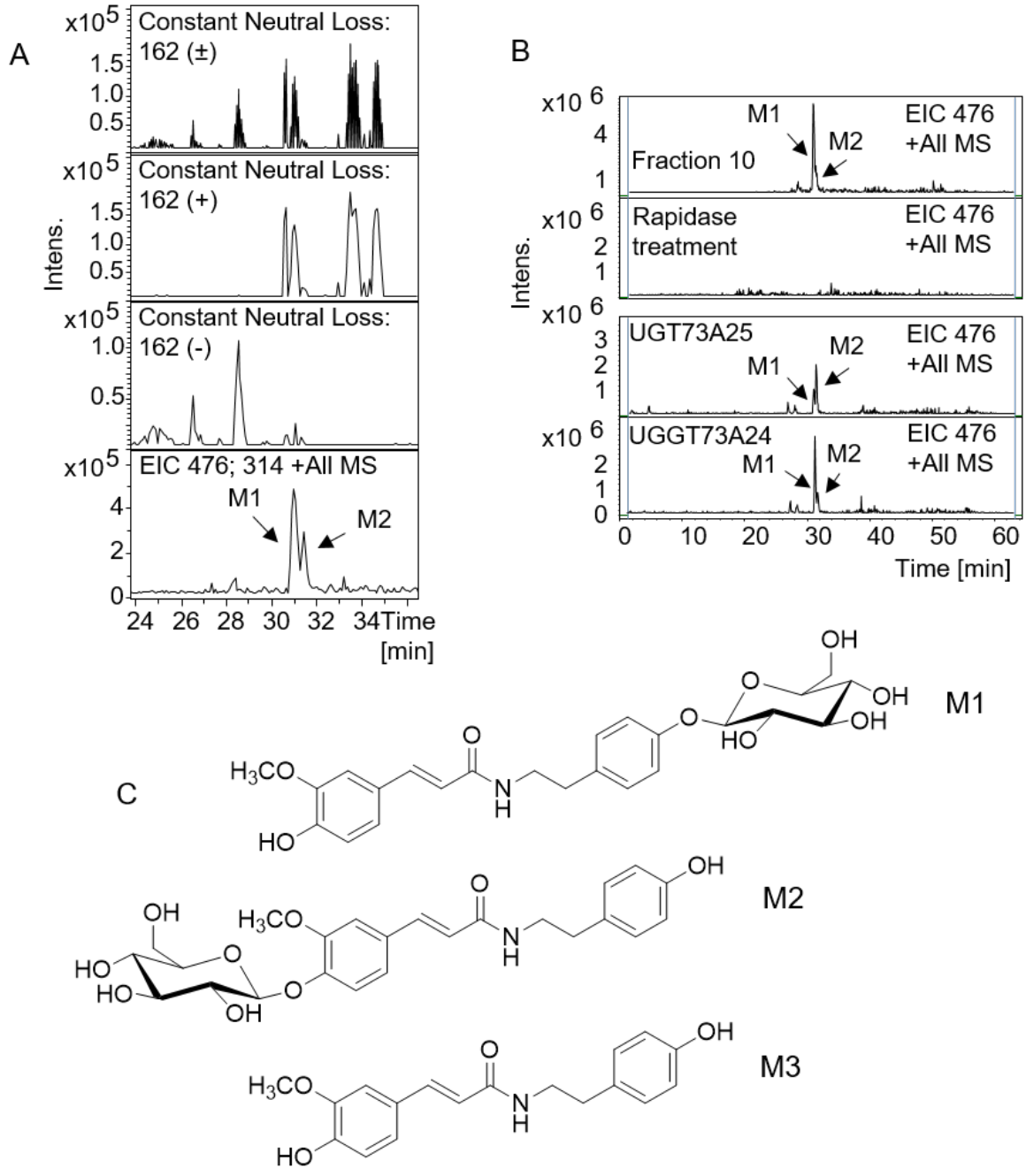

Figure 30. Identification of hexosides M1 and M2 as natural products of UGT73A24 and UGT73A25. (A) M1 and M2 were identified in fraction 10 after preparative LC isolation. Fraction 10 contains at least five additional hexosides (shown by constant neutral loss experiment of m/z 162 in positive and negative mode) in addition to M1 and M2 (EIC, extracted ion chromatogram *m/z* 476 and 314). **(B)** M1 and M2 are formed by UGT73A24 and UGT73A25. Fraction 10 was hydrolyzed by glycosidase (rapidase) and extracted aglycons incubated with UGT73A24 and UGT73A25. Formation of M1 and M2 was confirmed by EIC at *m/z* 476 in positive mode. **(C)** Chemical formulas of M1, M2 and M3 (N-feruloyl tyramine).

3.11 UGT73A24 and UGT73A25 glucosylate ferulic acid derivatives

Sine N-feruloyl tyramine was identified as *in planta* substrate of UGT73A24 and UGT73A25, additional ferulic acid derivatives and tyramine were tested as acceptor molecules for both enzymes. Enzymatic assays demonstrated the formation of glucosides when caffeic acid, trans-ferulic acid, 4-coumaric acid, N-caffeoyl *O*-methyltyramine, N-4-trans-coumaroyl tyramine, ethyl 4-hydroxy-3-methoxy-cinnamate, and N-trans-feruloyl-tyramine and tyramine were incubated with the recombinant proteins (Supplementary Figure S7). Two monoglucosides were produced from caffeic acid and tyramine, respectively, and both enzymes produced diglucosides from N-4-trans-coumaroyl tyramine and N-trans-feruloyl-tyramine. Among the amides, both enzymes favoured N-caffeoyl *O*-methyltyramine as a substrate (kcat/Km 431 M^{-1} s^{-1} and 471 M^{-1} s^{-1}; Table 12).

3.12 Modulation of pathogen-induced metabolites

Since N-feruloyl tyramine accumulated in considerable amount in *N. benthamiana* leaves agroinfiltrated with the empty vector (CO), we searched for additional Agrobacterium-induced metabolites in CO samples by targeted and non-targeted LC-MS analysis (Cho et al., 2012; Mhlongo et al., 2016a; Mhlongo et al., 2016b). Comparative LC-MS analysis showed that in addition to feruloyl tyramine agroinfiltration of empty vector (CO) induced the accumulation of coumaroyl quinic acid, feruloyl quinic acid, phenylalanine, coumaroyl tyramine, tryptophan, and two isomeric grossamides (dimers of feruloyl tyramine; (Baxendale et al., 2006); (Cardullo et al., 2016); Figure 31). Formation of caffeoly quinic acids (chlorogenic acids) seemed not to be induced as chlorogenic acids were already detected at high levels in untreated wild-type samples (WT). The WT samples lacked all other metabolites except phenylalanine and tryptophan, which occurred at low levels. Notably, overexpression of *UGT73A24* and *UGT73A25* resulted in a significant decrease in the levels of pathogen-responsive metabolites, including phenylalanine and tryptophan although the latter are no substrates of the encoded enzymes (Figure 31).

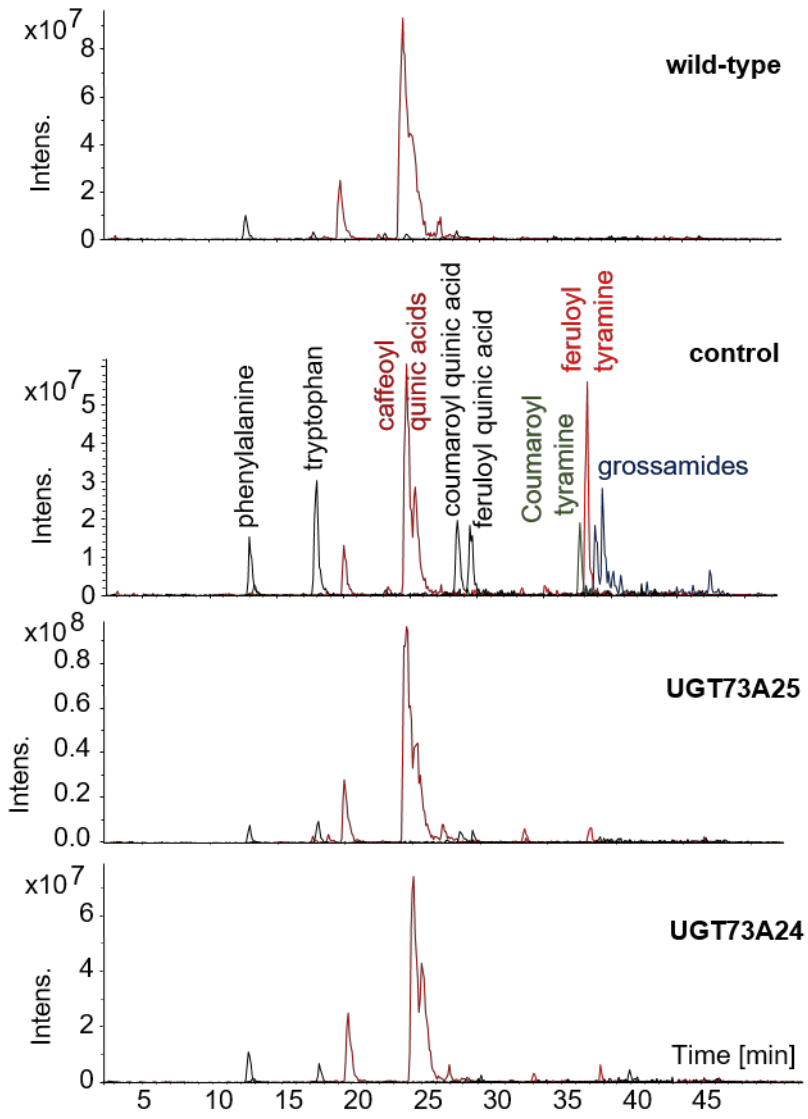

Figure 31. Modulation of pathogen-induced metabolites by agroinfiltration of *UGT73A24* and *UGT73A25* in *N. benthamiana* leaves. LC-MS analysis revealed accumulation of phenylalanine *m/z* 166 $[M+H]^+$, tryptophan *m/z* 205 $[M+H]^+$, caffeoyl quinic acids *m/z* 355 $[M+H]^+$, coumaroyl quinic acid *m/z* 339 $[M+H]^+$, feruloyl quinic acid *m/z* 369 $[M+H]^+$, coumaroyl tyramine *m/z* 284 $[M+H]^+$, feruloyl tyramine *m/z* 314 $[M+H]^+$, and grossamide diastereomers *m/z* 625 $[M+H]^+$ after agroinfiltration of an empty vector control (control). Untreated wild-type leaves contained only caffeoyl quinic acids and small amounts of phenylalanine and tryptophan. The raised levels of pathogen-responsive metabolites returned to normal when *UGT73A24* and *UGT73A25* were overexpressed in *N. benthamiana* leaves.

3.13 Production of quercetin rutinoside

Since the specificity constant kcat/K_M of UGT73A24 and UGT73A25 indicated a high preference for flavonoids quercetin and kaempferol, we re-evaluted the LC-MS data and specifically searched for flavonoid derivatives (Figure 32). Quercetin rutinoside (rutin), kaemperol rutinoside and a kaempferol diglucoside were found in the leaves

agroinfiltrated with *UGT73A25,* but were absent in the other three samples. The rutinosides were overlooked in the constant neutral loss experiment (Figure 29) because the MS2 spectra of the rutinosides mainly showed a loss of rhamnose (-146 Dalton) and rutinose (-308 Dalton), while the kaemperol diglucoside was already discernible but occurred at a low level. Therefore, UGT73A25 appeared to promote the formation of flavonoid rutinosides and a kaempferol diglucoside, while UGT73A24 did not.

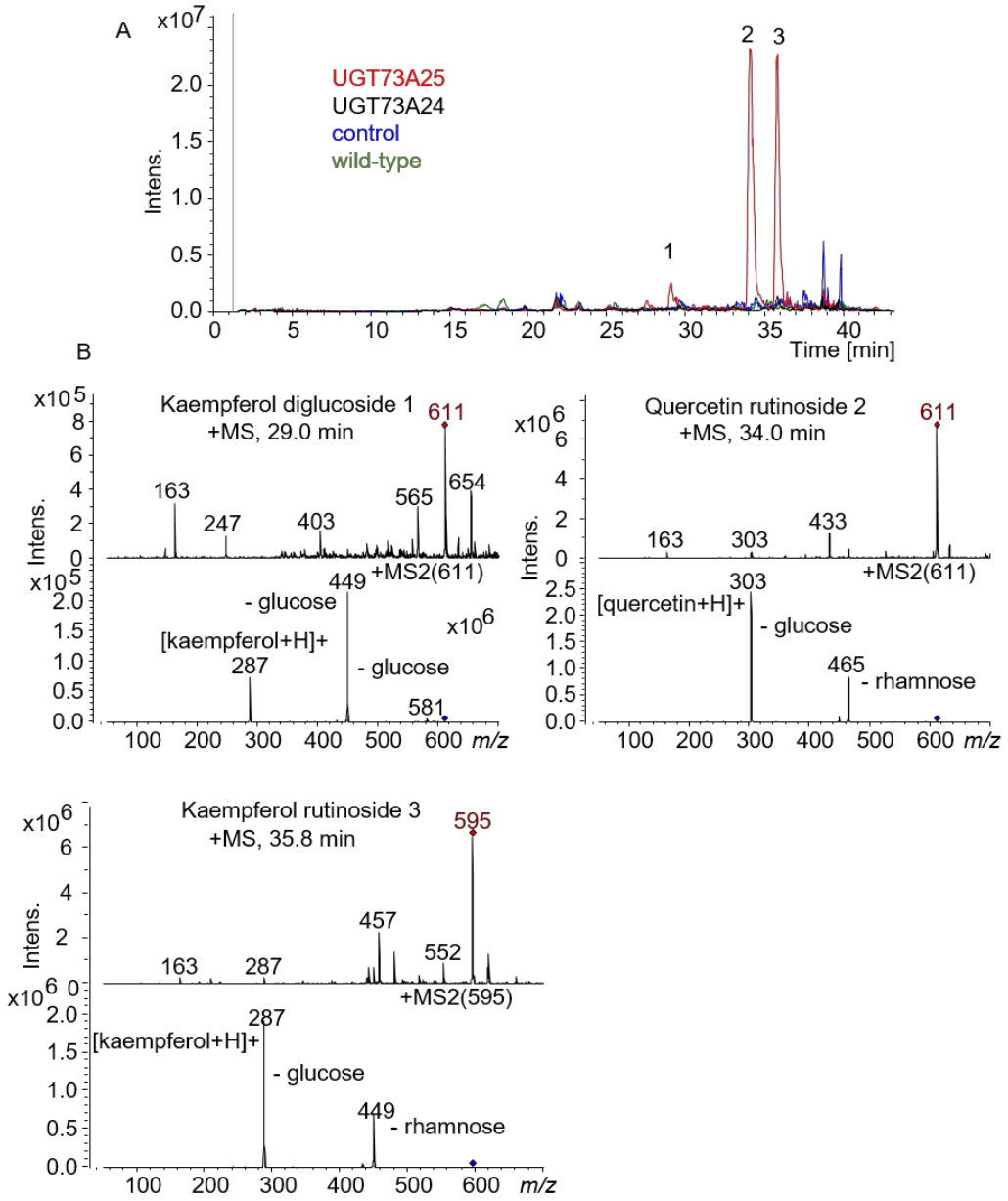

Figure 32. LC-MS analysis of kaempferol and quercetin derivatives in agroinfiltrated and wild-type leaves of *N. benthamiana*. (A) Leaves were agroinfiltrated with *UGT73A24*, *UGT73A25*, and the empty vector. Wild-type leaves remained untreated. Overlay of ion traces *m/z* (+) 287, 303, 449, 465, 595, 611, and 627 for the detection of kaempferol and quercetin glucoside, rutinoside and diglucosides. (B) Mass and product ion spectra of metabolite 1, 2 and 3.

3.14 Hydrolase activity assay for UGT72AY1

To characterize the UDP-glucose hydrolase activity of UGT72AY1 in more detail the UDP-Glo™ and glucose-Glo™ assay were used to quantify the amount of released UDP and glucose and to calculate the enzymatic activity. UGT72AY1 was incubated with increasing concentrations of UDP-glucose without acceptor substrate. As control, UGT73A25 and UGT73A24 were also used at their optimal reaction conditions (Table 5). Even without acceptor substrates, the amount of released UDP and glucose increased for the three UGTs with increasing UDP glucose concentration. (Figure 33). UGT72AY1 showed the highest UDP-glucose hydrolase activity of the three UGTs. The K_M values for UGT72AY1 based on released UDP and glucose were 24 and 35 µM, respectively, while for UGT73A25 and UGT73A24 the values were 144 (69 for glucose) and 144 (38 for glucose) µM, respectively. The kcat values for UGT72AY1, UGT73A25, and UGT73A24 were 0.1 (0.4 for glucose) s^{-1}, 0.02 (0.01 for glucose) and 0.02 (0.07 for glucose) s^{-1} respectively.

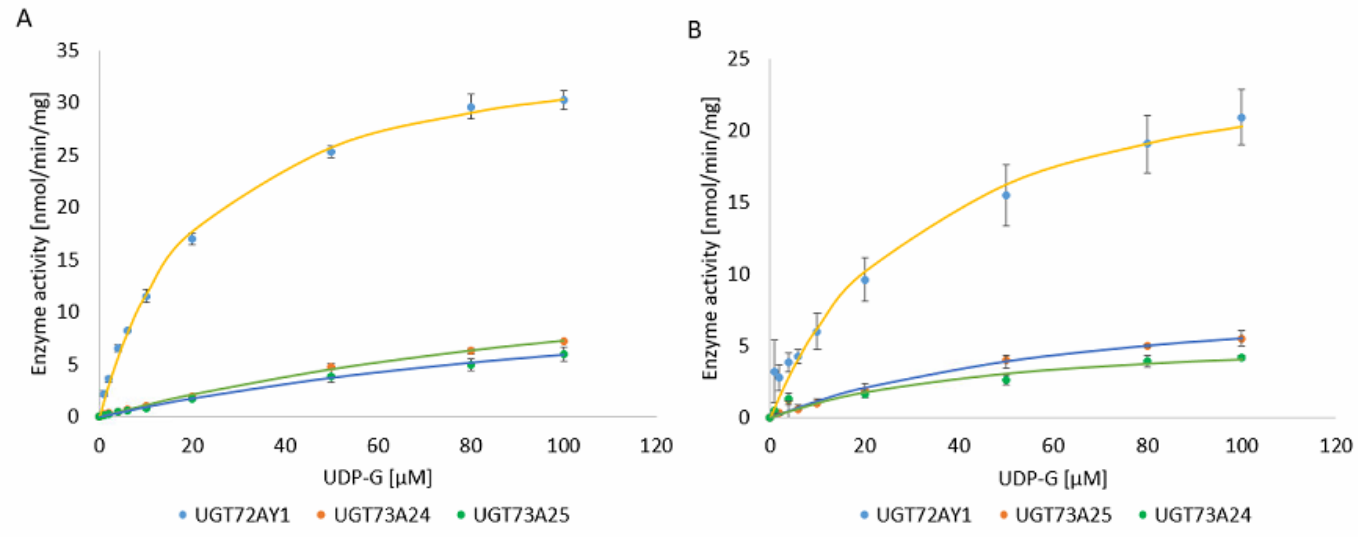

Figure 33. UDP-glucose hydrolase activity of three UGTs. Assays were performed with increasing concentrations of UDP-glucose for UGT72AY1, UGT73A25, and UGT73A24. UDP Glo™ (A) and glucose Glo™ (B) were used to quantify released UDP and glucose, respectively.

4. Discussion

Although glycosyltransferases are widely distributed in the plant kingdom, their substrate preferences and biological effects are largely unknown. This is also true for UGTs from peppermint and tobacco plants, although several *Nicotiana* species have emerged as model organisms in intra- and interspecies interaction studies, plant molecular biology and plant virology (Goodin et al., 2008). Due to the availability of expressed sequence tags (EST) for *Mentha x piperita* and the genome sequence of *N. benthamiana* and extensive transcriptome and metabolome data, we aimed to functionally characterize UGTs that are highly expressed in leaves, roots or flowers. The genome sequence of *N. benthamiana* contains approximately 290 UDP-glycosyltransferase genes (http://benthgenome.qut.edu.au/).

4.1 *In silico* analysis, substrate screening and kinetic assay of NbUGTs

Thirteen CAZy family 1 potential *NbUGTs* were selected and ten encoded proteins were successfully expressed in *E. coli*. Since UGT85A74 and UGT709Q1 failed to transform any of the tested substrates (Table 9) and lacked characteristic features of functional UGTs, such as the GSS motif (Huang et al., 2018) and the catalytic His (Offen et al., 2006), they may represent pseudogenes although they are expressed (Supplementary Figure S1). Even though they are not catalytically active as UGTs, they can still be functional, similar to other types of non-coding DNA and perform regulatory functions.

All remaining tobacco recombinant proteins produced glucosides from phenolic substrates preferring carvacrol, kaempferol, and scopoletin as acceptors, except for UGT85A73, which favored aliphatic alcohols (Figure 23; Table 9). UGT85 enzymes and UGT709Q1 (inactive) formed a separate group in the phylogenetic tree (Figure 12) that support the functional difference. Since considerable transcript levels of *UGT85A73* were found in tobacco flower and the encoded protein preferentially glucosylated non-polar, low molecular weight compounds, we conclude that this enzyme is involed in the conversion of tobacco flower volatiles (Song et al., 2018). Enzymes of the UGT85 family appear to be involved in the glucosylation of volatile alcohols in plants. UGT85s from grape, tea, and kiwifruit were shown to catalyze the

glucosylation of volatiles, including citronellol, geraniol, hexanol, (Z)-3-hexenol, 2-benzyl alcohol, phenylethanol, octanol, and 2,5-dimethyl-4-hydroxy-3(2H)-furanone (furaneol; (Bönisch et al., 2014; Jing et al., 2019; Song et al., 2018). Biochemical analysis of recombinant UGT709C2 protein showed that it possessed catalytic activity towards 7-deoxyloganetate, the precursor of the loganin and secologanin pathway (Asada et al., 2013).

Although members of the UGT family 71, 72 and 73 converted phenols, they could be distinguished by their activity against hydroquinone (Table 9). While UGT71AJ1, UGT72AX1, UGT72AY1, UGT72B35, and UGT72B34 converted benzene-1,4-diol, UGT73A24 and UGT73A25 failed to glucosylate the phenolic compound. Similarly, members of UGT71AJ1 and UGT72 convered benzyl alcohol, but members of the UGT73 family were inactive towards the alcohol. In contrast, borneol was a substrate for the UGT73 enzymes but not for UGT71AJ1 and the UGT72s. UGT71AJ1 does not glucosylate 1-octene-3-ol, which acts as a substrate for the UGT72 and UGT73 enzymes. Thus, the UGT71, 72, and 73 proteins exhibit broad substrate tolerance and overlapping enzymatic activities, but could be distinguished by their preferences for certain metabolites.

Members of the UGT71 family have been shown to be promiscuous enzymes that accept many hydroxycoumarins, flavonoids, naphthols and phytohormones such as (+)-S-abscisic acid (ABA; (Song et al., 2015). This group includes the ABA glucosyltransferase UGT71B6 ((Yonekura-Sakakibara and Hanada, 2011) and UGT71G1 from *Medicago truncatula,* which can glycosylate flavonoids (quercetin) and triterpenoids (medicagenic acid, hederagenin; (Shao et al., 2005)). Similarly, members of the UGT72 family have been shown to function in flavonol (Yin et al., 2017), flavanone, anthocyanin (Zhao et al., 2017) and monolignol glucosylation (Lanot et al., 2006; Lim et al., 2005) and are involved in lignin biosynthesis (Wang et al., 2012). Members of the UGT73 family catalyzed the 3-*O*-glucosylation of the sapogenins oleanolic acid and hederagenin (Augustin et al., 2012; Erthmann et al., 2018) and the conversion of brassinosteroid phytohormons (Poppenberger et al., 2005), while UGT73C6 transferred glucose from UDP-glucose to the 7-OH position of kaempferol 3-*O*-rhamnoside and quercetin 3-*O*-rhamnoside, respectively (Jones et al., 2003). UGT73B3 and UGT73B5 are implicated in the modification of salicylic acid and scopoletin (Simon et al., 2014). Thus, consistent with the published data, UGT71, 72

and 73 from *N. benthamiana* glucosylated phenolic compounds including flavonols, but also produced glucosides from aliphatic alcohols such as terpenoids (Table 9).

4.2 *In silico* analysis, substrate screening and kinetic assay of MpUGTs

Since no *GT*s from mint have yet been characterized, five CAZy family 1 potential *MpUGTs* were selected from an EST database and six encoded proteins were successfully expressed in *E. coli* due to the presence of an allelic form. UGT708M2 and UGT709C8 may represent pseudogenes because they could not accept any of the selected substrates (Table 8), UGT708M2 lacked the catalytic Asp but the highly similar UGT708M1, which also lacked the Asp showed minor enzymatic activity.

The selected MpUGTs showed a narrow substrate tolerance, except for UGT86C10, which accepted 37 out of 40 potential substrates (mainly aromatic compounds, aliphatic alcohols, terpenoids and phenols) and converted them to glucosides. UGT708M1, UGT709C7, and UGT709C6 transformed only 10, 15 and 15 substrates out of 40, respectively. Although the protein sequences of UGT708M1 and UGT708M2 as well as UGT709C7 and UGT709C8 were highly similar, they showed distinct substrate preferences, indicating that the exchange of amino acids altered their function.

Quantitative analysis indicated that UGT708M1 showed highest activity towards naringenin, which is a natural product in mint species but the overall catalytic activity was quite low. Carvacrol and farnesol, two natural volatiles from mint were the preferred substrates of UGT709C6 and UGT86C10 farnesol, respectively.

4.3 Glucosylation of noisoprenoid substrates

Because α- and β-ionol were efficiently glucosylted by seven UGTs from tobacco and mint (UGT72AY1, UGT85A73, UGT73A25, UGT73A24, UGT86C10, UGT709C6 and UGT73B24) additional norisoprenoids obtained by a whole-cell P450 monooxygenase biotransformation were tested as substrates with these UGTs. LC-MS analysis confirmed that the seven UGTs formed monoglucosides of 3-hydroxy-α-ionol, 4-hydroxy-β-ionol, 4-hydroxy-β-ionone, α-ionol and β-ionol. UGT86C10 from mint showed broad substrate tolerance and accepted all nine norisoprenoid substrates. It

readily glucosylated 3-hydroxy-α-ionone, 4-hydroxy-β-ionone, 3-hydroxy-α-damascone, and 4-hydroxy-β-damascone (Table 10). In tobacco, the norisoprenoids 3-hydroxy-β-damascone, 3-hydroxy-β-ionol, 3-hydroxy-7,8-dehydro-β-ionol, 3-oxo-α-ionol, 3-hydroxy-5,6-epoxy-β-ionol, blumenol C, 9-hydroxymegastigma-4,6-dien-3-one isomers, and vomifoliol have been found glycosidically bound while in mint glycosidically bound volatiles have not been characterized until now (Cai et al., 2014). It seems highly probably that the UGTs identified in this study participate in the formation of apocarotinal glucosides in tobacco leaves.

4.4 *In vitro* substrate preference

Since UGT71, 72, and 73 family members converted a number of substrates, quantitative substrate screening was performed using the UDP-Glo™ assay, which quantifies the amount of released UDP (Figure 23). Therefore, the same product was detected for each reaction and no specific standard was required. This allowed a high-throughput screening in a short period and direct comparison of different substrates. Since scopoletin, carvacrol, and kaempferol were converted by all active UGTs in this study, the same assay was used to determine the kinetics data of these substrates.

The substrate preferences (Table 9) are reflected by the kinetic data (Table 12). UGT71AJ1 and members of the UGT72 family exhibited preference for carvacrol expressed by the specificity constant K_{cat}/K_M, except for UGT72AY1, which showed a specificity constant of 233,159 M^{-1} s^{-1} for scopoletin. Although all tested enzymes transformed scopoletin, only TOGT1 (Q9AT54.1 and AAB36653.1 in Figure 12) and TOGT2 (AAB36652.1 and AAK28304.1 in Figure 12) have been characterized as scopoletin UGTs in *N. tabacum* until now (Chong et al., 2002; Chong et al., 1999; Fraissinet-Tachet et al., 1998; Gachon et al., 2004). Scopoletin is present in several plant species and is known to accumulate in *Solanaceous* plants upon infection. It is generally considered an antimicrobial compound, and in many plants and cell suspensions, scopoletin appears as its glucoside scopolin. TOGT1 and TOGT2 from *N. tabacum* are orthologues of UGT73A24 and UGT73A25, which in our study preferentially glucosylated kaempferol and quercetin. The flavonoids have not been previously tested as substrates for TOGT1 and TOGT2. *TOGT1/2* genes have been discovered by mRNA display due to their induction adter salicylic acid treatment of tobacco cell culture (Horvath and Chua, 1996). The induction occurred within the first

one to two hours and was observed upon exposure to a fungal elicitor or to an avirulent pathogen. However, in our study, 7 days after agroinfiltration of an empty vector control, the expression levels of the orthologues *UGT73A24* and *UGT73A25* were not significantly different from those of the untreated wild-type *N. benthamiana* (Figure 26). In contrast, agroinfiltration of *UGT73A24* and *UGT73A25* resulted in a significant increase in the amount of transcripts of both genes (Figure 26), accompanied by the accumulation of rutinosides of quercetin and kaempferol in case of *UGT73A25* (Figure 32) and isomeric glucosides of feruloyl tyramine in case of both genes in the leaves (Figure 29).

4.5 Formation of increased levels of rutinosides upon agroinfiltration

The production of quercetin and kaempferol glucoside, the precursors of the rutinosides, which have been detected in *UGT73A25* agroinfiltrated leaves (Figure 32), can be inferred from the kinetics data, highlighting the preference of UGT73A25 for the flavonoids (Table 12). A highly active rhamnosyltransferase must be present to transfer rhamnose to the flavonoid glucosides to produce the rutinosides. The production of rutin (quercetin rutinoside) by *N. tabacum* has been shown to be affected by light quality (Fu et al., 2016), radical producing agents (Steger-Hartmann et al., 1994) and the transcription factor gene *NtFLS2* (Shi et al., 2017). However, there was no change in rutin levels after treatment of *N. attenuata* with methyl jasmonate (Keinänen et al., 2001).

Since no flavonoids and flavonoid monoglucosides were detected in the leaf samples, it was assumed that they were completely converted to rutinoside. Unexpectedly, accumulation of rutinosides was observed only after agroinfiltration of *UGT73A25,* while the other samples, including the *UGT73A24*-agroinfiltrated leaves did not contain these glycosides (Figure 32). Similarly, overexpression of three homologous *UGT72E* genes, encoding functional UGTs showed only massive accumulation of coniferyl alcohol 4-*O*-glucoside in the case of *UGT72E3* and *UGT72E2,* but not when *UGT72E1* was overexpressed (Lanot et al., 2008). Interestingly, only *UGT72E2* was found to be wound and touch responsive. Therefore, UGT72E2 and UGT73A24 may have different roles in plants compared to other members of their cluster.

4.6 Accumulation of N-feruloyl tyramine glucoside after agroinfiltration

After agroinfiltration of *UGT73A24* and *UGT73A25* in *N. benthamiana* leaves, two glucosides of feruloyl tyramine were identified by untargeted metabolite profiling (Figures 29 and 30). The metabolites were absent in untreated wild-type leaves but were produced upon agroinfiltration of an empty vector and accumulated to high amounts in *UGT73A24* and *UGT73A25*-agroinfiltrated leaves. In contrast, the aglycon feruloyl tyramine was produced at high concentration in the empty vector control sample, but showed a reduced content in the leaves agroinfiltrated with the *UGT* genes. Glucosylation of feruloyl tyramine was independently confirmed by the aglycon library as the hydroxycinnamoyl amide glucosides could be isolated from *N. tabacum* leaves, hydrolyzed by a glycosidase and reconstituted by UGT73A24 and UGT73A25 (Figure 30).

N-feruloyl tyramine is considered to be a phytoalexin because it has antifungal activity and its biosynthesis is caused by wounding and pathogen attack in many species, in particular *Solanaceous* plants (Campos et al., 2014; Guillet and Luca, 2005; Kim et al., 2011; Macoy et al., 2015; Negrel and Jeandet, 1987; Negrel and Martin, 1984; Newman et al., 2001; Zacarés et al., 2007). The amide can be further integrated into cell walls via peroxidase-mediated catalysis yielding ether bonds (Guillet and Luca, 2005). Its main function in plants is probably to strengthen the cell walls and thereby prevent the entry of pathogens into suberizing tissue. The biosynthesis of hydroxycinnamoyl amides has been well studied, but a UGT capable of glucosylating phytoalexins has not been reported so far, although glucosides of the amides have been frequently found (Bolleddula et al., 2012; Geng et al., 2017; Nikolić et al., 2015; Nikolić et al., 2012; Oliveira Silva and Batista, 2017; Pei et al., 2015; Wang et al., 2017; Yahagi et al., 2010; Yang et al., 2012; Yim et al., 2012; Zhang et al., 2013). The biological function of glucosides of hydroxycinnamoyl amides are unclear but they might play a similar role in plant defence like monolignol glucosides (Le Roy et al., 2016). It is assumed that they are required for the transport and programmed delivery of a particular form of monolignols from the intracellular space to specific lignification sites in the cell wall.

4.7 Consequences of the glucosylation of N-feruloyl tyramine

Considering the kinetic data of the two UGTs for different hydroxycinnamoyl amides, it was unexpected to find large amounts of N-feruloyl tyramine glucosides in *UGT73A24*- and *UGT73A25*-agroinfiltrated *N. benthamiana* leaves (Table 12). However, regarding the massive amounts of N-feruloyl tyramine induced by agroinfiltration (Figure 29), it is conceivable that UGT73A24 and UGT73A25 catalyze the conversion of the amides near the maximum reaction rate. Quercetin is the preferred substrate for UGT73A25 *in vitro* and the reaction rate for the flavonol is only 4.4 times higher than that of N-feruloyl tyramine (0.264 sec^{-1} compared with 0.06 sec^{-1}) but the K_M value is 705-fold lower (Table 12). Thus, if the amide concentration clearly exceeds the quercetin content (free quercetin was not detectable in tobacco leaves), the maximum reaction rates become important for assessing product formation. For example, UGT73A25 shows the same reaction rate (0.46 nmol min^{-1} mg^{-1}) for 0.01 and 34 µM of quercetin and N-feruloyl tyramine, respectively (Table 13).

Table 13. Substrate concentrations of quercetin and N-feruloyl tyramine at identical reaction rates of UGT73A25 calculated by the Michaelis-Menten equation.

Reaction rate [nmol min^{-1} mg^{-1}]	Quercetin [µM]	N-feruloyl tyramine [µM]	Ratio (N-feruloyl tyramine/quercetin)
0.00046	0.00001	0.033	3323.1
0.0046	0.0001	0.33	3323.3
0.046	0.001	3.3	3326
0.46	0.01	34	3352
2.3	0.05	174	3473
4.5	0.1	364	3637
8.8	0.2	803	4017
17	0.4	2031	5077
31	0.8	8604	10755
37	1	24396	24396
40	1.1	73350	66682

This 3352-fold ratio, which is required for identical reaction rates rises only slowly at low substrate concentrations, but increases exponential when V_{max} for N-feruoyl tyramine (42 nmol min^{-1} mg^{-1}) is reached (Table 13; Supplemental Figure S8).

The competition between the two substrates for the enzyme was demonstrated by an experiment in which recombinant UGT73A25 was simultaneously incubated with quercetin and N-feruloyl tyramine to demonstrate the ability of the enzyme to produce

two glucosides in the presence of both substrates (Supplemental Figure S8). When N-feruloyl tyramine (3400 µM) was supplied in a 340-fold molar excess than quercetin (10 µM) a significant amount of N-feruloyl tyramine glucosides was produced while the quercetin derivative was hardly detectable. At constant level of N-feruloyl tyramine, increasing concentrations of the flavonol resulted in decreasing levels of N-feruloyl tyramine glucosides, while the amount of quercetin glucoside increased. Therefore, when discussing possible natural substrates for enzymes, it is important to consider the kinetic data of the catalytically active protein, its concentration, and the available substrate levels. In general, UGTs should be considered as multisubstrate enzymes that preferentially transform one substrate but also act on others. The importance of alternative substrate glucosylation becomes apparent when the concentrations of the substrates allow efficient transformation rates and thus product concentrations, as is the case with N-feruloyl-tyramine glucosides.

Due to the production of N-feruloyl amide glucosides during agroinfiltration of *UGT73A24* and *UGT73A25*, the levels of pathogen-responsive metabolites including quinic acid ester, tyramine amides, and aromatic amino acids were decreased in comparison with the sample agroinfiltrated with an empty vector (Figure 31).

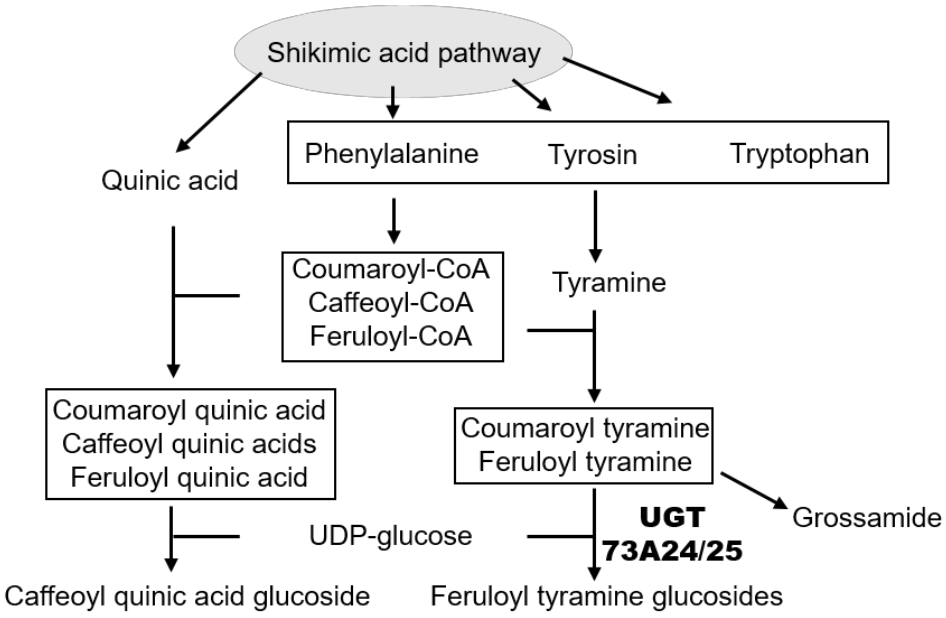

Figure 34. Biosynthetic pathway of feruloyl tyramine glucosides and competing pathways.

Although reduction of the levels of hydroxycinnamoyl amides and esters could be explained by glucosylation, catalyzed by the induced UGT, decreased phenylalanine

concentration, the precursor of the induced metabolites (Figure 34), and tryptophan indicated a feedback inhibition. Similarly, in a double mutant of *UGT78D1/UGT78D2* of *A. thaliana*, in which the initial 3-*O*-glycosylation of favonols was severely impaired, the committed step of the upstream, general phenylpropanoid pathway, phenylalanine ammonia-lyase (PAL), was down regulated in its enzyme activity and in the transcription of *PAL1* and *PAL2* (Yin et al., 2012). In the case of the pathogen-responsive amides, their production and their precursors might be induced at an early stage of the plant's response, but might act autocatalytically in a latter stage. Removal of the amides by glucosylation actually resulted in termination of the process and recovery of the initial levels (Figure 31).

UGTs show promiscuity which seems to be part of their biological role. Promiscuity becomes evident and plays a role when substances enter cell compartments where multi-substrate UGTs are expressed. An obvious example is the immediate conversion of pesticides by plants and the production of pathogen responsive metabolites. Similarly, in transgenic plants, when enzymes are produced in compartments where they are not normally present or when a large number of less preferred substrates are formed upon introduction of a new enzyme, promiscuity of UGTs plays an important role. Consequently, in addition to the enzyme amount and kinetic properties, substrate availability is a determining factor in product formation and accumulation.

Acknowledgement

This research was supported by the China Scholarship Council (CSC) (no. 201506060185) and International Graduate School of Science and Engineering (IGSSE) (no. 10.05)

References

Ahkami, A., Johnson, S.R., Srividya, N., Lange, B.M., 2015. Multiple levels of regulation determine monoterpenoid essential oil compositional variation in the mint family. Molecular Plant 8 (1), 188–191. 10.1016/j.molp.2014.11.009.

Ali, M.S., Saleem, M., Ahmad, W., Parvez, M., Yamdagni, R., 2002. A chlorinated monoterpene ketone, acylated b-sitosterol glycosides and a flavanone glycoside from *Mentha longifolia* (Lamiaceae). Phytochemistry 59, 889–895.

Asada, K., Salim, V., Masada-Atsumi, S., Edmunds, E., Nagatoshi, M., Terasaka, K., Mizukami, H., Luca, V. de, 2013. A 7-deoxyloganetic acid glucosyltransferase contributes a key step in secologanin biosynthesis in Madagascar periwinkle. The Plant Cell 25 (10), 4123–4134. 10.1105/tpc.113.115154.

Augustin, J.M., Drok, S., Shinoda, T., Sanmiya, K., Nielsen, J.K., Khakimov, B., Olsen, C.E., Hansen, E.H., Kuzina, V., Ekstrøm, C.T., Hauser, T., Bak, S., 2012. UDP-glycosyltransferases from the UGT73C subfamily in *Barbarea vulgaris* catalyze sapogenin 3-O-glucosylation in saponin-mediated insect resistance. Plant Physiology 160 (4), 1881–1895. 10.1104/pp.112.202747.

Bak, S., Olsen, C.E., Petersen, B.L., Mùller, B.L., Halkier, B.A., 1999. Metabolic engineering of p-hydroxybenzylglucosinolate in *Arabidopsis* by expression of the cyanogenic CYP79A1 from *Sorghum bicolor*. The Plant Journal 20 (6), 663–671.

Baldwin, I.T., 1999. Inducible nicotine production in native *Nicotiana* as an example of adaptive phenotypic plasticity. Journal of Chemical Ecology 25 (1), 3–30.

Bauer, K., Garbe, D., Surburg, H., 1990. Common fragrance and flavor materials: preparation, properties and uses.: Preparation, properties, and uses, Weinheim, New York.

Baxendale, I., Griffiths-Jones, C., Ley, S., Tranmer, G., 2006. Preparation of the neolignan natural product grossamide by a continuous-flow process. Synlett 2006 (03), 427–430. 10.1055/s-2006-926244.

Berger, R.G., 2007. Flavour and fragrance, 246–550.

Bevan, M.W., Flavell, R.B., Chilton, M.-D., 1983. A chimaeric antibiotic resistance gene as a selectable marker for plant cell transformation. Nature 304 (5922), 184–187. 10.1038/304184a0.

Bolleddula, J., Fitch, W., Vareed, S.K., Nair, M.G., 2012. Identification of metabolites in *Withania sominfera* fruits by liquid chromatography and high-resolution mass spectrometry. Rapid Communications in Mass Spectrometry 26 (11), 1277–1290. 10.1002/rcm.6221.

Bönisch, F., Frotscher, J., Stanitzek, S., Rühl, E., Wüst, M., Bitz, O., Schwab, W., 2014. Activity-based profiling of a physiologic aglycone library reveals sugar acceptor promiscuity of family 1 UDP-glucosyltransferases from grape. Plant Physiology 166 (1), 23–39. 10.1104/pp.114.242578.

Bouvier, F., Suire, C., Mutterer, J., Camaraa, B., 2002. Oxidative remodeling of chromoplast carotenoids: Identification of the carotenoid dioxygenase CsCCD and CsZCD genes involved in crocus secondary metabolite biogenesis. The Plant Cell Online 15 (1), 47–62. 10.1105/tpc.006536.

Bouwmeester, H.J., Roux, C., Lopez-Raez, J.A., Bécard, G., 2007. Rhizosphere communication of plants, parasitic plants and AM fungi. Trends in Plant Science 12 (5), 224–230. 10.1016/j.tplants.2007.03.009.

Bowles, D., Isayenkova, J., Lim, E.-K., Poppenberger, B., 2005. Glycosyltransferases: Managers of small molecules. Current Opinion in Plant Biology 8 (3), 254–263. 10.1016/j.pbi.2005.03.007.

Bowles, D., Lim, E.-K., Poppenberger, B., Vaistij, F.E., 2006. Glycosyltransferases of lipophilic small molecules. Annu. Rev. Plant Biol. 57, 567–597.

Bradford, M., 1976. A rapid and sensitive method for the quantitation of microgram quantities of protein utilizing the principle of protein-dye binding. Analytical Biochemistry 72 (1-2), 248–254. 10.1006/abio.1976.9999.

Brahmi, F., Khodir, M., Mohamed, C., Pierre, D., 2017. Chemical composition and biological activities of *Mentha* species, in: El-Shemy, H.A. (Ed.), Aromatic and Medicinal Plants - back to Nature. InTech, pp. 47–79.

Brandi, F., Bar, E., Mourgues, F., Horváth, G., Turcsi, E., Giuliano, G., Liverani, A., Tartarini, S., Lewinsohn, E., Rosati, C., 2011. Study of 'Redhaven' peach and its white-fleshed mutant suggests a key role of CCD4 carotenoid dioxygenase in carotenoid and norisoprenoid volatile metabolism. BMC Plant Biology 11, 24. 10.1186/1471-2229-11-24.

Breton, C., Snajdrová, L., Jeanneau, C., Koca, J., Imberty, A., 2006. Structures and mechanisms of glycosyltransferases. Glycobiology 16 (2), 29R-37R. 10.1093/glycob/cwj016.

Bungaruang, L., Gutmann, A., Nidetzky, B., 2013. Leloir glycosyltransferases and natural product glycosylation: Biocatalytic synthesis of the C-glucoside nothofagin, a major antioxidant of redbush herbal tea. Advanced Synthesis & Catalysis 355 (14-15), 2757–2763. 10.1002/adsc.201300251.

Burton, H.R., Kasperbauer, M.J., 1985. Changes in chemical composition of tobacco lamina during senescence and curing. 1. plastid pigments. Journal of Agricultural and Food Chemistry 33, 879–883.

Busch, M., Seuter, A., Hain, R., 2002. Functional analysis of the early steps of carotenoid biosynthesis in tobacco. Plant Physiology 128 (2), 439–453. 10.1104/pp.010573.

Cai, K., Zhao, H., Xiang, Z., Cai, B., Pan, W., Lei, B., 2014. Enzymatic hydrolysis followed by gas chromatography-mass spectroscopy for determination of glycosides in tobacco and method optimization by response surface methodology. Analytical Methods 6 (17), 7006. 10.1039/C4AY01056F.

Campos, L., Lisón, P., López-Gresa, M.P., Rodrigo, I., Zacarés, L., Conejero, V., Bellés, J.M., 2014. Transgenic tomato plants overexpressing tyramine N-hydroxycinnamoyltransferase exhibit elevated hydroxycinnamic acid amide levels and enhanced resistance to *Pseudomonas syringae*. Molecular Plant-Microbe Interactions 27 (10), 1159–1169. 10.1094/MPMI-04-14-0104-R.

Canadanovic-Brunet, J.M., Djilas, S.M., Cetkovic, G.S., Tumbas, V.T., 2005. Free-radical scavenging activity of wormwood (*Artemisia absinthium* L) extracts. Journal of the Science of Food and Agriculture 85 (2), 265–272. 10.1002/jsfa.1950.

Cardullo, N., Pulvirenti, L., Spatafora, C., Musso, N., Barresi, V., Condorelli, D.F., Tringali, C., 2016. Dihydrobenzofuran neolignanamides: laccase-mediated biomimetic synthesis and antiproliferative activity. Journal of Natural Products 79 (8), 2122–2134. 10.1021/acs.jnatprod.6b00577.

Chakraborty, A., Chattopadhyay, S., 2008. Stimulation of menthol production in *Mentha piperita* cell culture. In Vitro Cellular & Developmental Biology - Plant 44 (6), 518–524. 10.1007/s11627-008-9145-y.

Champagne, A., Boutry, M., 2013. Proteomic snapshot of spearmint (*Mentha spicata* L.) leaf trichomes: a genuine terpenoid factory. Proteomics 13 (22), 3327–3332. 10.1002/pmic.201300280.

Cho, K., Kim, Y., Wi, S.J., Seo, J.B., Kwon, J., Chung, J.H., Park, K.Y., Nam, M.H., 2012. Nontargeted metabolite profiling in compatible pathogen-inoculated tobacco (*Nicotiana tabacum* L. cv. Wisconsin 38) using UPLC-Q-TOF/MS. Journal of Agricultural and Food Chemistry 60 (44), 11015–11028. 10.1021/jf303702j.

Choi, S.-K., Osawa, A., Maoka, T., Hattan, J.-I., Ito, K., Uchiyama, A., Suzuki, M., Shindo, K., Misawa, N., 2013. 3-β-Glucosyl-3'-β-quinovosyl zeaxanthin, a novel carotenoid glycoside synthesized by *Escherichia coli* cells expressing the *Pantoea ananatis* carotenoid biosynthesis gene cluster. Applied Microbiology and Biotechnology 97 (19), 8479–8486. 10.1007/s00253-013-5101-9.

Chong, J., Baltz, R., Fritig, B., Saindrenan, P., 1999. An early salicylic acid-, pathogen- and elicitor-inducible tobacco glucosyltransferase: role in compartmentalization of phenolics and H_2O_2 metabolism. FEBS Letters 458 (2), 204–208. 10.1016/S0014-5793(99)01154-0.

Chong, J., Baltz, R., Schmitt, C., Beffa, R., Fritig, B., Saindrenanan, P., 2002. Downregulation of a pathogen-responsive tobacco UDP-Glc:Phenylpropanoid glucosyltransferase reduces scopoletin glucoside accumulation, enhances oxidative stress, and weakens virus resistance. The Plant Cell 14 (5), 1093–1107. 10.1105/tpc.010436.

Croteau, R.B., Davis, E.M., Ringer, K.L., Wildung, M.R., 2005. (-)-Menthol biosynthesis and molecular genetics. Die Naturwissenschaften 92 (12), 562–577. 10.1007/s00114-005-0055-0.

Crupi, P., Coletta, A., Milella, R.A., Palmisano, G., Baiano, A., La Notte, E., Antonacci, D., 2010. Carotenoid and chlorophyll-derived compounds in some wine grapes grown in apulian region. Journal of Food Science 75 (4), S191-8. 10.1111/j.1750-3841.2010.01564.x.

Dong, L., Jongedijk, E., Bouwmeester, H., van der Krol, A., 2016. Monoterpene biosynthesis potential of plant subcellular compartments. The New Phytologist 209 (2), 679–690. 10.1111/nph.13629.

Dong, L., Miettinen, K., Goedbloed, M., Verstappen, F.W.A., Voster, A., Jongsma, M.A., Memelink, J., van der Krol, S., Bouwmeester, H.J., 2013. Characterization of two geraniol synthases from *Valeriana officinalis* and *Lippia dulcis*: Similar activity but difference in subcellular localization. Metabolic Engineering 20, 198–211. 10.1016/j.ymben.2013.09.002.

Dorman, H.J.D., Koşar, M., Kahlos, K., Holm, Y., Hiltunen, R., 2003. Antioxidant properties and composition of aqueous extracts from *Mentha* species, hybrids, varieties, and cultivars. Journal of Agricultural and Food Chemistry 51 (16), 4563–4569. 10.1021/jf034108k.

Eccles, R., 1994. Menthol and related cooling compounds. J. Pharm. Pharmacol. 46, 618–630.

Enyedi, A.J., Raskin, I., 1993. Induction of UDP-Glucose:Salicylic acid glucosyltransferase activity in Tobacco Mosaic Virus-inoculated tobacco (*Nicotiana tabacum*) leaves. Plant Physiology 101 (4), 1375–1380. 10.1104/pp.101.4.1375.

Enzell, C., 1985. Biodegradation of carotenoids—an important route to aroma compounds. Pure & Appl. Chem. 57 (5), 693–700.

Erthmann, P.Ø., Agerbirk, N., Bak, S., 2018. A tandem array of UDP-glycosyltransferases from the UGT73C subfamily glycosylate sapogenins, forming a spectrum of mono- and bisdesmosidic saponins. Plant Molecular Biology 97 (1-2), 37–55. 10.1007/s11103-018-0723-z.

Fernández-García, E., Carvajal-Lérida, I., Jarén-Galán, M., Garrido-Fernández, J., Pérez-Gálvez, A., Hornero-Méndez, D., 2012. Carotenoids bioavailability from foods: from plant pigments to efficient biological activities. Food Research International 46 (2), 438–450. 10.1016/j.foodres.2011.06.007.

Fraissinet-Tachet, L., Baltz, R., Chong, J., Kauffmann, S., Fritig, B., Saindrenan, P., 1998. Two tobacco genes induced by infection, elicitor and salicylic acid encode glucosyltransferases acting on phenylpropanoids and benzoic acid derivatives, including salicylic acid. FEBS Letters 437 (3), 319–323.

Frusciante, S., Diretto, G., Bruno, M., Ferrante, P., Pietrella, M., Prado-Cabrero, A., Rubio-Moraga, A., Beyer, P., Gomez-Gomez, L., Al-Babili, S., Giuliano, G., 2014. Novel carotenoid cleavage dioxygenase catalyzes the first dedicated step in saffron crocin biosynthesis. Proceedings of the National Academy of Sciences of the United States of America 111 (33), 12246–12251. 10.1073/pnas.1404629111.

Fu, B., Ji, X., Zhao, M., He, F., Wang, X., Wang, Y., Liu, P., Niu, L., 2016. The influence of light quality on the accumulation of flavonoids in tobacco (*Nicotiana tabacum* L.) leaves. Journal of Photochemistry and Photobiology. B, Biology 162, 544–549. 10.1016/j.jphotobiol.2016.07.016.

Gachon, C., Baltz, R., Saindrenan, P., 2004. Over-expression of a scopoletin glucosyltransferase in *Nicotiana tabacum* leads to precocious lesion formation during the hypersensitive response to

Tobacco Mosaic Virus but does not affect virus resistance. Plant Molecular Biology 54 (1), 137–146. 10.1023/B:PLAN.0000028775.58537.fe.

Geng, P., Harnly, J.M., Sun, J., Zhang, M., Chen, P., 2017. Feruloyl dopamine-O-hexosides are efficient marker compounds as orthogonal validation for authentication of black cohosh (*Actaea racemosa*)-an UHPLC-HRAM-MS chemometrics study. Analytical and Bioanalytical Chemistry 409 (10), 2591–2600. 10.1007/s00216-017-0205-1.

Gomez-Roldan, V., Fermas, S., Brewer, P.B., Puech-Pagès, V., Dun, E.A., Pillot, J.-P., Letisse, F., Matusova, R., Danoun, S., Portais, J.-C., Bouwmeester, H., Bécard, G., Beveridge, C.A., Rameau, C., Rochange, S.F., 2008. Strigolactone inhibition of shoot branching. Nature 455 (7210), 189–194. 10.1038/nature07271.

Goodin, M.M., Zaitlin, D., Naidu, R.A., Lommel, S.A., 2008. *Nicotiana benthamiana*: its history and future as a model for plant-pathogen interactions. Molecular Plant-Microbe Interactions 21 (8), 1015–1026. 10.1094/MPMI-21-8-1015.

Guedon, D.J., Pasquier, B.P., 1994. Analysis and distribution of flavonoid glycosides and rosmarinic acid in 40 *Mentha x piperita* clones. Journal of Agricultural and Food Chemistry 42 (3), 679–684. 10.1021/jf00039a015.

Gui, J., Fu, X., Zhou, Y., Katsuno, T., Mei, X., Deng, R., Xu, X., Zhang, L., Dong, F., Watanabe, N., Yang, Z., 2015. Does enzymatic hydrolysis of glycosidically bound volatile compounds really contribute to the formation of volatile compounds during the oolong tea manufacturing process? Journal of Agricultural and Food Chemistry 63 (31), 6905–6914. 10.1021/acs.jafc.5b02741.

Guillet, G., Luca, V. de, 2005. Wound-inducible biosynthesis of phytoalexin hydroxycinnamic acid amides of tyramine in tryptophan and tyrosine decarboxylase transgenic tobacco lines. Plant Physiology 137 (2), 692–699. 10.1104/pp.104.050294.

Gulati, J., Kim, S.-G., Baldwin, I.T., Gaquerel, E., 2013. Deciphering herbivory-induced gene-to-metabolite dynamics in *Nicotiana attenuata* tissues using a multifactorial approach. Plant Physiology 162 (2), 1042–1059. 10.1104/pp.113.217588.

Guvenalp, Z., Ozbek, H., Karadayi, M., Gulluce, M., Kuruuzum-Uz, A., Salih, B., Demirezer, O., 2015. Two antigenotoxic chalcone glycosides from *Mentha longifolia* subsp. *longifolia*. Pharmaceutical Biology 53 (6), 888–896. 10.3109/13880209.2014.948633.

Heider, S.A.E., Peters-Wendisch, P., Netzer, R., Stafnes, M., Brautaset, T., Wendisch, V.F., 2014. Production and glucosylation of C50 and C 40 carotenoids by metabolically engineered *Corynebacterium glutamicum*. Applied Microbiology and Biotechnology 98 (3), 1223–1235. 10.1007/s00253-013-5359-y.

Heiling, S., Khanal, S., Barsch, A., Zurek, G., Baldwin, I.T., Gaquerel, E., 2016. Using the knowns to discover the unknowns: MS-based dereplication uncovers structural diversity in 17-hydroxygeranyllinalool diterpene glycoside production in the *Solanaceae*. The Plant Journal 85 (4), 561–577. 10.1111/tpj.13119.

Hellemans, J., Mortier, G., Paepe, A. de, Speleman, F., Vandesompele, J., 2007. qBase relative quantification framework and software for management and automated analysis of real-time quantitative PCR data. Genome Biology 8 (2), R19. 10.1186/gb-2007-8-2-r19.

Hino, F., Okazaki, M., Miura, Y., 1982. Effect of 2,4-dichlorophenoxyacetic acid on glucosylation of scopoletin to scopolin in tobacco tissue culture. Plant Physiology 69 (4), 810–813.

Hirschberg, J., 2001. Carotenoid biosynthesis in flowering plants. Physiology and Metabolism 4, 210–218.

Höfer, R., Dong, L., André, F., Ginglinger, J.-F., Lugan, R., Gavira, C., Grec, S., Lang, G., Memelink, J., van der Krol, S., Bouwmeester, H., Werck-Reichhart, D., 2013. Geraniol hydroxylase and hydroxygeraniol oxidase activities of the CYP76 family of cytochrome P450 enzymes and potential

for engineering the early steps of the (seco)iridoid pathway. Metabolic Engineering 20, 221–232. 10.1016/j.ymben.2013.08.001.

Hoffman, B.G., Lunder, L.T., 1984. Flavonoids from *Mentha piperita* leaves. Planta Med. (51), 361.

Höfgen, R., Willmitzer, L., 1988. Storage of competent cells for *Agrobacterium* transformation. Nucleic Acids Research 16 (20), 9877.

Horvath, D.M., Chua, N.H., 1996. Identification of an immediate-early salicylic acid-inducible tobacco gene and characterization of induction by other compounds. Plant Molecular Biology 31 (5), 1061–1072.

Hu, Y., Walker, S., 2002. Remarkable structural similarities between diverse glycosyltransferases. Chemistry & Biology 9 (12), 1287–1296. 10.1016/S1074-5521(02)00295-8.

Huang, F.-C., Giri, A., Daniilidis, M., Sun, G., Härtl, K., Hoffmann, T., Schwab, W., 2018. Structural and functional analysis of UGT92G6 suggests an evolutionary link between mono- and disaccharide glycoside-forming transferases. Plant & Cell Physiology 59 (4), 857–870. 10.1093/pcp/pcy028.

Huang, F.-C., Hinkelmann, J., Schwab, W., 2015. Glucosylation of aroma chemicals and hydroxy fatty acids. Journal of Biotechnology 216, 100–109. 10.1016/j.jbiotec.2015.10.011.

Huang, F.-C., Studart-Witkowski, C., Schwab, W., 2010. Overexpression of hydroperoxide lyase gene in *Nicotiana benthamiana* using a viral vector system. Plant Biotechnology Journal 8 (7), 783–795. 10.1111/j.1467-7652.2010.00508.x.

Ibdah, M., Dubey, N.K., Eizenberg, H., Dabour, Z., Abu-Nassar, J., Gal-On, A., Aly, R., 2014. Cucumber Mosaic Virus as a carotenoid inhibitor reducing *Phelipanche aegyptiaca* infection in tobacco plants. Plant Signaling & Behavior 9 (10), e972146. 10.4161/psb.32096.

Jassbi, A.R., Gase, K., Hettenhausen, C., Schmidt, A., Baldwin, I.T., 2008. Silencing geranylgeranyl diphosphate synthase in *Nicotiana attenuata* dramatically impairs resistance to tobacco hornworm. Plant Physiology 146 (3), 974–986. 10.1104/pp.107.108811.

Jassbi, A.R., Zamanizadehnajari, S., Baldwin, I.T., 2010. 17-Hydroxygeranyllinalool glycosides are major resistance traits of *Nicotiana obtusifolia* against attack from tobacco hornworm larvae. Phytochemistry 71 (10), 1115–1121. 10.1016/j.phytochem.2010.04.014.

Jassbi, A.R., Zare, S., Asadollahi, M., Schuman, M.C., 2017. Ecological roles and biological activities of specialized metabolites from the genus *Nicotiana*. Chemical Reviews 117 (19), 12227–12280. 10.1021/acs.chemrev.7b00001.

Jing, T., Zhang, N., Gao, T., Zhao, M., Jin, J., Chen, Y., Xu, M., Wan, X., Schwab, W., Song, C., 2019. Glucosylation of (Z)-3-hexenol informs intraspecies interactions in plants: A case study in Camellia sinensis. Plant, Cell & Environment 42 (4), 1352–1367. 10.1111/pce.13479.

Jones, P., Messner, B., Nakajima, J.-I., Schäffner, A.R., Saito, K., 2003. UGT73C6 and UGT78D1, glycosyltransferases involved in flavonol glycoside biosynthesis in *Arabidopsis thaliana*. The Journal of Biological Chemistry 278 (45), 43910–43918. 10.1074/jbc.M303523200.

Jones, P., Vogt, T., 2001. Glycosyltransferases in secondary plant metabolism: Tranquilizers and stimulant controllers. Planta 213 (2), 164–174. 10.1007/s004250000492.

Kaiser, R., 1993. The scent of orchids: Olfactory and chemical investigations. New York; Elsevier Science Publishers; Editiones Roche, Amsterdam, Basel, 259 pp.

Keinänen, M., Oldham, N.J., Baldwin, I.T., 2001. Rapid HPLC screening of jasmonate-induced increases in tobacco alkaloids, phenolics, and diterpene glycosides in *Nicotiana attenuata*. Journal of Agricultural and Food Chemistry 49 (8), 3553–3558.

Kim, S.-G., Yon, F., Gaquerel, E., Gulati, J., Baldwin, I.T., 2011. Tissue specific diurnal rhythms of metabolites and their regulation during herbivore attack in a native tobacco, *Nicotiana attenuata*. PloS one 6 (10), e26214. 10.1371/journal.pone.0026214.

Kodama, H., Fujimori, T., Kato, K., 1984. A nor-sesquiterpene glycoside, rishitin-β-sophoroside, from tobacco. Phytochemistry 23 (3), 690–692. 10.1016/S0031-9422(00)80412-4.

Kohlen, W., Charnikhova, T., Lammers, M., Pollina, T., Tóth, P., Haider, I., Pozo, M.J., Maagd, R.A. de, Ruyter-Spira, C., Bouwmeester, H.J., López-Ráez, J.A., 2012. The tomato carotenoid cleavage DIOXYGENASE8 (SlCCD8) regulates rhizosphere signaling, plant architecture and affects reproductive development through strigolactone biosynthesis. The New Phytologist 196 (2), 535–547. 10.1111/j.1469-8137.2012.04265.x.

Koşar, M., Dorman, H.J.D., Can Başer, K.H., Hiltunen, R., 2004. Screening of free radical scavenging compounds in water extracts of *Mentha* samples using a postcolumn derivatization method. Journal of Agricultural and Food Chemistry 52 (16), 5004–5010. 10.1021/jf0496189.

Krammer, G., Winterhalter, P., Schwab, M., Schreier, P., 1991. Glycosidically bound aroma compounds in the fruits of *Prunus* species: Apricot (*P*. *armeniaca*, L.), peach (*P*. *persica*, L.), yellow plum (*P*. *domestica*, L. ssp. syriaca). Journal of Agricultural and Food Chemistry 39 (4), 778–781. 10.1021/jf00004a032.

Kumar, P., Mishra, S., Malik, A., Satya, S., 2011. Insecticidal properties of *Mentha* species: A review. Industrial Crops and Products 34 (1), 802–817. 10.1016/j.indcrop.2011.02.019.

Kumar, R., Sangwan, R.S., Mishra, S., Sabir, F., Sangwan, N.S., 2012. In silico motif diversity analysis of the glycon preferentiality of plant secondary metabolic glycosyltransferases. Plant Omics Journal 5 (3), 200–210.

Lairson, L.L., Henrissat, B., Davies, G.J., Withers, S.G., 2008. Glycosyltransferases: Structures, functions, and mechanisms. Annual Review of Biochemistry 77, 521–555. 10.1146/annurev.biochem.76.061005.092322.

Lanot, A., Hodge, D., Jackson, R.G., George, G.L., Elias, L., Lim, E.-K., Vaistij, F.E., Bowles, D.J., 2006. The glucosyltransferase UGT72E2 is responsible for monolignol 4-O-glucoside production in *Arabidopsis thaliana*. The Plant Journal 48 (2), 286–295. 10.1111/j.1365-313X.2006.02872.x.

Lanot, A., Hodge, D., Lim, E.-K., Vaistij, F.E., Bowles, D.J., 2008. Redirection of flux through the phenylpropanoid pathway by increased glucosylation of soluble intermediates. Planta 228 (4), 609–616. 10.1007/s00425-008-0763-8.

Le Roy, J., Huss, B., Creach, A., Hawkins, S., Neutelings, G., 2016. Glycosylation is a major regulator of phenylpropanoid availability and biological activity in plants. Frontiers in Plant Science 7, 735. 10.3389/fpls.2016.00735.

Lee, H.I., Raskin, I., 1999. Purification, cloning, and expression of a pathogen inducible UDP-glucose:Salicylic acid glucosyltransferase from tobacco. The Journal of Biological Chemistry 274 (51), 36637–36642.

Lee, P.C., Schmidt-Dannert, C., 2002. Metabolic engineering towards biotechnological production of carotenoids in microorganisms. Applied Microbiology and Biotechnology 60 (1-2), 1–11. 10.1007/s00253-002-1101-x.

Liang, D.-M., Liu, J.-H., Wu, H., Wang, B.-B., Zhu, H.-J., Qiao, J.-J., 2015. Glycosyltransferases: Mechanisms and applications in natural product development. Chemical Society Reviews 44 (22), 8350–8374. 10.1039/c5cs00600g.

Liao, Z., Chen, M., Guo, L., Gong, Y., Tang, F., Sun, X., Tang, K., 2004. Rapid isolation of high-quality total RNA from taxus and ginkgo. Preparative Biochemistry & Biotechnology 34 (3), 209–214. 10.1081/PB-200026790.

Lim, E.-K., Jackson, R.G., Bowles, D.J., 2005. Identification and characterisation of *Arabidopsis* glycosyltransferases capable of glucosylating coniferyl aldehyde and sinapyl aldehyde. FEBS Letters 579 (13), 2802–2806. 10.1016/j.febslet.2005.04.016.

Ma, G., Zhang, L., Matsuta, A., Matsutani, K., Yamawaki, K., Yahata, M., Wahyudi, A., Motohashi, R., Kato, M., 2013. Enzymatic formation of β-citraurin from β-cryptoxanthin and zeaxanthin by carotenoid cleavage dioxygenase4 in the flavedo of citrus fruit. Plant Physiology 163 (2), 682–695. 10.1104/pp.113.223297.

Macoy, D.M., Kim, W.-Y., Lee, S.Y., Kim, M.G., 2015. Biotic stress related functions of hydroxycinnamic acid amide in plants. Journal of Plant Biology 58 (3), 156–163. 10.1007/s12374-015-0104-y.

Maicas, S., Mateo, J.J., 2005. Hydrolysis of terpenyl glycosides in grape juice and other fruit juices: a review. Applied Microbiology and Biotechnology 67 (3), 322–335. 10.1007/s00253-004-1806-0.

Maldonado-Robledo, G., Rodriguez-Bustamante, E., Sanchez-Contreras, A., Rodriguez-Sanoja, R., Sanchez, S., 2003. Production of tobacco aroma from lutein. Specific role of the microorganisms involved in the process. Applied Microbiology and Biotechnology 62 (5-6), 484–488. 10.1007/s00253-003-1315-6.

Manosroi, J., Dhumtanom, P., Manosroi, A., 2006. Anti-proliferative activity of essential oil extracted from Thai medicinal plants on KB and P388 cell lines. Cancer Letters 235 (1), 114–120. 10.1016/j.canlet.2005.04.021.

Marillonnet, S., Giritch, A., Gils, M., Kandzia, R., Klimyuk, V., Gleba, Y., 2004. In planta engineering of viral RNA replicons: Efficient assembly by recombination of DNA modules delivered by *Agrobacterium*. Proceedings of the National Academy of Sciences of the United States of America 101 (18), 6852–6857. 10.1073/pnas.0400149101.

Marillonnet, S., Thoeringer, C., Kandzia, R., Klimyuk, V., Gleba, Y., 2005. Systemic *Agrobacterium* tumefaciens-mediated transfection of viral replicons for efficient transient expression in plants. Nature Biotechnology 23 (6), 718–723. 10.1038/nbt1094.

Matros, A., Mock, H.-P., 2004. Ectopic expression of a UDP-glucose:Phenylpropanoid glucosyltransferase leads to increased resistance of transgenic tobacco plants against infection with *Potato Virus Y*. Plant & Cell Physiology 45 (9), 1185–1193. 10.1093/pcp/pch140.

McKay, D.L., Blumberg, J.B., 2006. A review of the bioactivity and potential health benefits of peppermint tea (*Mentha piperita* L.). Phytotherapy Research 20 (8), 619–633. 10.1002/ptr.1936.

Mein, J.R., Dolnikowski, G.G., Ernst, H., Russell, R.M., Wang, X.-D., 2011. Enzymatic formation of apo-carotenoids from the xanthophyll carotenoids lutein, zeaxanthin and β-cryptoxanthin by ferret carotene-9',10'-monooxygenase. Archives of Biochemistry and Biophysics 506 (1), 109–121. 10.1016/j.abb.2010.11.005.

Mhlongo, M.I., Piater, L.A., Madala, N.E., Steenkamp, P.A., Dubery, I.A., 2016a. Phenylpropanoid defences in *Nicotiana tabacum* cells: Overlapping metabolomes indicate common aspects to priming responses induced by lipopolysaccharides, chitosan and flagellin-22. PloS one 11 (3), e0151350. 10.1371/journal.pone.0151350.

Mhlongo, M.I., Steenkamp, P.A., Piater, L.A., Madala, N.E., Dubery, I.A., 2016b. Profiling of altered metabolomic states in *Nicotiana tabacum* cells induced by priming agents. Frontiers in Plant Science 7, 1527. 10.3389/fpls.2016.01527.

Mohammad Hosein Farzaei, Roodabeh Bahramsoltani, Ali Ghobadi, Fatemeh Farzaei, Fariba Najafi, 2017. Pharmacological activity of *Mentha longifolia* and its phytoconstituents. J Tradit Chin Med 37 (5), 710–720.

Monte, F.J.Q., Kintzinger J.P., Trendel J.M., Poinsot, J., 1997. Mixture of closely related isomeric triterpenoid derivatives: Separation and purification by reversed-phase high-performance liquid chromatography. Chromatographia (46), 251–255.

Moreno, J.C., Cerda, A., Simpson, K., Lopez-Diaz, I., Carrera, E., Handford, M., Stange, C., 2016. Increased *Nicotiana tabacum* fitness through positive regulation of carotenoid, gibberellin and chlorophyll pathways promoted by Daucus carota lycopene β-cyclase (Dclcyb1) expression. Journal of Experimental Botany 67 (8), 2325–2338. 10.1093/jxb/erw037.

Negrel, J., Jeandet, P., 1987. Metabolism of tyramine and feruloyltyramine in TMV inoculated leaves of *Nicotiana tabacum*. Phytochemistry 26 (8), 2185–2190. 10.1016/S0031-9422(00)84681-6.

Negrel, J., Martin, C., 1984. The biosynthesis of feruloyltyramine in *Nicotiana tabacum*. Phytochemistry 23 (12), 2797–2801. 10.1016/0031-9422(84)83018-6.

Newman, M.A., Roepenack-Lahaye, E. von, Parr, A., Daniels, M.J., Dow, J.M., 2001. Induction of hydroxycinnamoyl-tyramine conjugates in pepper by *Xanthomonas campestris*, a plant defense response activated by *hrp* gene-dependent and *hrp* gene-independent mechanisms. Molecular Plant-Microbe Interactions 14 (6), 785–792. 10.1094/MPMI.2001.14.6.785.

Nikolić, D., Gödecke, T., Chen, S.-N., White, J., Lankin, D.C., Pauli, G.F., van Breemen, R.B., 2012. Mass spectrometric dereplication of nitrogen-containing constituents of black cohosh (*Cimicifuga racemosa* L.). Fitoterapia 83 (3), 441–460. 10.1016/j.fitote.2011.12.006.

Nikolić, D., Lankin, D.C., Cisowska, T., Chen, S.-N., Pauli, G.F., van Breemen, R.B., 2015. Nitrogen-containing constituents of black cohosh: Chemistry, structure elucidation, and biological activities. Recent Advances in Phytochemistry 45, 31–75. 10.1007/978-3-319-20397-3_2.

Nugroho, L.H., Verpoorte, R., 2002. Secondary metabolism in tobacco. Plant Cell, Tissue and Organ Culture 68 (2), 105–125. 10.1023/A:1013853909494.

Offen, W., Martinez-Fleites, C., Yang, M., Kiat-Lim, E., Davis, B.G., Tarling, C.A., Ford, C.M., Bowles, D.J., Davies, G.J., 2006. Structure of a flavonoid glucosyltransferase reveals the basis for plant natural product modification. The EMBO Journal 25 (6), 1396–1405. 10.1038/sj.emboj.7600970.

Oliveira Silva, E. de, Batista, R., 2017. Ferulic acid and naturally occurring compounds bearing a feruloyl moiety: a review on their structures, occurrence, and potential health benefits. Comprehensive Reviews in Food Science and Food Safety 16 (4), 580–616. 10.1111/1541-4337.12266.

Onkokesung, N., Gaquerel, E., Kotkar, H., Kaur, H., Baldwin, I.T., Galis, I., 2012. MYB8 controls inducible phenolamide levels by activating three novel hydroxycinnamoyl-coenzyme A:Polyamine transferases in *Nicotiana attenuata*. Plant Physiology 158 (1), 389–407. 10.1104/pp.111.187229.

Osmani, S.A., Bak, S., Møller, B.L., 2009. Substrate specificity of plant UDP-dependent glycosyltransferases predicted from crystal structures and homology modeling. Phytochemistry 70 (3), 325–347. 10.1016/j.phytochem.2008.12.009.

Pang, T., Yuan, Z., Dai, Y., Wang, C., Yang, J., Peng, L., Xu, G., 2007. Identification and determination of glycosides in tobacco leaves by liquid chromatography with atmospheric pressure chemical ionization tandem mass spectrometry. Journal of Separation Science 30 (3), 289–296. 10.1002/jssc.200600236.

Pei, K., Ou, J., Huang, C., Ou, S., 2015. Derivatives of ferulic acid: structure, preparation and biological activities. Annual Research & Review in Biology 5 (6), 512–528. 10.9734/ARRB/2015/14104.

Pereira, O.R., Cardoso, S.M., 2013. Overview on *Mentha* and *Thymus* polyphenols. Current Analytical Chemistry 9, 382–396.

Petitpierre, B., Kueffer, C., Broennimann, O., Randin, C., Daehler, C., Guisan, A., 2012. Climatic niche shifts are rare among terrestrial plant invaders. Science 335 (6074), 1344–1348. 10.1126/science.1215933.

Pflugmacher, S., Schroeder, P., Sandermann Jr., H., 2000. Taxonomic distribution of plant glutathione S-transferases acting on xenobiotics. Phytochemistry 54, 267–273.

Poppenberger, B., Fujioka, S., Soeno, K., George, G.L., Vaistij, F.E., Hiranuma, S., Seto, H., Takatsuto, S., Adam, G., Yoshida, S., Bowles, D., 2005. The UGT73C5 of *Arabidopsis thaliana* glucosylates brassinosteroids. Proceedings of the National Academy of Sciences of the United States of America 102 (42), 15253–15258. 10.1073/pnas.0504279102.

Reed, J., Osbourn, A., 2018. Engineering terpenoid production through transient expression in *Nicotiana benthamiana*. Plant Cell Reports 37 (10), 1431–1441. 10.1007/s00299-018-2296-3.

Ring, L., Yeh, S.-Y., Hücherig, S., Hoffmann, T., Blanco-Portales, R., Fouche, M., Villatoro, C., Denoyes, B., Monfort, A., Caballero, J.L., Muñoz-Blanco, J., Gershenson, J., Schwab, W., 2013. Metabolic interaction between anthocyanin and lignin biosynthesis is associated with peroxidase FaPRX27 in strawberry fruit. Plant Physiology 163 (1), 43–60. 10.1104/pp.113.222778.

Rodríguez-Bustamante, E., Maldonado-Robledo, G., Ortiz, M.A., Díaz-Avalos, C., Sanchez, S., 2005. Bioconversion of lutein using a microbial mixture--maximizing the production of tobacco aroma compounds by manipulation of culture medium. Applied Microbiology and Biotechnology 68 (2), 174–182. 10.1007/s00253-004-1868-z.

Rodríguez-Bustamante, E., Sánchez, S., 2007. Microbial production of C13-norisoprenoids and other aroma compounds via carotenoid cleavage. Critical Reviews in Microbiology 33 (3), 211–230. 10.1080/10408410701473306.

Rubio, A., Rambla, J.L., Santaella, M., Gómez, M.D., Orzaez, D., Granell, A., Gómez-Gómez, L., 2008. Cytosolic and plastoglobule-targeted carotenoid dioxygenases from *Crocus sativus* are both involved in beta-ionone release. The Journal of Biological Chemistry 283 (36), 24816–24825. 10.1074/jbc.M804000200.

Ryle, M.J., Hausinger, R.P., 2002. Non-heme iron oxygenases. Current Opinion in Chemical Biology 6, 193–201.

Saini, R.K., Nile, S.H., Park, S.W., 2015. Carotenoids from fruits and vegetables: Chemistry, analysis, occurrence, bioavailability and biological activities. Food Research International 76 (Pt 3), 735–750. 10.1016/j.foodres.2015.07.047.

Salin, O., Törmäkangas, L., Leinonen, M., Saario, E., Hagström, M., Ketola, R.A., Saikku, P., Vuorela, H., Vuorela, P.M., 2011. Corn mint (*Mentha arvensis*) extract diminishes acute *Chlamydia pneumoniae* infection in vitro and in vivo. Journal of Agricultural and Food Chemistry 59 (24), 12836–12842. 10.1021/jf2032473.

Salvador, Â.C., Rudnitskaya, A., Silvestre, A.J.D., Rocha, S.M., 2016. Metabolomic-based strategy for fingerprinting of *Sambucus nigra* L. berry volatile terpenoids and norisoprenoids: Influence of ripening and cultivar. Journal of Agricultural and Food Chemistry 64 (26), 5428–5438. 10.1021/acs.jafc.6b00984.

Sánchez-Contreras, A., Jiménez, M., Sanchez, S., 2000. Bioconversion of lutein to products with aroma. Applied Microbiology and Biotechnology 54 (4), 528–534. 10.1007/s002530000421.

Santos, J., Oliveira, M.B.P.P., Ibáñez, E., Herrero, M., 2014. Phenolic profile evolution of different ready-to-eat baby-leaf vegetables during storage. Journal of Chromatography A 1327, 118–131.

Schneider, R., Razungles, A., Augier, C., Baumes, R., 2001. Monoterpenic and norisoprenoidic glycoconjugates of *Vitis vinifera* L. cv. Melon B. as precursors of odorants in Muscadet wines. Journal of Chromatography A. 936, 145–157.

Schwab, W., Fischer, T., Wüst, M., 2015a. Terpene glucoside production: Improved biocatalytic processes using glycosyltransferases. Engineering in Life Sciences 15 (4), 376–386. 10.1002/elsc.201400156.

Schwab, W., Fischer, T.C., Giri, A., Wüst, M., 2015b. Potential applications of glucosyltransferases in terpene glucoside production: Impacts on the use of aroma and fragrance. Applied Microbiology and Biotechnology 99 (1), 165–174. 10.1007/s00253-014-6229-y.

Seto, Y., Hamada, S., Ito, H., Masuta, C., Matsui, H., Nabeta, K., Matsuura, H., 2011. Tobacco salicylic acid glucosyltransferase is active toward tuberonic acid (12-hydroxyjasmonic acid) and is induced by mechanical wounding stress. Bioscience, Biotechnology, and Biochemistry 75 (12), 2316–2320. 10.1271/bbb.110454.

Sgorbini, B., Cagliero, C., Pagani, A., Sganzerla, M., Boggia, L., Bicchi, C., Rubiolo, P., 2015. Determination of free and glucosidically-bound volatiles in plants. Two case studies: L-menthol in

peppermint (*Mentha x piperita* L.) and eugenol in clove (*Syzygium aromaticum* (L.) Merr. & L.M.Perry). Phytochemistry 117, 296–305. 10.1016/j.phytochem.2015.06.017.

Shaikh, S., Yaacob, H.B., Rahim, Z.H.A., 2014. Prospective role In treatment of major illnesses and potential benefits as a safe insecticide and natural food preservative of mint (*Mentha* spp.): A review. Asian Journal of Biomedical and Pharmaceutical Sciences 4 (35), 1–12. 10.15272/ajbps.v4i35.559.

Shao, H., He, X., Achnine, L., Blount, J.W., Dixon, R.A., Wang, X., 2005. Crystal structures of a multifunctional triterpene/flavonoid glycosyltransferase from *Medicago truncatula*. The Plant Cell 17 (11), 3141–3154. 10.1105/tpc.105.035055.

Shariatmadari, Z., Riahi, H., Abdi, M., Hashtroudi, M.S., Ghassempour, A.R., 2015. Impact of cyanobacterial extracts on the growth and oil content of the medicinal plant *Mentha piperita* L. Journal of Applied Phycology 27 (6), 2279–2287. 10.1007/s10811-014-0512-2.

She, G., Xu, C., Liu, B., Shi, R., 2010. Two new monoterpenes from *Mentha haplocalyx* briq. Helv Chim Acta 93, 2495–2498.

Shi, J., Li, W., Gao, Y., Wang, B., Li, Y., Song, Z., 2017. Enhanced rutin accumulation in tobacco leaves by overexpressing the NtFLS2 gene. Bioscience, Biotechnology, and Biochemistry 81 (9), 1721–1725. 10.1080/09168451.2017.1353401.

Simon, C., Langlois-Meurinne, M., Didierlaurent, L., Chaouch, S., Bellvert, F., Massoud, K., Garmier, M., Thareau, V., Comte, G., Noctor, G., Saindrenan, P., 2014. The secondary metabolism glycosyltransferases UGT73B3 and UGT73B5 are components of redox status in resistance of *Arabidopsis* to *Pseudomonas syringae* pv. tomato. Plant, Cell & Environment 37 (5), 1114–1129. 10.1111/pce.12221.

Singh, S., Vishwakarma, R.K., Kumar, R.J.S., Sonawane, P.D., Ruby, Khan, B.M., 2013. Functional characterization of a flavonoid glycosyltransferase gene from *Withania somnifera* (Ashwagandha). Applied Biochemistry and Biotechnology 170 (3), 729–741. 10.1007/s12010-013-0230-2.

Song, C., Härtl, K., McGraphery, K., Hoffmann, T., Schwab, W., 2018. Attractive but toxic: Emerging roles of glycosidically bound volatiles and glycosyltransferases involved in their formation. Molecular Plant 11 (10), 1225–1236. 10.1016/j.molp.2018.09.001.

Song, C., Le Gu, Liu, J., Zhao, S., Hong, X., Schulenburg, K., Schwab, W., 2015. Functional characterization and substrate promiscuity of UGT71 glycosyltransferases from strawberry (*Fragaria × ananassa*). Plant & Cell Physiology 56 (12), 2478–2493. 10.1093/pcp/pcv151.

Stahl, W., Sies, H., 2003. Antioxidant activity of carotenoids. Molecular Aspects of Medicine 24 (6), 345–351. 10.1016/S0098-2997(03)00030-X.

Stahl-Biskup, E., Intert, F., Holthuijzen, J., Stengele, M., Schulz, G., 1993. Glycosidically bound volatiles-a review 1986-1991. Flavour and Fragrance Journal 8, 61–80.

Steger-Hartmann, T., Koch, U., Dunz, T., Wagner, E., 1994. Induced accumulation and potential antioxidative function of rutin in two cultivars of *Nicotiana tabacum* L. Zeitschrift für Naturforschung C 49 (1-2), 57–62. 10.1515/znc-1994-1-210.

Taguchi, G., Imura, H., Maeda, Y., Kodaira, R., Hayashida, N., Shimosaka, M., Okazaki, M., 2000. Purification and characterization of UDP-glucose: Hydroxycoumarin 7-O-glucosyltransferase, with broad substrate specificity from tobacco cultured cells. Plant Science 157 (1), 105–112. 10.1016/S0168-9452(00)00270-3.

Taguchi, G., Nakamura, M., Hayashida, N., Okazaki, M., 2003. Exogenously added naphthols induce three glucosyltransferases, and are accumulated as glucosides in tobacco cells. Plant Science 164, 231–240.

Taguchi, G., Yazawa, T., Hayashida, N., Okazaki, M., 2001. Molecular cloning and heterologous expression of novel glucosyltransferases from tobacco cultured cells that have broad substrate specificity and are induced by salicylic acid and auxin. European Journal of Biochemistry 268 (14), 4086–4094.

Takaichi, S., 2011. Carotenoids in algae: Distributions, biosyntheses and functions. Marine Drugs 9 (6), 1101–1118. 10.3390/md9061101.

Tang, K.S.C., Konczak, I., Zhao, J., 2016. Identification and quantification of phenolics in Australian native mint (*Mentha australis* R. Br.). Food Chemistry 192, 698–705. 10.1016/j.foodchem.2015.07.032.

Villa-Ruano, N., Pacheco-Hernandez, Y., Rubio-Rosas, E., Cruz-Duran, R., Lozoya-Gloria, E., 2017. Essential oil composition, carotenoid profile, antioxidant and antimicrobial activities of the parasitic plant *Cuscuta mitraeformis*. Boletín Latinoamericano y del Caribe de Plantas Medicinales y Aromáticas 16 (5), 463–470.

Villasenor, I.M., Sanchez, A.C., 2009. Menthalactone, a new analgesic from *Mentha cordifolia* opiz. leaves. Z. Naturforsch. 64, 809–812.

Vinas, M., Gruschwitz, M., Schweiggert, R.M., Guevara, E., Carle, R., Esquivel, P., Jimenez, V.m., 2012. Identification of phenolic and carotenoid compounds in coffee (*Coffea arabica*) pulp, peels and mucilage by HPLC electrospray ionization mass spectrometry, 127–135.

Vogt, T., Jones, P., 2000. Glycosyltransferases in plant natural product synthesis: Characterization of a supergene family. Trends in Plant Science 5 (9), 380–386.

Wahlberg, I., Enzell C.R., 1987. Tobacco isoprenoids, Natural Product Reports, 237-276.

Walter, M.H., Fester, T., Strack, D., 2000. Arbuscular mycorrhizal fungi induce the non-mevalonate methylerythritol phosphate pathway of isoprenoid biosynthesis correlated with accumulation of the 'yellow pigment' and other apocarotenoids. The Plant Journal 21 (6), 571–578.

Walter, M.H., Floss, D.S., Strack, D., 2010. Apocarotenoids: Hormones, mycorrhizal metabolites and aroma volatiles. Planta 232 (1), 1–17. 10.1007/s00425-010-1156-3.

Walter, M.H., Strack, D., 2011. Carotenoids and their cleavage products: biosynthesis and functions. Natural Product Reports 28 (4), 663–692. 10.1039/c0np00036a.

Wang, H., Xie, M., Charpin-El Hamri, G., Ye, H., Fussenegger, M., 2018. Treatment of chronic pain by designer cells controlled by spearmint aromatherapy. Nature Biomedical Engineering 2 (2), 114–123. 10.1038/s41551-018-0192-3.

Wang, S., Suh, J.H., Zheng, X., Wang, Y., Ho, C.-T., 2017. Identification and quantification of potential anti-inflammatory hydroxycinnamic acid amides from wolfberry. Journal of Agricultural and Food Chemistry 65 (2), 364–372. 10.1021/acs.jafc.6b05136.

Wang, X., 2009. Structure, mechanism and engineering of plant natural product glycosyltransferases. FEBS Letters 583 (20), 3303–3309. 10.1016/j.febslet.2009.09.042.

Wang, X., Bennetzen, J.L., 2015. Current status and prospects for the study of *Nicotiana* genomics, genetics, and nicotine biosynthesis genes. Molecular Genetics and Genomics 290 (1), 11–21. 10.1007/s00438-015-0989-7.

Wang, Y.-W., Wang, W.-C., Jin, S.-H., Wang, J., Wang, B., Hou, B.-K., 2012. Over-expression of a putative poplar glycosyltransferase gene, PtGT1, in tobacco increases lignin content and causes early flowering. Journal of Experimental Botany 63 (7), 2799–2808. 10.1093/jxb/ers001.

Williams, G.J., Gantt, R.W., Thorson, J.S., 2008. The impact of enzyme engineering upon natural product glycodiversification. Current Opinion in Chemical Biology 12 (5), 556–564. 10.1016/j.cbpa.2008.07.013.

Winterhalter, P., 1990. Bound terpenoids in the juice of the purple passion fruit (*Passiflora edulis* Sims). Journal of Agricultural and Food Chemistry 38 (2), 452–455. 10.1021/jf00092a026.

Winterhalter, P., Rouseff, R., 2002. Carotenoid-derived aroma compounds: an introduction. ACS Symposium series 802 Washington DC:. American Chemical Society, 1–17.

Winterhalter, P., Schreier, P., 1994. C13-Norisoprenoid glycosides in plant tissues: An overview on their occurrence, composition and role as flavour precursors. Flavour and Fragrance Journal 9 (6), 281–287. 10.1002/ffj.2730090602.

Xu, S., Brockmöller, T., Navarro-Quezada, A., Kuhl, H., Gase, K., Ling, Z., Zhou, W., Kreitzer, C., Stanke, M., Tang, H., Lyons, E., Pandey, P., Pandey, S.P., Timmermann, B., Gaquerel, E., Baldwin, I.T., 2017. Wild tobacco genomes reveal the evolution of nicotine biosynthesis. Proceedings of the National Academy of Sciences of the United States of America 114 (23), 6133–6138. 10.1073/pnas.1700073114.

Yahagi, T., Yamashita, Y., Daikonnya, A., Wu, J.-b., Kitanaka, S., 2010. New feruloyl tyramine glycosides from *Stephania hispidula* YAMAMOTO. Chem. Pharm. Bull. 58 (3), 415–417. 10.1248/cpb.58.415.

Yahyaa, M., Bar, E., Dubey, N.K., Meir, A., Davidovich-Rikanati, R., Hirschberg, J., Aly, R., Tholl, D., Simon, P.W., Tadmor, Y., Lewinsohn, E., Ibdah, M., 2013. Formation of norisoprenoid flavor compounds in carrot (*Daucus carota* L.) roots: characterization of a cyclic-specific carotenoid cleavage dioxygenase 1 gene. Journal of Agricultural and Food Chemistry 61 (50), 12244–12252. 10.1021/jf404085k.

Yahyaa, M., Berim, A., Isaacson, T., Marzouk, S., Bar, E., Davidovich-Rikanati, R., Lewinsohn, E., Ibdah, M., 2015. Isolation and functional characterization of carotenoid cleavage sioxygenase-1 from *Laurus nobilis* L. (Bay Laurel) fruits. Journal of Agricultural and Food Chemistry 63 (37), 8275–8282. 10.1021/acs.jafc.5b02941.

Yamamura, S., Ozawa, K., Ohtani, K., Kasai, R., Yamasaki, K.e.a., 1998. Antihistaminic flavones and aliphatic glycosides from *Mentha Spicata*. Phytochemistry 48 (1), 131–136.

Yang, C., Tanaka, O., 1997. Advances in plant glycosides, chemistry and biology: Proceedings of the international symposium on plant glycosides. Studies in Plant Science August 12-15, Kunming, China.

Yang, L., Jiang, H., Wang, Q.-H., Yang, B.-Y., Kuang, H.-X., 2012. A new feruloyl tyramine glycoside from the roots of *Achyranthes bidentata*. Chinese Journal of Natural Medicines 10 (1), 16–19. 10.3724/SP.J.1009.2012.00016.

Yao, J., Weng, Y., Dickey, A., Wang, K.Y., 2015. Plants as factories for human pharmaceuticals: Applications and challenges. International Journal of Molecular Sciences 16 (12), 28549–28565. 10.3390/ijms161226122.

Yim, S.-H., Kim, H.-J., Jeong, N.-R., Park, K.-D., Lee, Y.-J., Cho, S.-D., Lee, I.-S., 2012. Structure-guided identification of novel phenolic and phenolic amide allosides from the rhizomes of *Cimicifuga heracleifolia*. Bulletin of the Korean Chemical Society 33 (4), 1253–1258. 10.5012/bkcs.2012.33.4.1253.

Yin, Q., Shen, G., Chang, Z., Tang, Y., Gao, H., Pang, Y., 2017. Involvement of three putative glucosyltransferases from the UGT72 family in flavonol glucoside/rhamnoside biosynthesis in *Lotus japonicus* seeds. Journal of Experimental Botany 68 (3), 597–612. 10.1093/jxb/erw420.

Yin, R., Messner, B., Faus-Kessler, T., Hoffmann, T., Schwab, W., Hajirezaei, M.-R., Saint Paul, V. von, Heller, W., Schäffner, A.R., 2012. Feedback inhibition of the general phenylpropanoid and flavonol biosynthetic pathways upon a compromised flavonol-3-O-glycosylation. Journal of Experimental Botany 63 (7), 2465–2478. 10.1093/jxb/err416.

Yonekura-Sakakibara, K., Hanada, K., 2011. An evolutionary view of functional diversity in family 1 glycosyltransferases. The Plant Journal 66 (1), 182–193. 10.1111/j.1365-313X.2011.04493.x.

Yuan, F., Qian, M.C., 2016. Development of C13-norisoprenoids, carotenoids and other volatile compounds in *Vitis vinifera* L. Cv. Pinot noir grapes. Food Chemistry 192, 633–641. 10.1016/j.foodchem.2015.07.050.

Yuan, Y., Zhou, R., Li, D., Luo, C., Li, G., 2018. Simultaneous quantitative assessment of nine glycosides in tobacco by liquid chromatography-tandem mass spectrometry. Journal of Separation Science 41 (5), 1009–1016. 10.1002/jssc.201700880.

Zacarés, L., López-Gresa, M.P., Fayos, J., Primo, J., Bellés, J.M., Conejero, V., 2007. Induction of p-coumaroyldopamine and feruloyldopamine, two novel metabolites, in tomato by the bacterial pathogen *Pseudomonas syringae*. Molecular Plant-Microbe Interactions 20 (11), 1439–1448. 10.1094/MPMI-20-11-1439.

Zaia, M.G., Di Cagnazzo, T.O., Feitosa, K.A., Soares, E.G., Faccioli, L.H., Allegretti, S.M., Afonso, A., Anibal, F.d.F., 2016. Anti-inflammatory properties of menthol and menthone in *Schistosoma mansoni* infection. Frontiers in Pharmacology 7, 170. 10.3389/fphar.2016.00170.

Zeevaart, J.A.D., 1988. Metabolism and physiology of abscisic acid. Annual Review of Plant Physiology and Plant Molecular Biology 39 (1), 439–473. 10.1146/annurev.arplant.39.1.439.

Zhang, C., Chen, X., Lindley, N.D., Too, H.-P., 2018. A "plug-n-play" modular metabolic system for the production of apocarotenoids. Biotechnology and Bioengineering 115 (1), 174–183. 10.1002/bit.26462.

Zhang, F., Han, L.-F., Pan, G.-X., Peng, S., Andre, N., 2013. A new phenolic amide glycoside from *Cimicifuga dahurica*. Yao xue xue bao = Acta pharmaceutica Sinica 48 (8), 1281–1285.

Zhao, J., Li, L., Zhao, Y., Zhao, C., Chen, X., Liu, P., Zhou, H., Zhang, J., Hu, C., Chen, A., Liu, G., Peng, X., Lu, X., Xu, G., 2018. Metabolic changes in primary, secondary, and lipid metabolism in tobacco leaf in response to topping. Analytical and Bioanalytical Chemistry 410 (3), 839–851. 10.1007/s00216-017-0596-z.

Zhao, X., Dai, X., Gao, L., Guo, L., Zhuang, J., Liu, Y., Ma, X., Wang, R., Xia, T., Wang, Y., 2017. Functional analysis of an uridine diphosphate glycosyltransferase involved in the biosynthesis of polyphenolic glucoside in tea plants (*Camellia sinensis*). Journal of Agricultural and Food Chemistry 65 (50), 10993–11001. 10.1021/acs.jafc.7b04969.

Supplement

UGT72B35

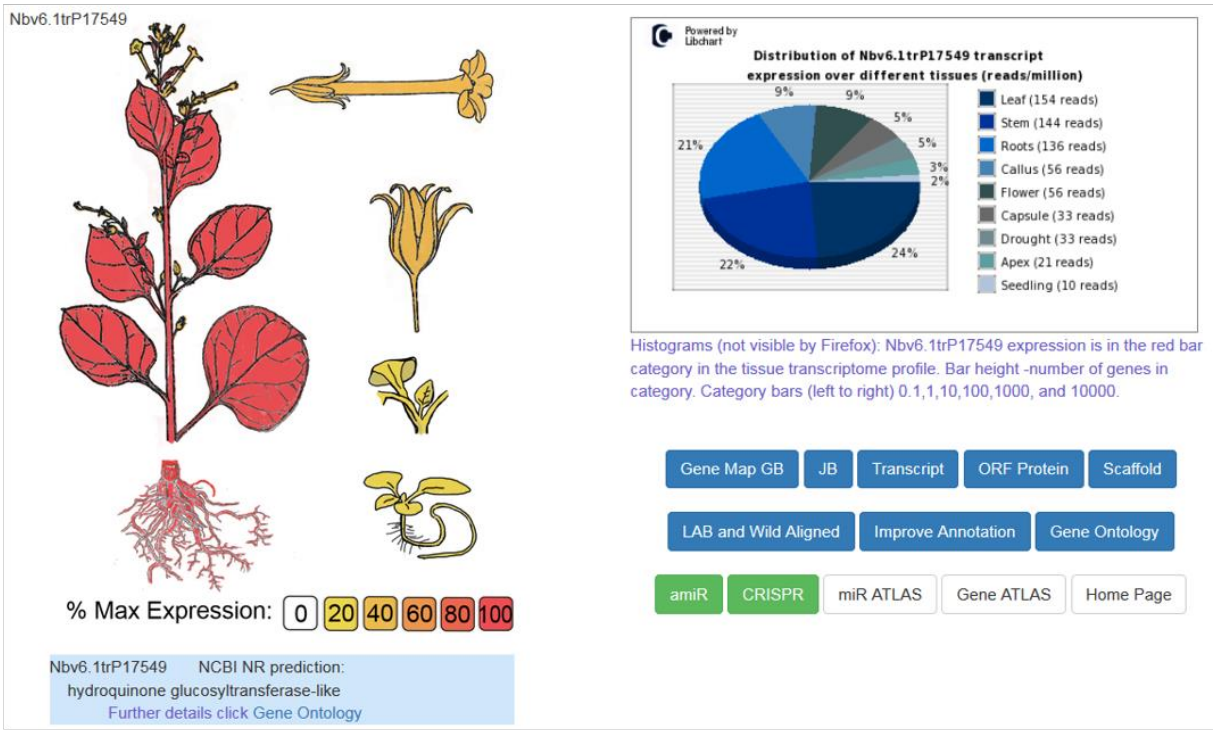

UGT72AX1

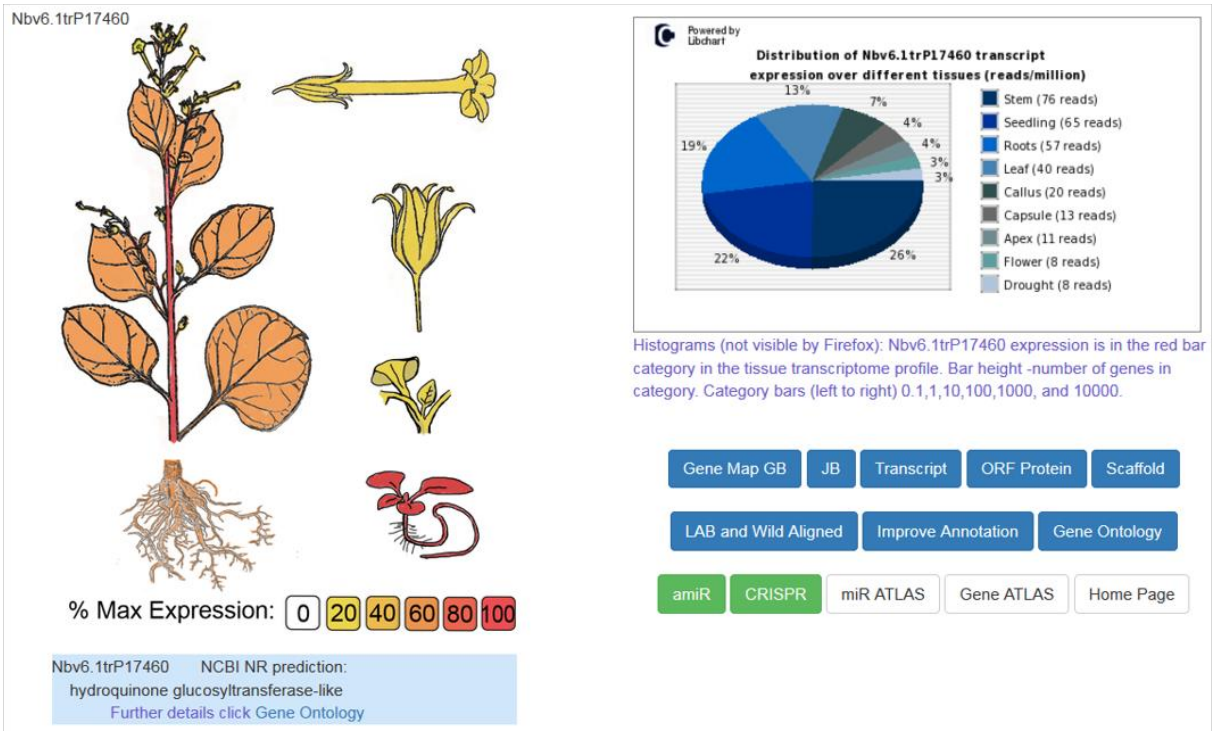

Figure S1a. Expression profiles of selected UGTs from *N. benthamiana* (http://benthgenome.qut.edu.au/).

UGT72AY1

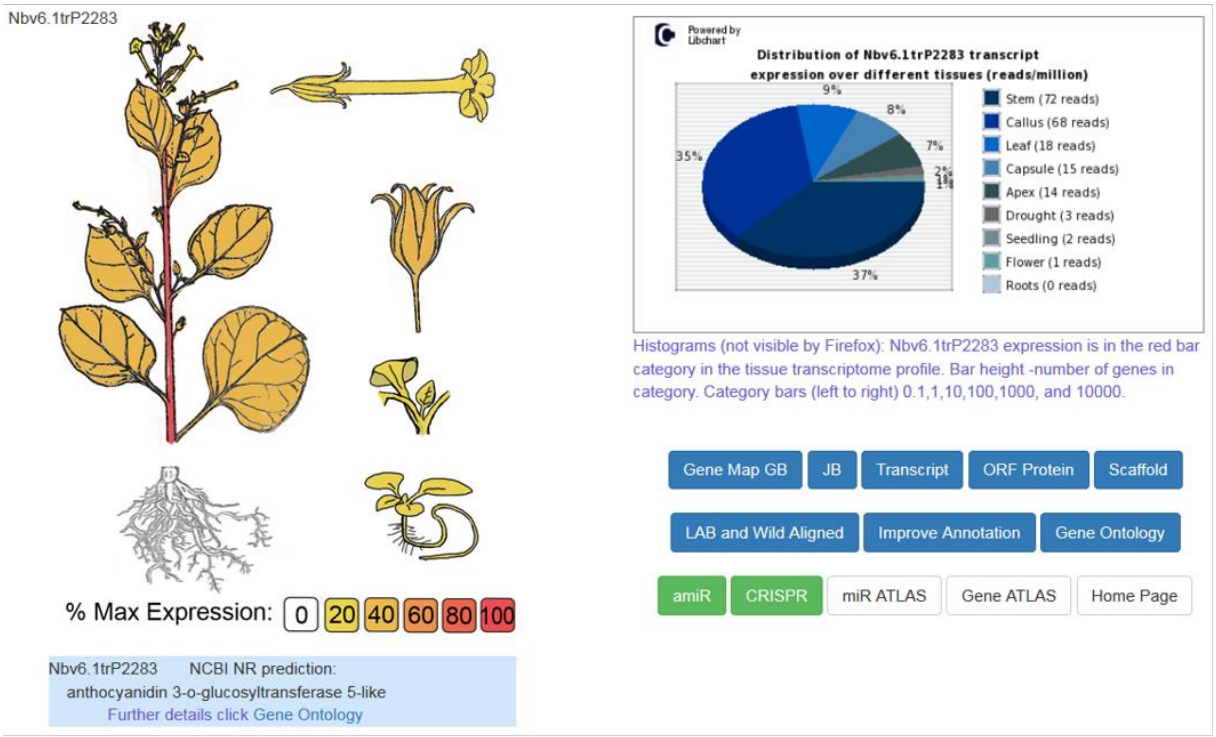

UGT85A73

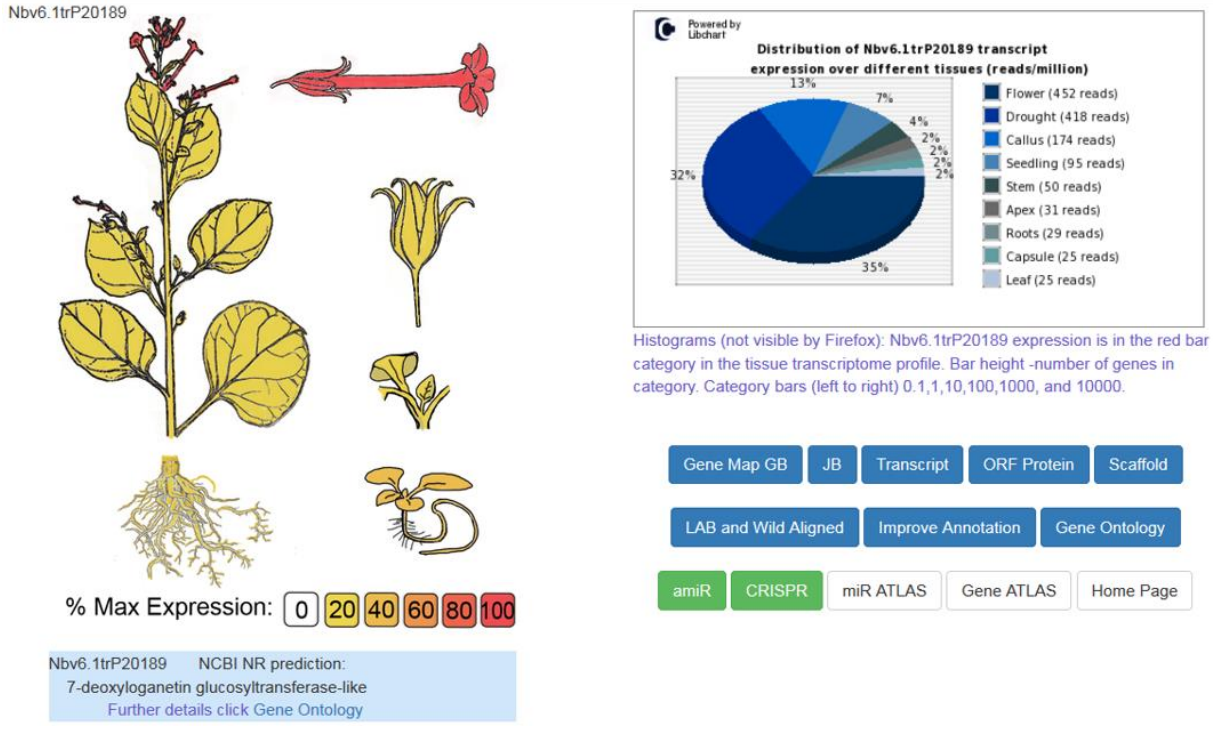

Figure S1b. Expression profiles of selected UGTs from *N. benthamiana* (http://benthgenome.qut.edu.au/).

UGT73A25

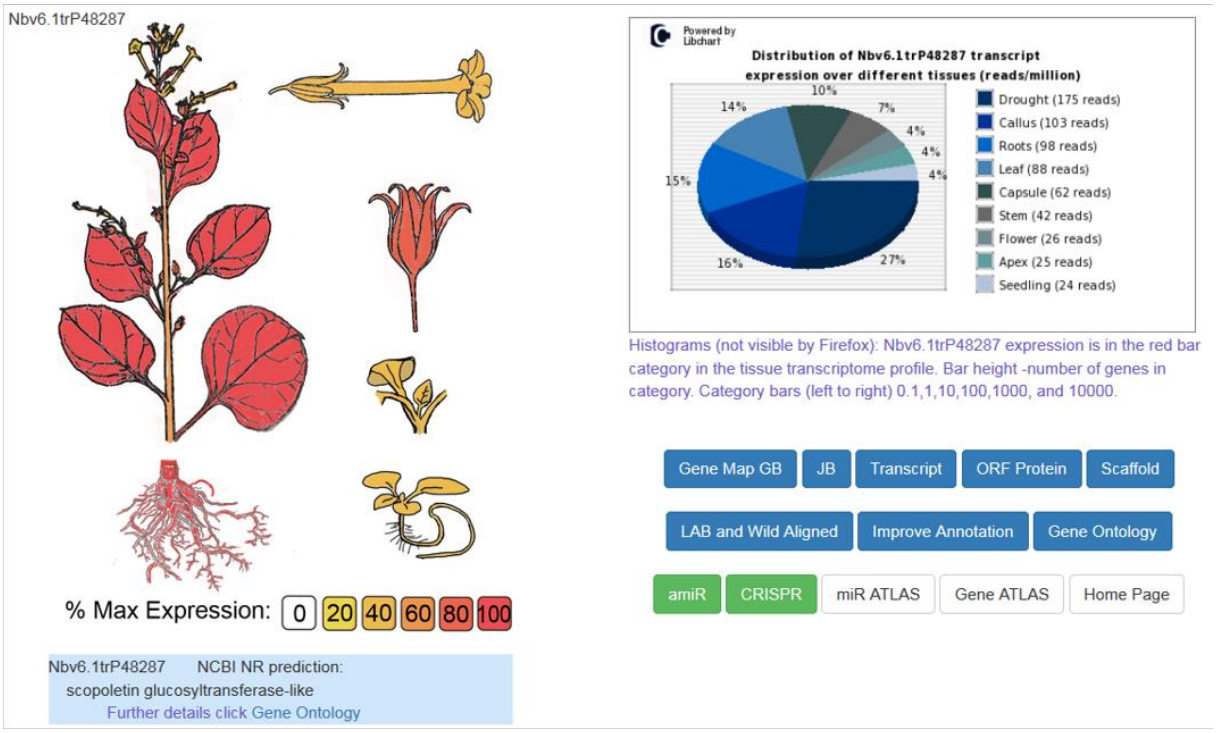

UGT85A74

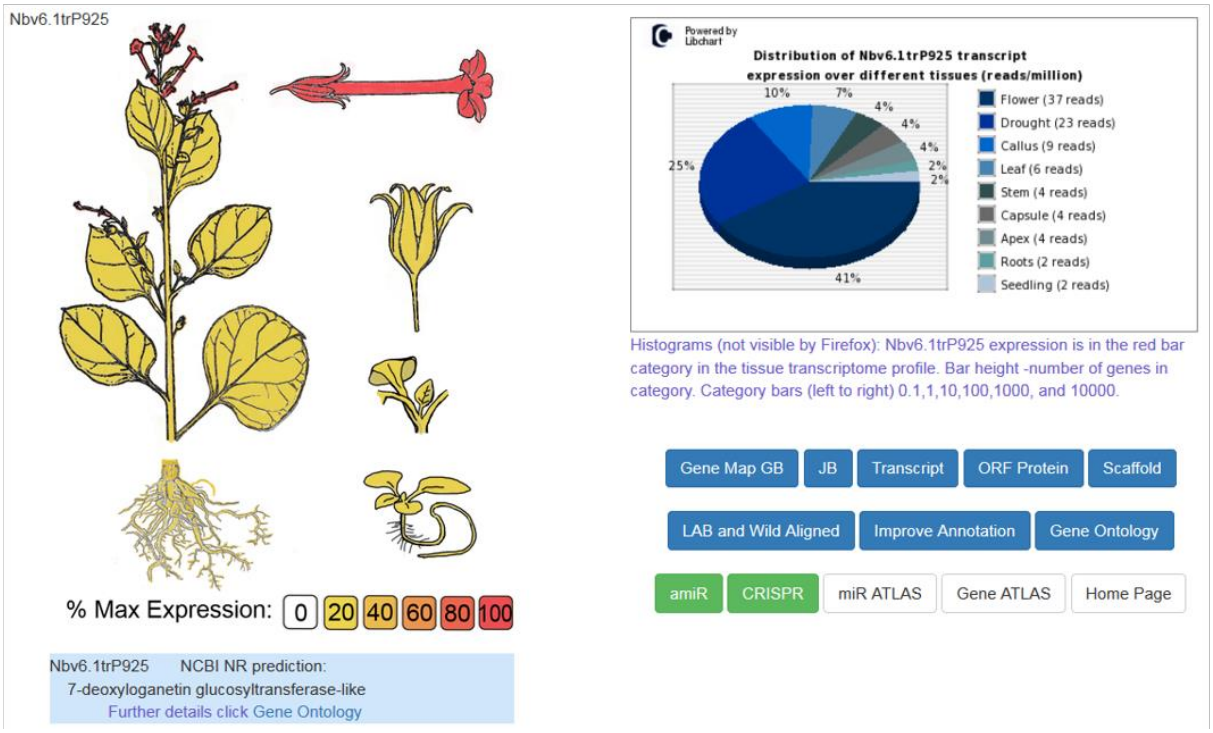

Figure S1c. Expression profiles of selected UGTs from *N. benthamiana* (http://benthgenome.qut.edu.au/).

UGT73A24

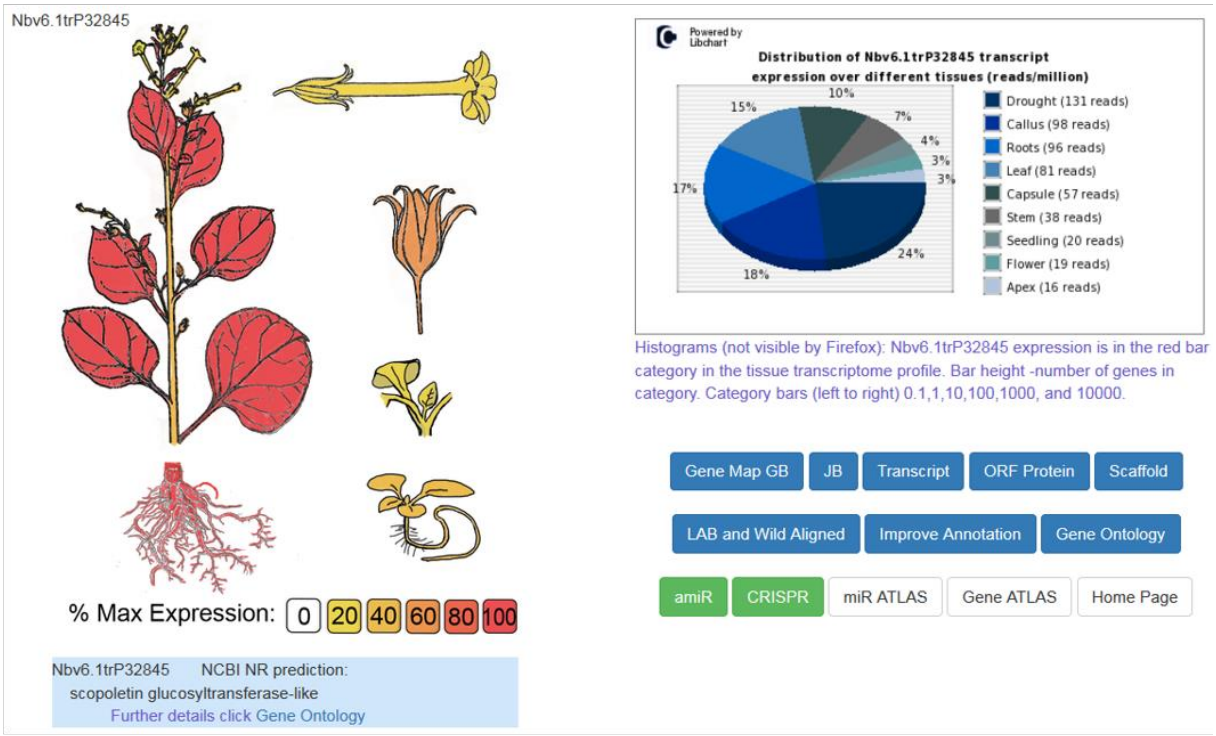

UGT71AJ1

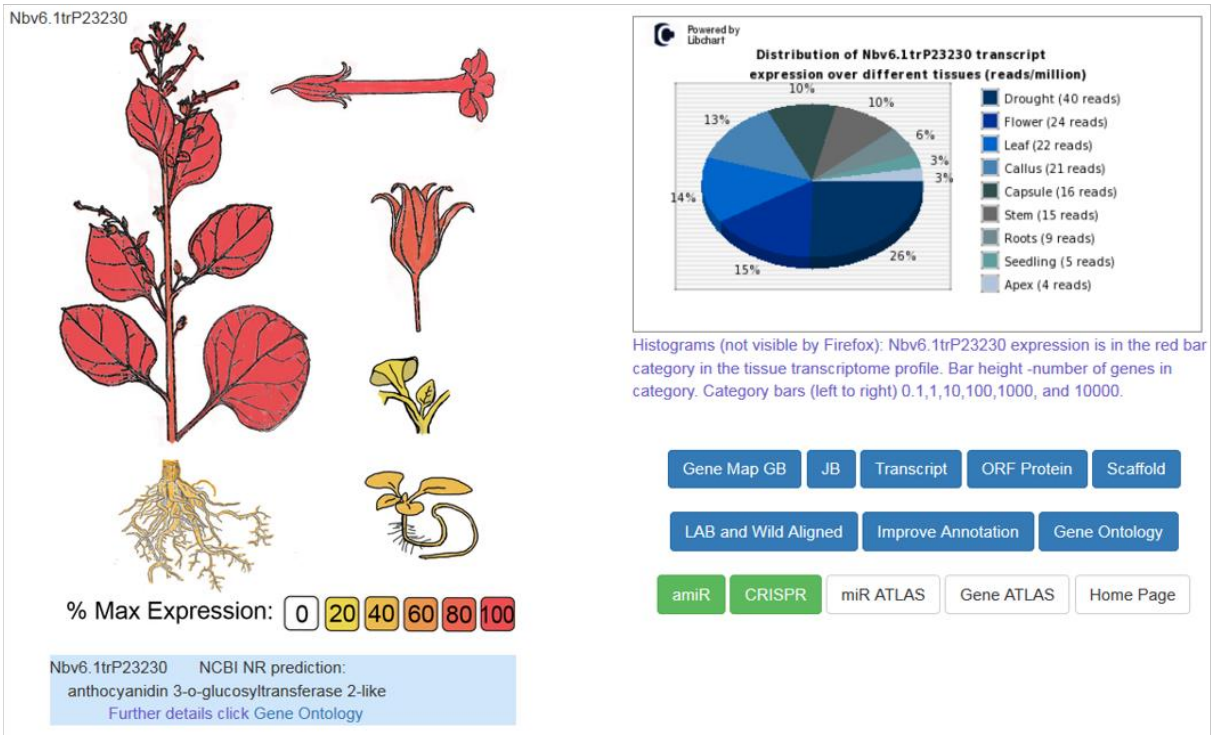

Figure S1d. Expression profiles of selected UGTs from *N. benthamiana* (http://benthgenome.qut.edu.au/).

UGT72B34

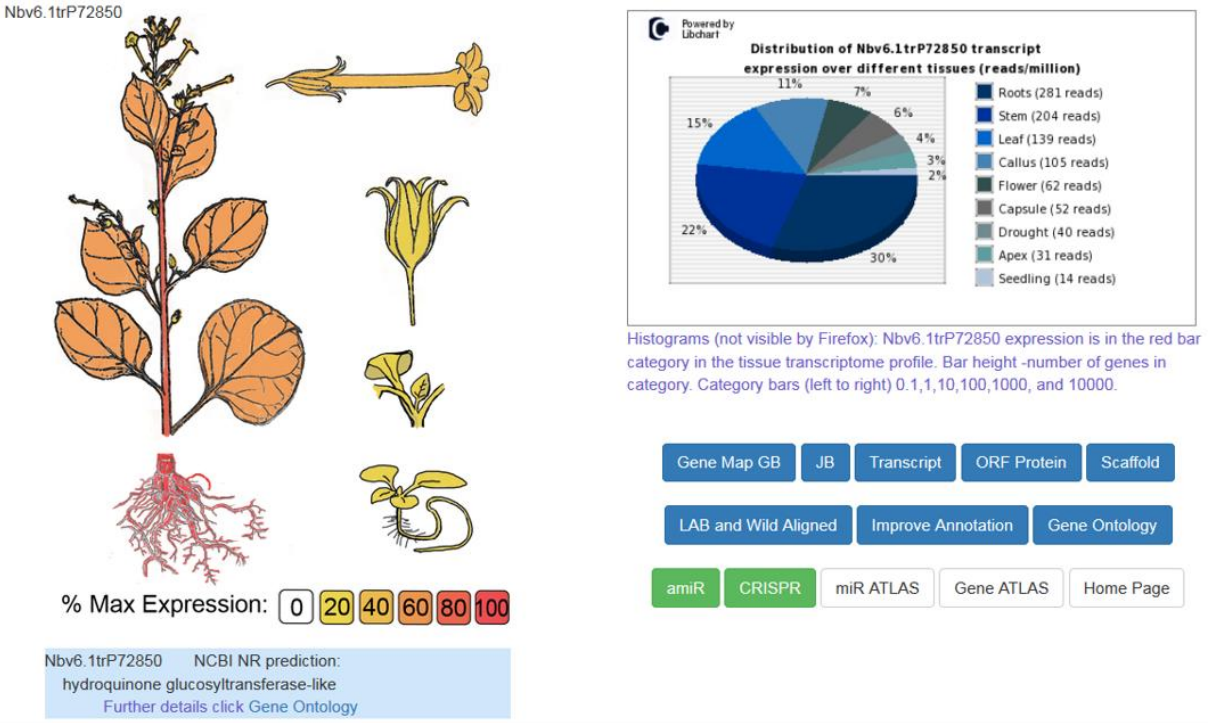

UGT709Q1

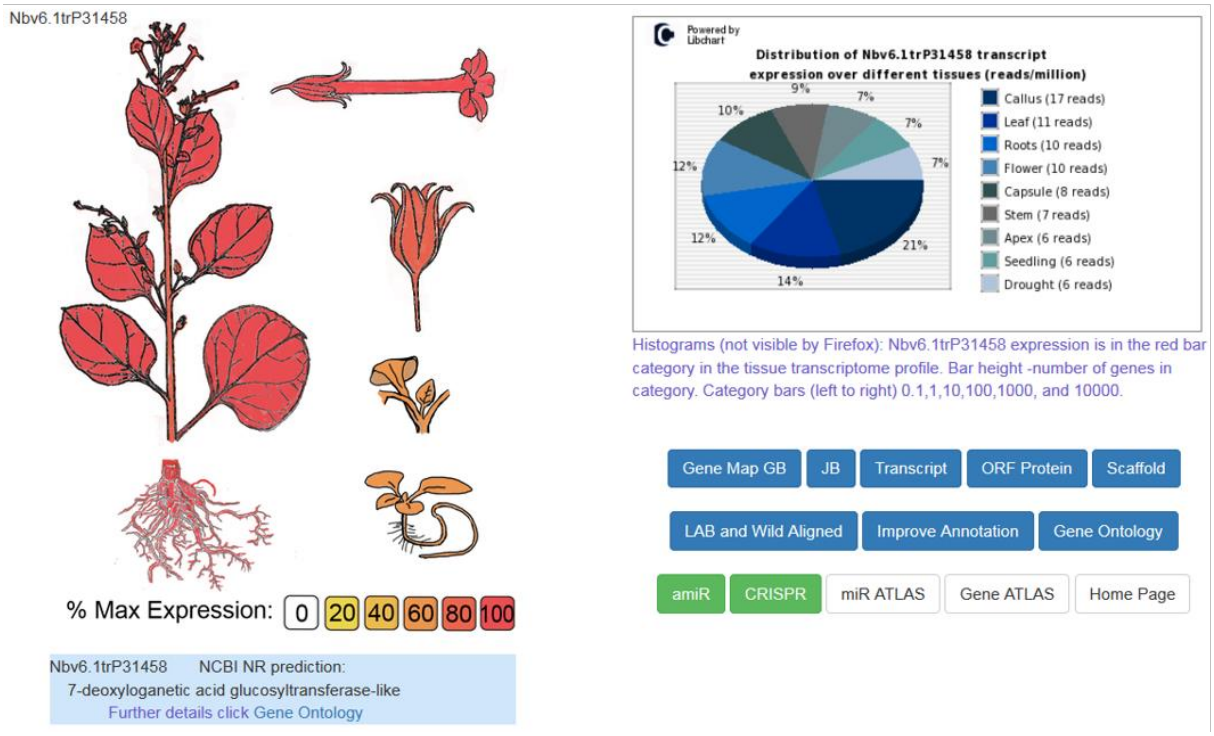

Figure S1e. Expression profiles of selected UGTs from *N. benthamiana* (http://benthgenome.qut.edu.au/).

NbGTms6

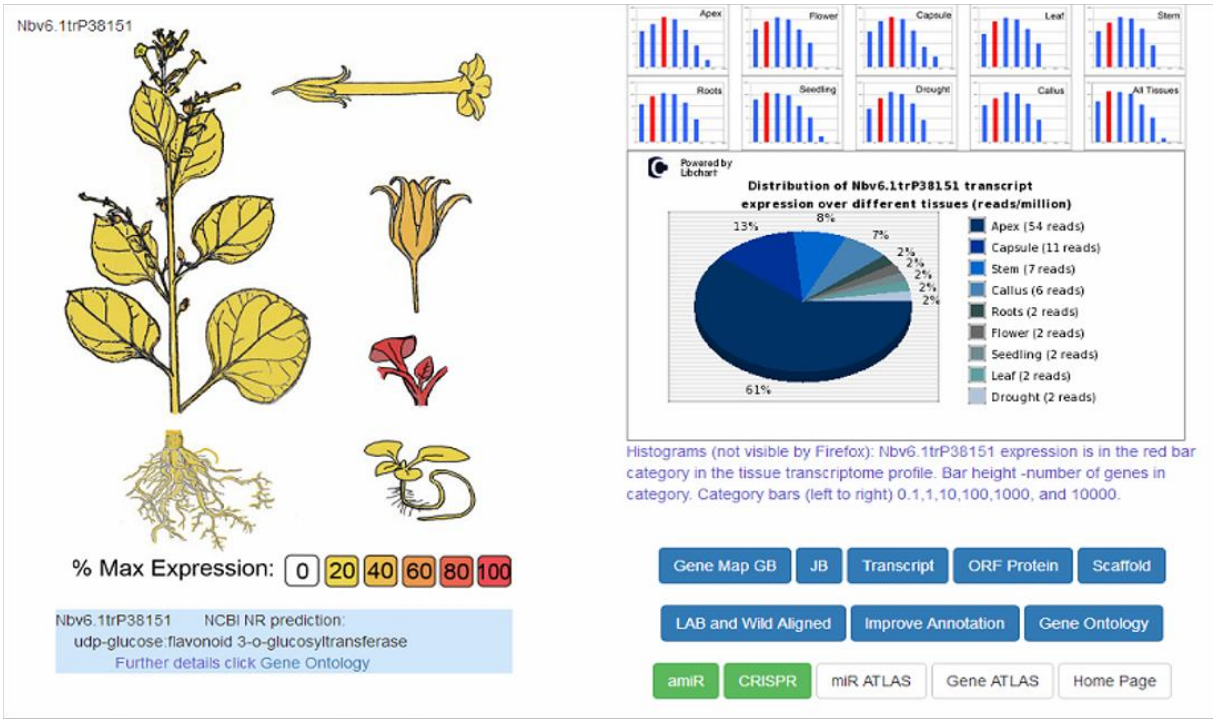

NbGTms7

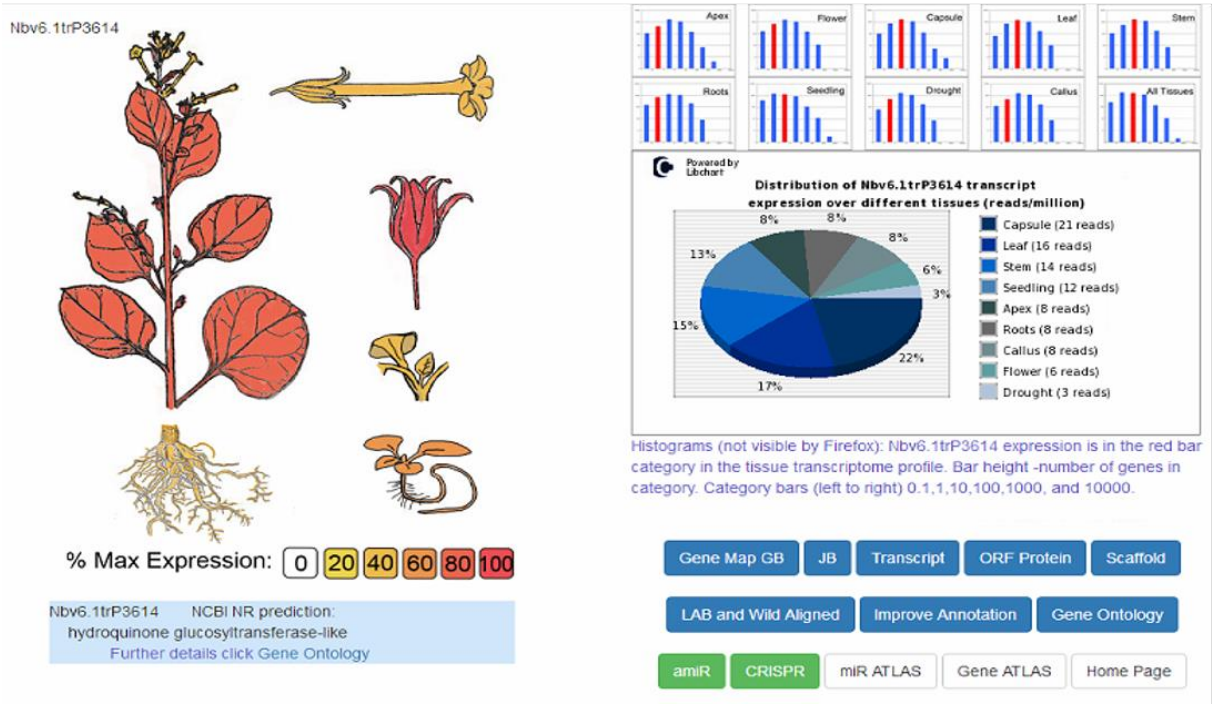

Figure S1f. Expression profiles of selected UGTs from *N. benthamiana* (http://benthgenome.qut.edu.au/).

NbGTfc1

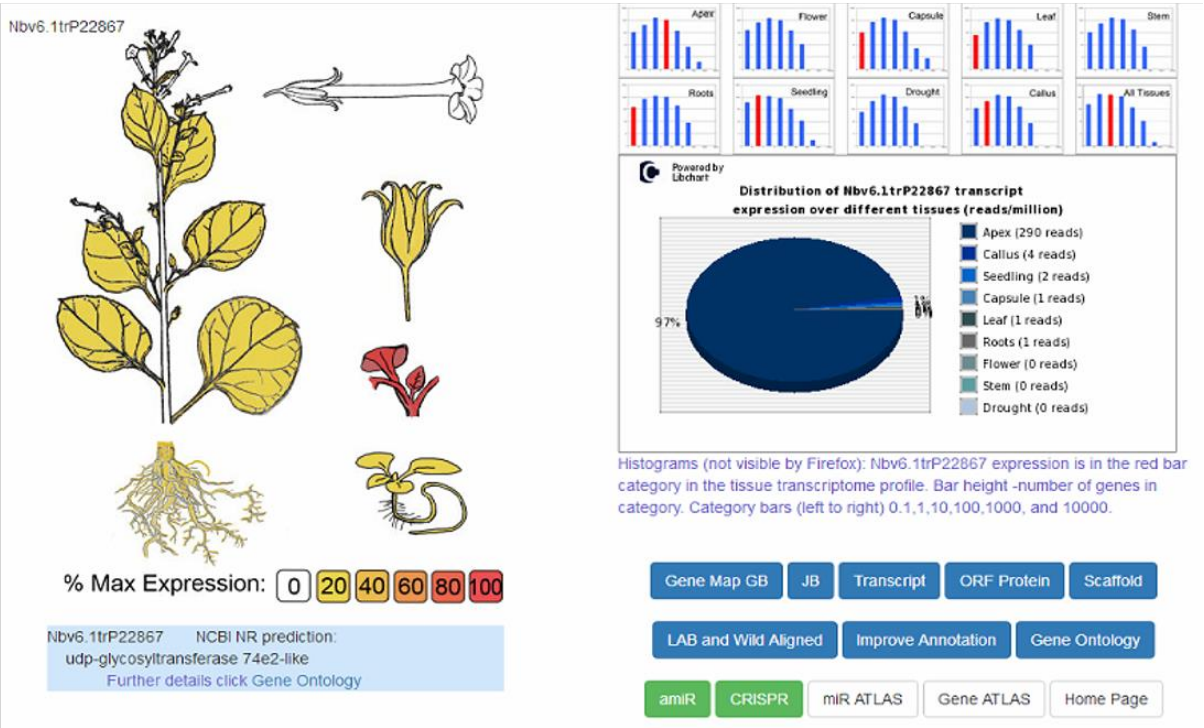

Figure S1g. Expression profiles of selected UGTs from *N. benthamiana* (http://benthgenome.qut.edu.au/).

Figure S2a. Phytogenetic analysis of of UGTs from *N. benthamiana* analysed in this study and biochemically characterized GTs from *N. tabacum*. Default values of the Geneious program (http://www.geneious.com/) were used.

Figure S2b. Phytogenetic analysis of of UGTs from *N. benthamiana* analysed in this study and biochemically characterized GTs from *N. tabacum*. Default values of the Geneious program (http://www.geneious.com/) were used.

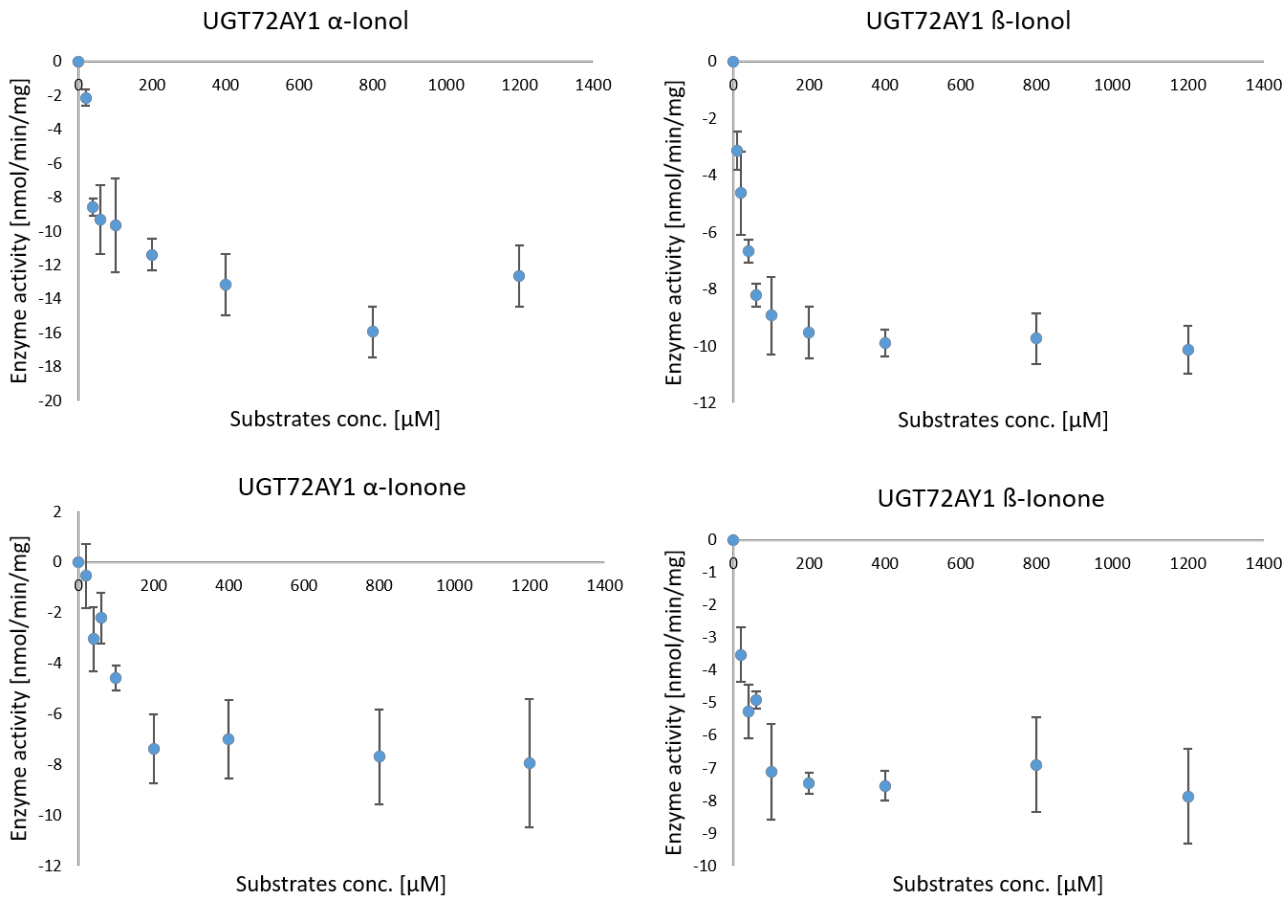

Figure S3a: Michaelis-Menten kinetics of UGT72AY1 anlyzed by UDP-Glo™. Enzyme activity of UGT72AY1 fitted to the Michaelis-Menten equation using α-ionol, ß-ionol, α-ionone, and ß-ionone. Released UDP was quantified.

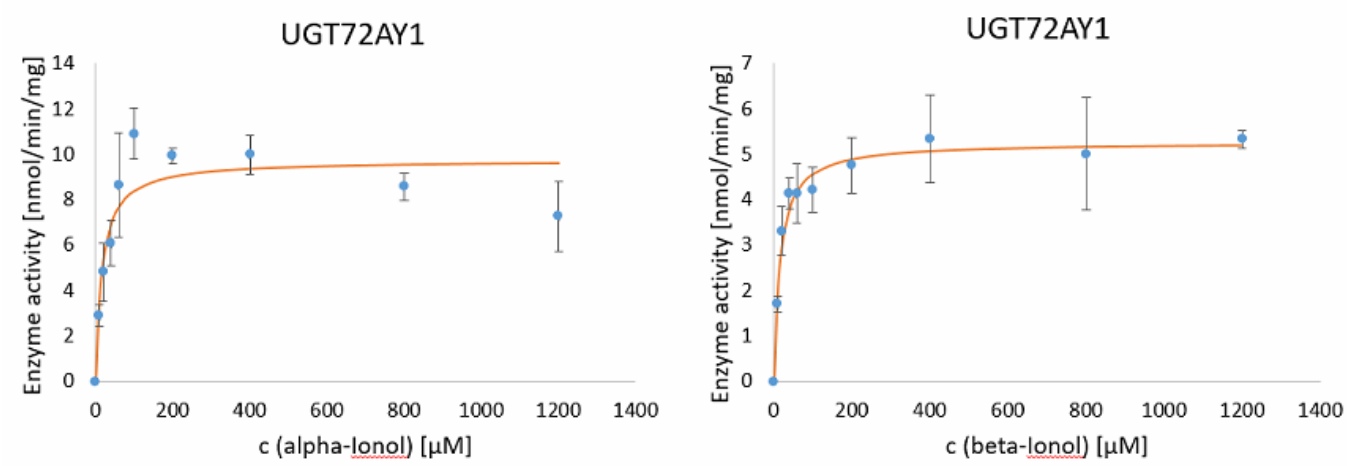

Figure S3b. Michaelis-Menten kinetics curve of UGT72AY1 by LC-MS. Enzyme activity of UGT72AY1 fitted to the Michaelis-Menten equation using α-ionol, ß-ionol. Glucoside formation was quantified.

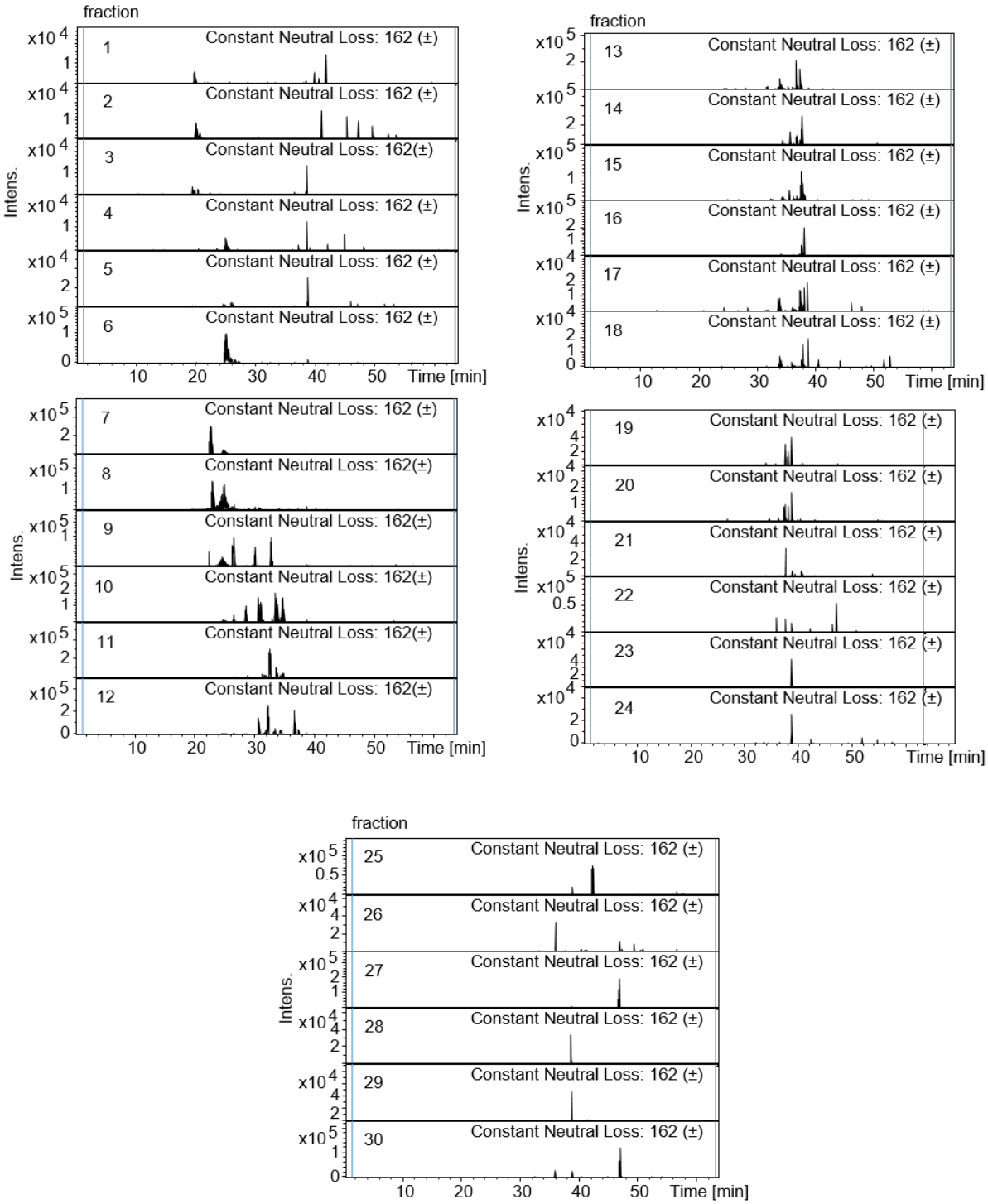

Figure S4. LC-MS analysis (constant neutral loss experiments in positive and negative mode) of 30 fractions obtained by semi-preparative LC fractionation of an extract isolated by XAD solid phase from tobacco leaves (*N. tabacum*)

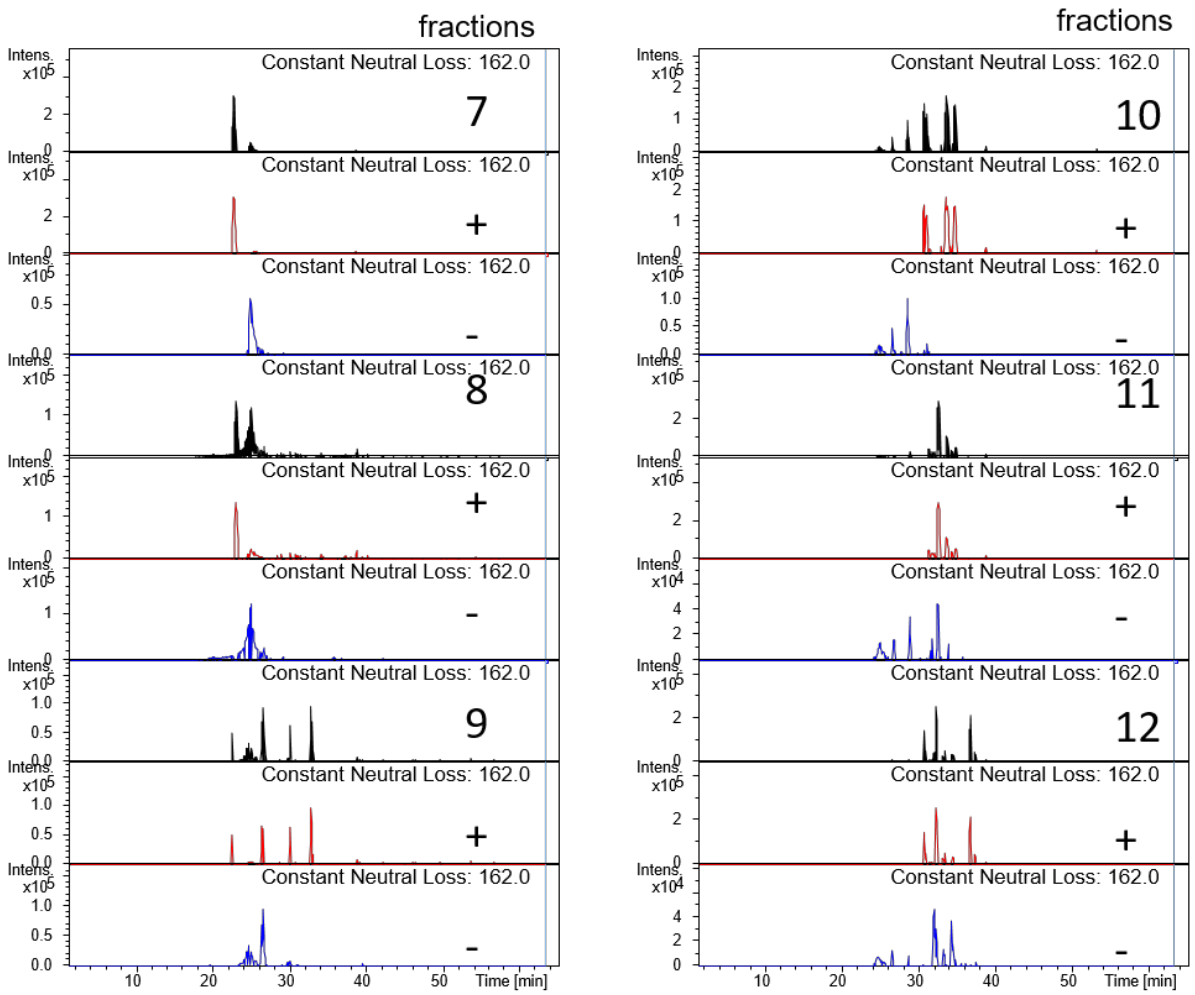

Figure S5. LC-MS analysis of selected fractions (7-12) of the tobacco extract. Different putative hexosides (neutral loss of 162) can be inferred from the neutral loss experiments in the positive and negative mode.

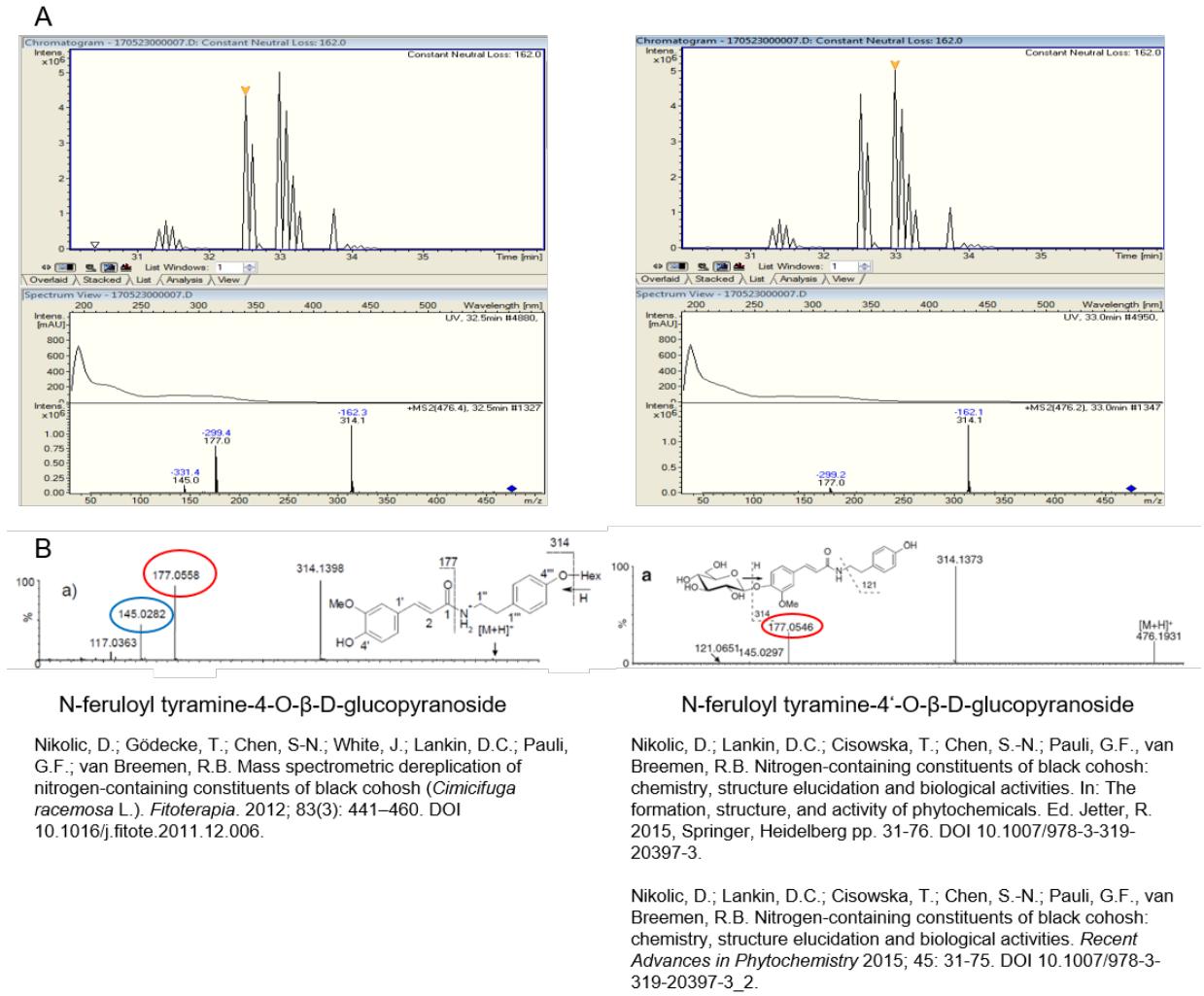

Nikolic, D.; Gödecke, T.; Chen, S-N.; White, J.; Lankin, D.C.; Pauli, G.F.; van Breemen, R.B. Mass spectrometric dereplication of nitrogen-containing constituents of black cohosh (*Cimicifuga racemosa* L.). *Fitoterapia*. 2012; 83(3): 441–460. DOI 10.1016/j.fitote.2011.12.006.

Nikolic, D.; Lankin, D.C.; Cisowska, T.; Chen, S.-N.; Pauli, G.F., van Breemen, R.B. Nitrogen-containing constituents of black cohosh: chemistry, structure elucidation and biological activities. In: The formation, structure, and activity of phytochemicals. Ed. Jetter, R. 2015, Springer, Heidelberg pp. 31-76. DOI 10.1007/978-3-319-20397-3.

Nikolic, D.; Lankin, D.C.; Cisowska, T.; Chen, S.-N.; Pauli, G.F., van Breemen, R.B. Nitrogen-containing constituents of black cohosh: chemistry, structure elucidation and biological activities. *Recent Advances in Phytochemistry* 2015; 45: 31-75. DOI 10.1007/978-3-319-20397-3_2.

Figure S6. Identification of hexosides M1 and M2 by LC-MS. M1 and M2 produced by UGT73A24 and UGT73A25 (A), reference mass spectra from literature (B) and proposed fragmentation pattern explaining the formation of fragment ion *m/z* 145 from product ion *m/z* 177 (C) according to Martens, S.M.; Marta, R.A.; Martens, J.K.; McMahon, T.B. Consecutive Fragmentation Mechanisms of Protonated Ferulic Acid Probed by Infrared Multiple Photon Dissociation Spectroscopy and Electronic Structure Calculations. *Journal of The American Society for Mass Spectrometry.* 2012; 23:1697Y1706. DOI: 10.1007/s13361-012-0438-3.

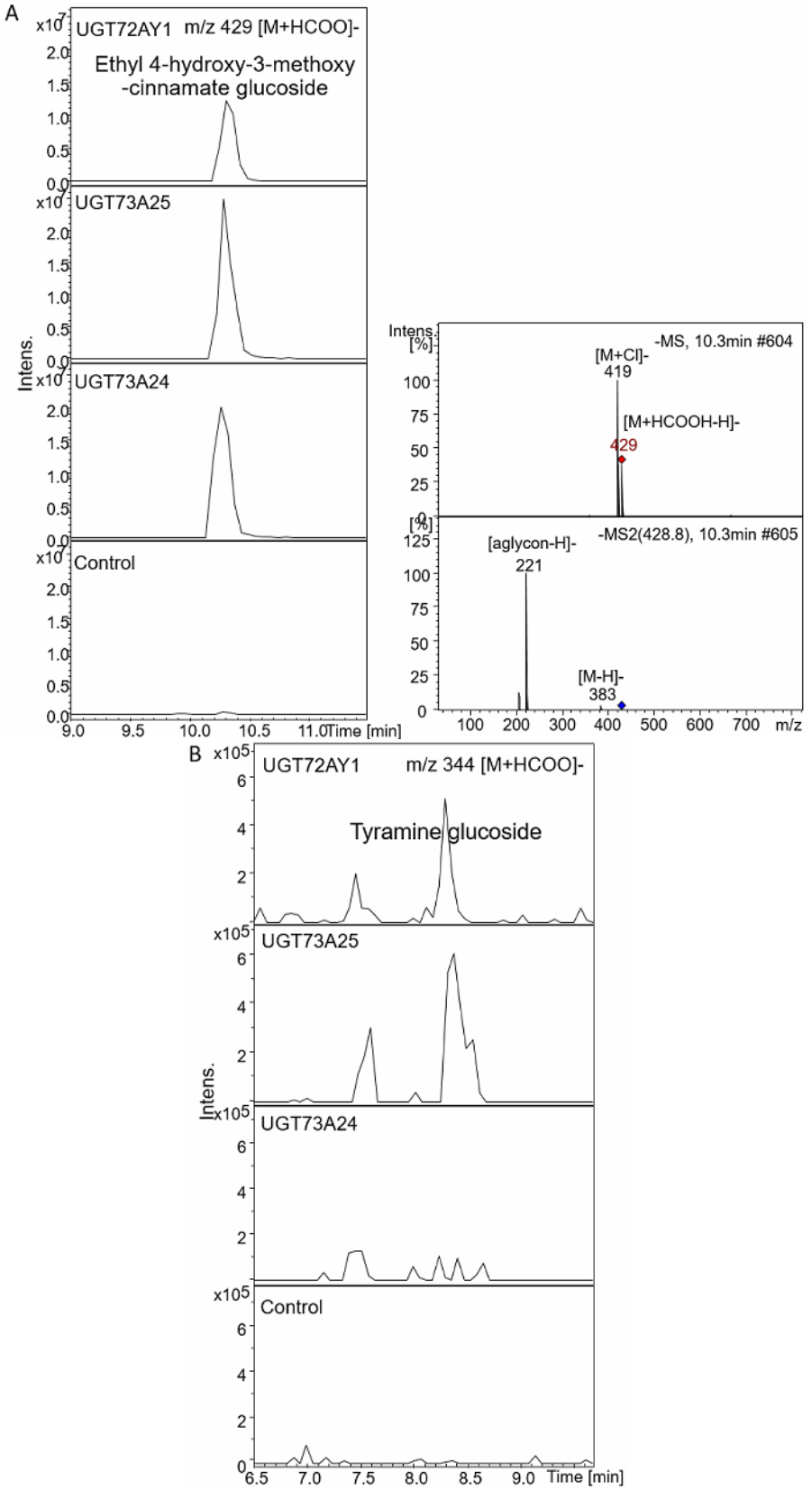

Figure S7a. LC-MS analysis of products formed by UGT72AY1, UGT73A24 and UGT73A25 from different substrates.

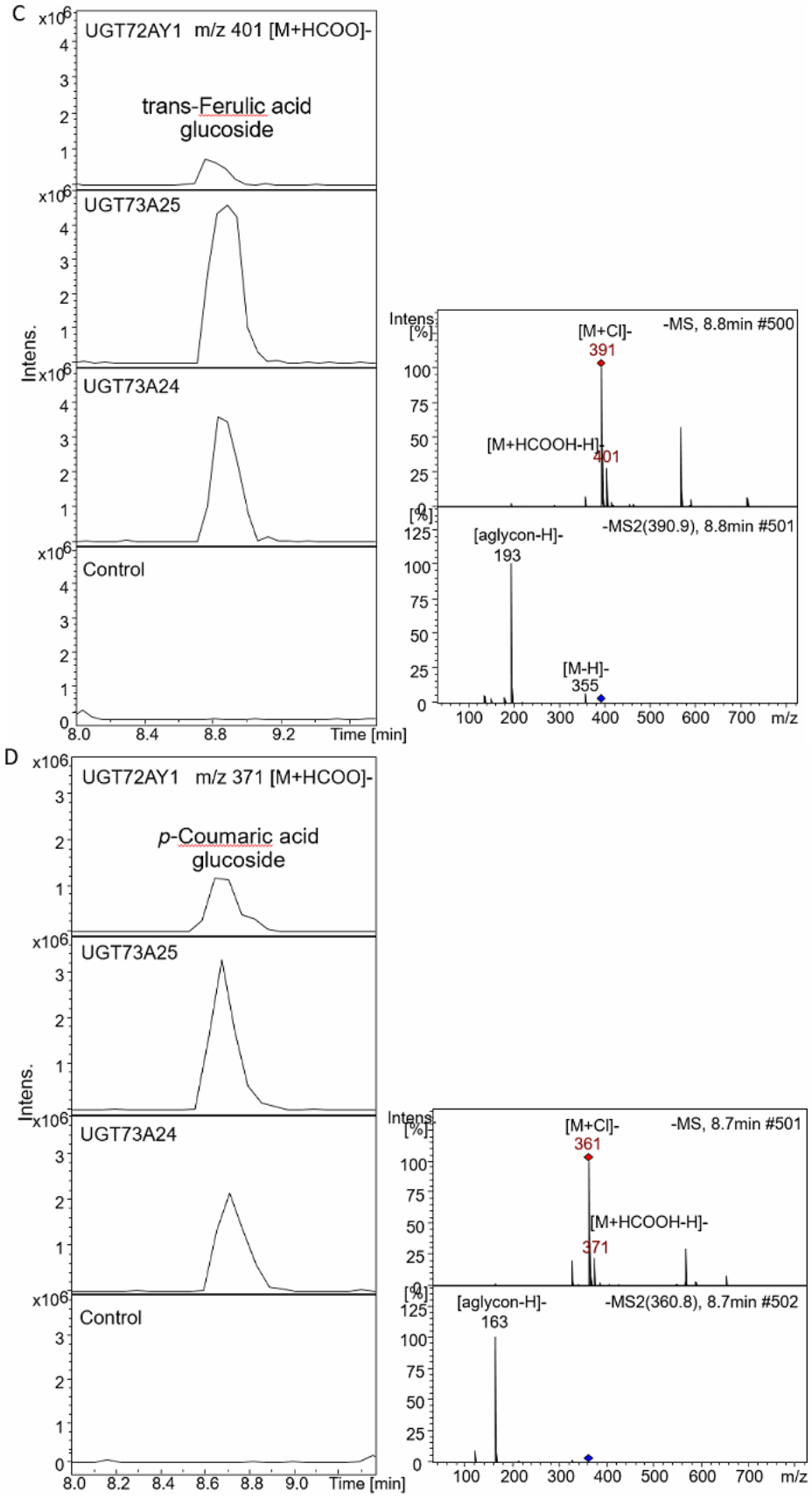

Figure S7b. LC-MS analysis of products formed by UGT72AY1, UGT73A24 and UGT73A25 from different substrates.

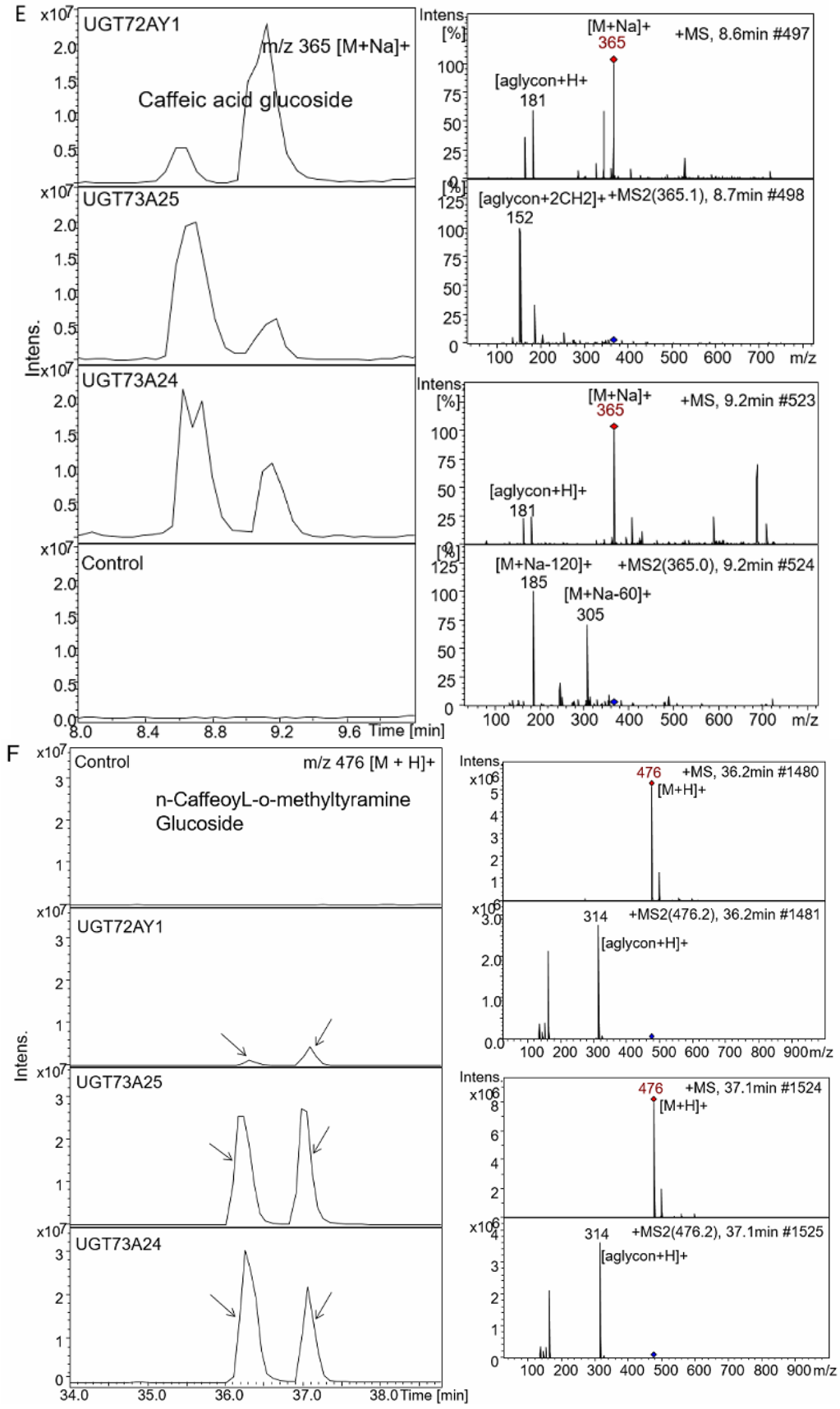

Figure S7c. LC-MS analysis of products formed by UGT72AY1, UGT73A24 and UGT73A25 from different substrates.

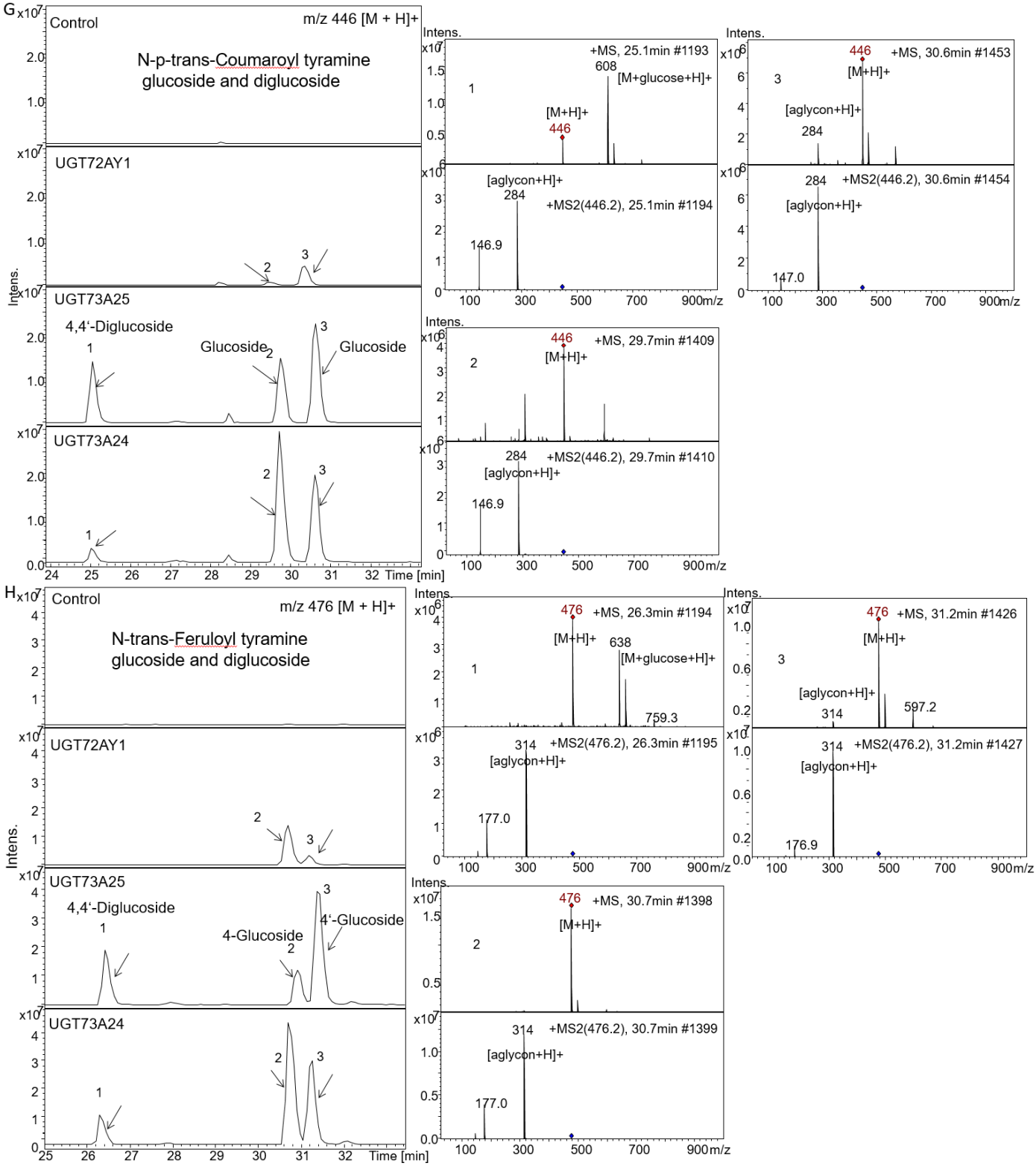

Figure S7d. LC-MS analysis of products formed by UGT72AY1, UGT73A24 and UGT73A25 from different substrates.

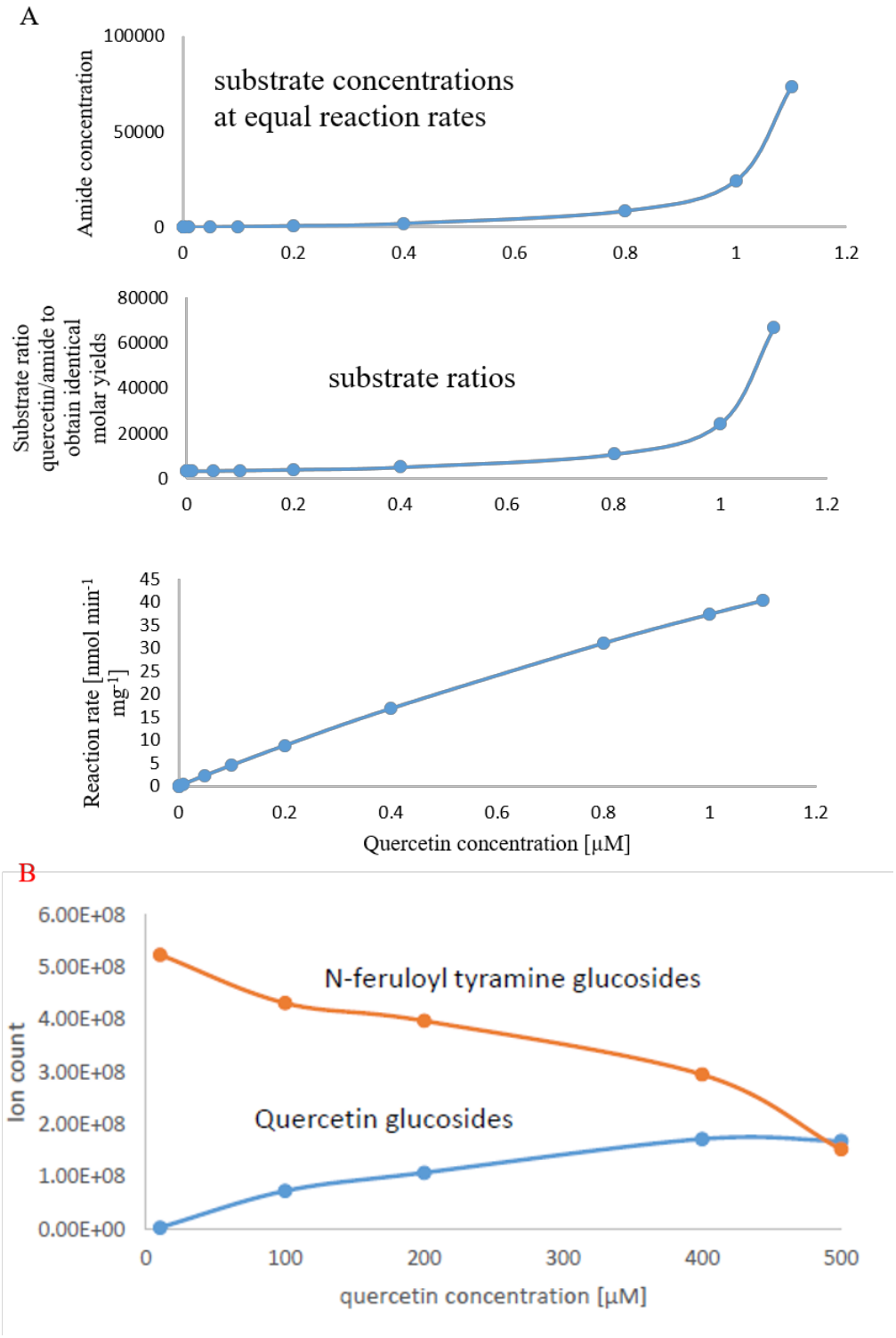

Figure S8. UGT73A25 substrate concentrations of quercetin and N-feruloyl tyramine (amide) at identical reaction rate and their glucoside production. (A) Substrate concentrations of quercetin and N-feruloyl tyramine (amide) at identical reaction rate. **(B)** Glucoside production by UGT73A25. N-feruloyl tyramine (3640 µM) and increasing concentrations of quercetin were co-incubated with UGT73A25 and products simultaneously analyzed by LC-MS.

Amino acid sequences of MpGTs and NbGTs, which have been functionally characterized.

UGT709C6 (MpGT 85A3-P-C748)

MRSEEGKDVPPHVLIFPYPVQGHLNSMLNLAHIFCLADFHVTFIISDFSHRRLLRHTT
VAATFARFPGFQFRLLPDGLPEDHPRSGERVMEMMSSVATITFPLFKKMIIGENFFA
ADGRRPVTCYVADGLMTFAADFAEENGLPLIYFRTATASYFWAIFCFPELLEAQEIP
FNGKSMDGLVKSVPGMKDFLRRRDLPSFYRADDVNDPILQKVAAVTRKITRAQAAI
FNTCEDLEGKILAEIQKHVPRIFSIGPIHEQTKSRLTEKNAEPSIITASLWAEDRSCVD
WLDAQPPKSVIYVSFGSITILTREQLFEIWHGLIDSCQRFLWVMRPDSVAGEDQIPA
ELTERSREKGLLVEWAPQEKVLNHPSVGGFFTHSGWNSTLESISAGVPMICWPYF
ADQTINSRFVSEVWKIGLDIKDSCDRFIIEKAVRELMEERKGEFLERAEEMATIVKRA
VSKGGSSYSNLDGLIEYIKSLVG*

UGT86C10 (MpGT86A1-S-C8335)

MGEIEKNLHAIMICVPFQGHLNPFVTLALKLASKGIIVTFVHLEFLHRKLCAANRSDD
ETQVDFFSAARDSGLDIRFTTMNDPFPLEFDRDAHSEEYWESMVRDFAPLVDEFV
GKLVNSHPDLLHFLVADTVYTWPAEIAEKYKLVNVSLWTQSALVYTLGYHWDLLQQ
NGHFPCKDGVEEEINYVPGVETINTNDIMPYLKESLKESVLSWSARLFFHNGKKAD
FVLQNTVEELEPETLSALNQYLPNYAIGPINFSKNLPSMTQSFWSQSDCTGWLDSK
PPGSVLYISFGSLVHANKHVIEEVAYGLALSGVNFLWVIREGILGDGDTEVLPPGFK
DEVKDRGMTVGWCDQIKVLSHPAVAGFWTHNGWNSTLESMWSGVPMICYPIGFD
QPCNRKLVVDNWEIGVNLCEGGSLDRGHVAETIKIFMNGGGSEKLRKNAGRVKEI
MHNAMEMNGSSEKNFERFIMDLEGKVRATKV*

UGT708M1 (MpGT71B5-c13929-23)

MSKSENEAPAPHVALFPCAGMGHLIPFLRLAAQLHTRGCAVTVITVEPTVSAAESN
HLSSFFSTFPRIKRLEFRLLPHQKSELTNDDPFFIQMERIGNSVHLLQPLLSSLSPPL
AAAVVDLPVLSRLASALSLPIYTLITTSARFFSLMASLSHLQKNADSVEIPNFGPIPLS
SVPPPMLDPNHFFAASITTNTSSLLKSAGVIINTFTSLESQAIEALRRNGVDQILPIGP
LPPFSETSALDLPWLDEQAPSSVLYISFGSRTALSKEQITELASALEISGCKFLWVLK
GGKVDREDKEEVGEMVGAEFVERTKGKGKVIKGWVEQEQILSHAAIGGFVSHCG
WNSVTEAAAVGVPVLAWPLHGDQRVNAAVVEEVGLGIWVREWGWGGERLIGRD
EIAKQLRMVMGDEMLRKKAEELKKKAREAREINGSSETLIRGLMESFKRK*

UGT708M2 (MpGT71B5-c13929-26)

MSKSENEAPHVALFPCAGMGHLIPFLRLAEQLHSHGCAVTVITVEPTVSAAESNHL
SSFFSTFPRIKRLEFRLLPHRKSELINYDPFFIQMERIGNSVHLLQPLLSSLSPPLSAA
VVDLPVLSRLASALSLPIYTLITTSARFFSLMASLSHLQKNADSVEIPYFGPIPFSNVP
PPMLDPNHFFAASITTNTSSLSKSAGVIINTFTSLESQAIEALRRNGVDQILPIGPLLP
FSETSALDLPWLDEQAPSSVLYISFGSRTALSKEQITELASALEISGCKFLWVLKGG
KVDREDKEEVGEMVGAEFVERTKGKGKVIKGWVEQEQILSHAAIGGFVSHCGWNS
VTEAAAVGVPVLAWPLHGDQRVNAAVVEEVGLGIWVREWGWGGERLIGRDEIAK
QLRMVMGDEMLRKKAEELKKKAREAREINGSSETLIRGLMESFKRK*

UGT709C8 (MpGT85A3-W-c10000: MpGT85-10-1)

MRSEEGKDVPPHVLIFPYPVQGHLNSMLNLAHIFCLADFHVTFIISDFSHRRLLRHTT
VATTFARFPGFQFRLLPDGLPEDHPRSGERVMEMMSSVATITFPLFKKMITGENFF
AADSRRPVTCYVADGLMTFAADFAEENGLPLIYFRTATASYFWAIFRFPELLEAQEI
PFNGKSMDGLVKSVPGMEDFLRRRDLPSFYRGDDIIDPILRKVAAVTRQITRAQAAI
FNTCEDLEGKILAEMQKHVPRIFSIGPIHEQTKSRLTEKKAELSIITASLWAEDRSCV
DWLDAQPPKSVIYVSFGSITILTREQLIEIWHGLLDSCLRFLWVMRPDSVAGGDQIP
AELTERSREKGFLVEWAPQEKVLNHPSVGGFFTHSGWNSTLESISAGVPMICWPY
FADQAINSRFVSEVWKIGLDIKDSCDRFIIEKAVRELMEERKGEFLERAEEMATIVKR
AVSKGGSSYSNLDGLIEYIKSLVV*

UGT709C7 (MpGT85A3-W-c10000: MpGT85-10-3)

MRSEEGKDVPPHVLIFPYPVQGHLNSMLNLAHIFCLADFHVTFIISDFSHRRLLRHTT
VASTFARFPGFQFRLLPDGLPEDHPRSGERVMEMMSSVATITFPLFKKMIIGENFFA
ADGRRPVTCYVADGLMTFAADFAEENGLPLIYFRTATASYFWAIFCFPLLLEAQEIP
FNGKSMDELVKSVPGMDDFLRRRDLPSFYRVDDVNDPILQKVAAVTRKITRAQAAI
FNTCEDLEGKILAEIQKHVPRIFSIGPIHEQTKSRLTEKKAEPLIITASLWAEDRSCVE
WLDAQPPKSVIYVSFGSITILTREQLFEIWHGLLDSCQRFLWVMRPDSVAGGDQIPA
ELTERSREKGLLVEWAPQEEVLNHPSVGGFFTHSGWNSTLESISAGVPMICWPYF
ADQAINSRFVSEVWKIGLDIKDSCDRFIIEKAVRELMEERKGEFLERAEEMATIVKRA
VSKGGSSYSNLDGLIEYIKSLVV*

UGT72B35 (NbGTfc2)

MAETAIVTKSENPHIVILPSPGMGHLIPLVEFSKRLISQHQFSVTLILPTEGPISNSQKI
FLNSLPSCMDYHLLPPVNFDDLPLDVKIETRISLTVTRSLSSLRDVFKTLVDSKKVVA
FVVDLFGTDAFDVAIDFNVSPYIFFPSTAMALSLFLYLPKLDGTVSCEYREVTDPVQI
PGCIPIHGKDLLDPVQDRKNEAYKWLLHHSKRYRMAEGVVANSFKELEGGAIKALQ
EEEPGKPPVYPVGPLIQMDWGSKVDGSGCLTWLDEQPRGSVLYISYGSGGTLSHE
QLIEVASGLETSEQRFLWVIRCPNDTIANATYFNVQDSDNPLDFLPKGFLERTKGLG
LVLPNWAPQAQILSHGSTGGFLTHCGWNSTLESVVHGVPLIAWPLYAEQKMNAVM
LTEDIKVALRPKANENGLVGRLEIAKVVKGLMEGEEGKGVRTRMRDLKDAAAKVLS
QDGSSTKALAELATKLKNKVLNN*

UGT72AX1 (NbGTfc3)

MDISTTTATAEQKEKPHVAFLPSPGMGHIIPLFEFAKRLVINHGFHVSFFVISTGASA
AQNELFRSDNIPAGFHAVEIPPVENISSFFTDDMRIVTRLSIIVRESLKQYLSLLLITHR
PKALIIDLFCTDAFEICKEVSIPVYSFFTASTLLMAFSLYLPTLDREVNGEFVDLPEPIQ
TPGCNPICPHDLLDQVKDRKNDEYKWYLLHVSRLPLAAGIFVNSWDDLEPVTLEAL
KRNSFFQNIPIPPVHTIGPLIKQDEVVTEKDAQILTWLDNQPPDSVLFVVFGSGGTLT
SEQLTELAWGLEMSHQRFILVARKPSDASASAAFFNVGSDENDPLMYLPEGFAKKT
EGRGLVVPSWASQVAILNHPSTRAFFSHCGWNSTLESVVHGVPMIAWPLYAEQRM
NATFLAEEVGVTMKFPLVPGEELISRKEIEKMVRIVMEGEKGMAMRRRAEELKESA
KIALSNGGSSDDSLCRVVQFWKSDQSLCG*

UGT72AY1 (NbGTfc4)

MDSSQLHVAIVSSPGMGHLIPVLVLGNRLATHHNIKITILAITTTSSSAETEFLKKTTLT
NEEKTIEIIPVPSVDISHLINSSTKIFTQLRLLVREALPKIHSTIASMTHRPDALIVDIFCT
QILPIAEEFNISKYTYHPTTAWTLALAIYCQVFDKEIEGEYVELKEPLKIPGCKALRPD
DVVDPLLDRSDQQYEEYVKLGKEYTDFDGILINTWEDLEPETINALRYNEKLRLLLK
VPVFPIGPLRRKVETTLNDEVIQWLDKQNNESVLFVSFGSGGTLSTKQMTELAWGL
ELSQQKFVWVVRPPSDGDADSAYLNSAGKDTRDMSEYLPEGFLTRTKDMGLVVP
MWANQVEILSHSSVGGFLTHCGWNSTVESLTNGVPMIAWPLHAEQKMNAAMLTE
ELGVAIRPAVLPTKKLVKREEIQGMVRILMQTKEGKRIKEKAKKLKKSAENALSDGG
SSYNSICELVKDIRSREL*

UGT85A73 (NbGTfc5)

MGSIGAELTKPHAVCIPYPAQGHINPMLKLAKILHHKGFHITFVNTEFNHRRLLKSRG
PDSLKGLSSFRFETIRDGLPPCEADATQDIPSLCESTTTTCLGPFKDLLAKLNDTNTS
NVPPVSCIVSDGVMSFTLAAAQELGVPEVLFWTTSACGLLGYMHYYKVIEKGYAPL
KDATDLTNGYLETTLDFIPGMKDVRLRDLPSFLRTTNPDEFMIKFVLQETQRARKAS
AIILNTFETLEAEVLETLRNLLPPVYPIGPLHFLVKHADDENLKGLRSSLWKEEPECIQ
WLDTKEPNSVVYVNFGSITVMTPNQLIEFAWGLANSQQTFLWIIRPDIVSGDASILPP
EFVEETKNRGMLASWCSQEEVLSHPAIGGFLTHSGWNSTLESISSGVPMICWPFFA
EQQTNCWFSVTKWDIGMEIDSDVKRDEVESLVRELMVGEKGIKMKKKAMEWKELA
EESAKEHSGLSYVNIEKVVNDILLSSKH*

UGT73A25 (NbGTfc6)

MGQLHFFFFPMMAQGHMIPTLDMAKLVASRGVKATIITTPLNESVFSKSIQRNKHLG
IEIEIRLIKFPAIENDLPEECERLDQIPSDEKLPNFFKATAMMQEPLEQLIEECRPNCL
VSDMFLPWTTDSAAKFNIPRIVFHGTSFFALCVENSVRLNKPFKNVSSDSETFVVPN
LPHEIKLTRTQVSPFEQSGEETTMARMIKTVWESDSRSYGVVFNSFYELETDYVEH
YTKVLGRRAWAIGPLSMCNRDIEDKAERGKKSSIDKHECLKWLDSKKPSSVVYICF
GSVANFTASQLHELAMGIEASGQEFIWVVRTELDNEDWLPEGFEERTREKGLIIRG
WAPQVVILDHESVGAFVTHCGWNSTLEGVSGGVPMVTWPVFAEQFFNEKLVTEVL
RTGADVGSIQWKRSASEGVKREAIAKAIQRVMVSEEAEGFRNRAKAYKEMARKAV
EEGGSSYTGLTTLLEDISTYSSTGH*

UGT85A74 (NbGTms5)

MGSVEGKKAQKPHAVCIPFPSQGHINPMKISILLHSKGFHITFVNSEYNHKRLLKSR
GPYSLKGLQDFVFETIPDGLPPIDAHTTQHIPSLCLSTKENCLAPFKELLIKINSSNDV
PKVTCIIFDGIMTFAVLAAQEIGVPSVCFRTTNACSFMCNKHLPLLIEKGILPLKDTSDI
TNGYLDTVIDCIPSMKNVRLREFPSQIRTTDINDKLLNFIMGETEGASKASAIIFHTFD
TLEFNVLRDLSLICPPLYTIGPLHLLTHQLPENSLKFLGANLWKEDEDCIQWLNSKEE
KSVVYVNFGSITVLTKNQLMEFAWGLANSKKNFFWVIRSDAVIGDDSAMLPNSFVE
ETKERGLISRWCCQEQVLKHSSIAAFLTHCGWNSVMESIGIGVPMICWPFFADQHI
NCRNVCCEWGVGLEIGKNVNRNEVDKIVREVMDGEKGKKVKKKVSEWKKLAERLL
E*

UGT73A24 (NbGTms8)

MGQLHIFFFPMMAHGHMIPTLDMAKLFASRGVKATIITTPLNESVFSKAIQRNKHLGI
EIEIRLIKFPAVENDLPEECERLDQIPSDEKLPNFFKAVAMMQEPLEKLIQECRPNCL
VSDMFLPWTTDSAAKFNIPRIVFHGTSFFALCVENSVRLNKPFKNVSSDSETFVVPN
LPHEIKLTRTQVSPFERSGEETAMTRMIKTVRESDSKSYGVVFNSFYELETDYVEHY
TKVLGRRAWAIGPLSMCNRDIVDKAERGKKSSIDKHECLKWLDSKKPSSVVYICFG
SVANFTASQLHELAMGIEASGQEFIWVVRTELDNEDWLPEGFEERTKEKGLIIRGW
APQVLILDHESVGAFVTHCGWNSTLEGVSGGVPMVTWPVFAEQFFNEKLVTVVLK
TGAGVGSIQWKRSASEGVKREAIAKAVKRVMVSEEADGFRNRAKAYKEMATKAIE
KGGSSYTGLTTLLEDISTYSSTDH*

UGT71AJ1 (NbGTms9)

MSKLELVFLPAPAVGHLVSSCKFAENLLSKEQRLCITILIIRPPAPWDAGIDVYIKRSS
STPHGSRIRYITLPQVEPPSSDKLEKSIENYFSLLIASYRPLVKEAIISNKWPDSDPKII
GLVIDMFSSSMIDVANELGVPSYLFFTSGAGFLGFLFYLSVWHEKFGRELNKYDAD
LNIAAYANPVPSKVLPTFAFNKEGFNSFREHGVRFKDTKGILINTVAELENHAVNALA
SNPELPPVYTVGFLLDLEGQKTKGNSNIEYDEIMKWLDQQPPSSVVFLCFGSSGIFE
PPQLIEMAIALEQSGVSFVWSIRRPVDDEYAKLEEILPEGFLERTKSRGIVCGWAPQ
VNILAHKATGAFVSHCGWNSTLESLWNGVPIVTWPLYAEQQINAFQLVKDLEMAVE
LRLDYKMRGSDRGEIVKAEEMERAIRCIMDSENPVRKRVKELGEICKNALMEGGSS
FNSIGRFVKTILDSWN*

UGT72B34 (NbGTms10)

MAETAIVTKSENPHIVILPSPGMGHLIPLVEFSKRLISQHQFSVTLILPTDGPISNSQKI
FLNSLPSCMDYHLLPPVNFDDLPLDVKIETRISLTVTRSLSSLRDVFKTLVESKKVVA
FVVDLFGTDAFDVAIDFNVSPYIFFPSTAMALSLFLYLPKLDATVSCEYRDLPDPIQIP
GCIPIYGKDLLDPVQDRKNEAYKWLLHHSKRYGMAEGVIANSFKELEGGAIKALQE
EEPGKPPVYPVGPLIQMDSGSNVDGSGCLTWLDEQPLGSVLYISYGSGGTLSHEQ
LIEVASGLEMSEQRFLWVIRCPDDTVANATYFNGQDSTNPLDFLPKGFLERTKSLG
LVVPNWAPQAQILAHGSTGGFLTHCGWNSILESVIHGVPLIAWPLYAEQKMNAVML
AEDIKVALRPKANENGLMGRLEIAKVVKGLMEGEEGKGVRTRMRDLKDAAAKVLS
QDGSSTKALAELATKLKNKVLYN*

UGT709Q1 (NbGTms11)

MDHPSPHVLLFPLPIQSPINSMLQLAELFCLAGLQVTFLNTNHNQKLLLRYTNVESR
FRQYPRFRFRTISDGLPEENPRSSVQFGELISSLQAVAEPFLREILIGSSSSSDGDTE
APLTCVIPDGLFYYAVDIGNEMGVPVIPFDTISPCCLWIYLCIPKLIQAGEIPFKGNDL
DVLFENVAGMQGLLRRRDFPFYRLIDYATDPYCQIALKEVESIPQCNGLILNTFEDLD
GPLLSLIRSHCPQTYATGPLHLHLKTKLADKRIPISASSNSLWEEDHSSIQWLDAQPI
ESVIYVSFGSMATLSKEEILEFWHGLVNSGIRFLWVMRSNLLRGEEMNHQFVKELA
EGCKERAYIVSWAPQEKVLAHSAIGGFLTHSGWNSTMESIVQGKPMICWAVYVDQ
RVTSRFVGEVWKIGVDMKDTCDRYIIEKMVKDLMVTNRDEFKKSAEKLSILAKESVG
EGGSSYNALECLVDDIKKLSRRGKDIKSNCIE*